A COMPARATIVE STUDY OF ERODIBILITY MODELS AND INVESTIGATION OF INFLUENTIAL FACTORS IN ESTIMATION OF THEIR PARAMETERS FROM LABORATORY MINI-JETS

By

ANISH KHANAL

Bachelor of Science in Civil Engineering
Institute of Engineering
Tribhuvan University
Lalitpur, Nepal
2008

Master of Science in Civil Engineering
Southern Illinois University
Carbondale, Illinois
2012

Submitted to the Faculty of the
Graduate College of the
Oklahoma State University
in partial fulfillment of
the requirements for
the Degree of
DOCTOR OF PHILOSOPHY
May, 2016

A COMPARATIVE STUDY OF
ERODIBILITY MODELS
AND
INVESTIGATION OF INFLUENTIAL FACTORS IN
ESTIMATION OF THEIR PARAMETERS FROM
LABORATORY MINI-JETS

Dissertation Approved:

Dr. Garey Fox

Dissertation Adviser

Dr. Daniel Storm

Dr. Sherry Hunt

Dr. Rifat Bulut

.

ACKNOWLEDGEMENTS

I would like to express my most sincere gratitude towards my advisor, Dr. Garey Fox. I am grateful to him for providing me the opportunity to pursue my PhD and his guidance and support to complete it. I appreciate his patience and effort through these four years. He has been a phenomenal teacher and mentor to me and I will always cherish my days working as his student. I would also like to thank my committee members, Dr. Daniel Storm, Dr. Sherry Hunt and Dr. Rifat Bulut for their invaluable input and feedback.

I appreciate all the help and support I received from my colleagues and friends; Dr. A. T. Al-Madhhachi, Dr. Erin Daly, Kate Klavon, Whitney Lisenbee, Holly Enlow. Yan Zhou Cole Niblett, Abigail Parnell and Kevin Moore. I thank them for their hard work and tireless effort in laboratory, field and office. I have really enjoyed working and collaborating with them. I would also like to acknowledge the support from Biosystems laboratory manager Wayne Kiner and his staff.

I would like to thank all my friends in Stillwater and Tulsa for all the wonderful memories. I would not have been able to make it through these four years if I didn't have their company. Finally, I would like to thank my parents, Rishi Khanal and Sushila Khanal, my sister Anaga Khanal and my wife, Safala Acharya for their unending, unconditional love. I owe them everything I have achieved and I will always strive to make them proud.

Acknowledgements reflect the views of the author and are not endorsed by committee members or Oklahoma State University.

Name: ANISH KHANAL

Date of Degree: MAY, 2016

Title of Study: A COMPARATIVE STUDY OF ERODIBILITY MODELS AND INVESTIGATION OF INFLUENTIAL FACTORS IN ESTIMATION OF THEIR PARAMETERS FROM LABORATORY MINI-JETS

Major Field: BIOSYSTEMS ENGINEERING

Abstract: Modeling and predicting detachment of cohesive particles and consequently erosion of cohesive soil mass remains an unconquered problem. The linear excess shear stress model and the non-linear Wilson model are some of the prominent process based models used extensively. The parameters of these models can be statistically estimated from various experimental methods like the Jet Erosion Test (JET). A miniaturized version of the JETS called the mini-JETs has added advantage of portability and in-situ use. However, lack of a standard operating procedure can lead to wide variability in estimation of the parameters of the erodibility equation. Besides the operation of the device, analysis procedure of the data obtained from the JETs is also not adequately established. This study focused on the mini-JET device and the parameters of the erodibility equation. Precision of the mini-JET in terms of the parameters of the erodibility models was calculated. Recommendations were made regarding the head setting, initial interval and termination interval to establish uniformity in operation of the mini-JET. The influence of vegetation roots on the parameters of the erodibility equations was also quantified using the mini-JET and correlations between root properties and the erodibility parameters were identified. The influence of the moisture content on the soil erodibility was investigated in terms of the parameters of the erodibility equation using the mini-JET. Different solution techniques to derive the parameters of the linear model were compared with respect to the variability of the parameters. The performance of the linear model and non-linear model was applied in a reach scale stream bank stability simulation in order to evaluate their performance in an application setting. The non-linear model was shown to be more appropriate than the linear model in predicting the erosion rates at a wider range of applied shear stress. This research highlighted the usefulness of the mini-JET in modeling the detachment of cohesive soil and advantages of using the non-linear model in modeling long term streambank retreat. This study also identified the critical areas of research to further improve the process based approach to modeling the erosion of cohesive soil.

TABLE OF CONTENTS

LIST OF FIGURES

Figure **Page No**

LIST OF TABLES

Table **Page**

CHAPTER 1

INTRODUCTION

Erosion is a key process in geomorphology. It is a natural watershed process and determines the formation and evolution of channels such as rills, gullys and streambanks. It is also inherently associated with quality of the floodplain environment, habitat and ecological functions. Streambank erosion is combination of three separate erosion processes: sub-aerial erosion, fluvial erosion and mass failure.

Sub-aerial processes contribute in loosening, weathering and weakening particles from the parent material. This process mostly depends on climatic factors such as surface temperature, precipitation, wind, etc. This process acts on large scales (watershed scale) and is continuous temporally. Mass failure is an episodic process which occurs at much smaller scale (site scale) due to a lack of equilibrium between driving and resisting forces. The process depends mostly on intrinsic properties of the parent material such as weight, moisture content, texture and permeability. Fluvial erosion acts a precursor to mass failure (ASCE, 1998; Rinaldi and Darby, 2008). Fluvial erosion occurs due to detachment of particles from parent material of a bank when acted upon by a fluvial force. It is a quasi-continuous process which is initiated when a threshold of fluvial force is exceeded in a particular flow event. It is dependent on the hydraulic forces acting on the bank as well as physical properties of the bank (Simon et al., 2000).

Inherent variability of different fluvial forces acting on a streambank and heterogeneity of the physical properties of the bank material make measurement, modeling and prediction of fluvial erosion complex and challenging. Streambank erosion is one of the most abundant and prominent manifestations of the fluvial erosion in nature. Streambank erosion, while a natural process, also can be driven by anthropogenic factors and contribute significantly to pollution of natural streams. The sediment detached from the streambanks can be a significant source of excessive sediments, nutrients and other pollutants which can lead to problems of eutrophication, loss of habitat and overall degradation of ecological functions. Streambank erosion has been identified as a significant source of sediment both in UK (Walling et al, 1999) and USA (USEPA, 2011). Hence, reliable measurement and modeling of the sediment detachment from streambanks as well as other natural channels is of great concern to engineers, geomorphologists and water managers.

Different attempts have been made to model and predict cohesive particle detachment due to fluvial forces. Earliest attempts at such modeling have focused on deriving the hydraulic variables that act to detach and transport (Knapen et al, 2007). Other attempts have focused on empirically estimating the amount of sediment loss from large scales with a multiplying factor, for example, the K factor in USLE and RUSLE (Renard et. al., 1997). The most popular model to quantify fluvial erosion remains the excess shear stress equation (Partheniades, 1965):

$$\varepsilon_r = k_d(\tau - \tau_c)^a \tag{1.1}$$

where ε_r is the erosion rate (cms^{-1}), k_d is coefficient of erodibility ($cm^3N^{-1}s^{-1}$), τ is the applied shear stress (Pa), τ_c is the critical shear stress (Pa), and a is an exponent usually assumed to be unity.

An alternative to the excess shear stress model is Wilson's model (Wilson, 1993a, b). Wilson's model is based on the balance of all the forces and moments driving and resisting detachment of a two dimensional representation of a particle or an aggregate of particle:

$$\varepsilon_r = b_0\sqrt{\tau}\left[1-\exp\left\{-\exp\left(3-\frac{b_1}{\tau}\right)\right\}\right] \qquad (1.2)$$

where ε_r is the erosion rate (cms^{-1}), τ is the applied shear (Pa), and Wilson's model has two parameters; b_0 ($gm^{-1}s^{-1}N^{0.5}$) and b_1 (Pa). These parameters, unlike parameters of the excess shear stress equation, are mechanistically defined.

The main difference between these models is the relation between the τ and predicted ε_r. In most of applications of the excess shear stress equation, the value of the exponent is assumed to be unity. Consequently, the relationship between τ and ε_r predicted by the excess shear stress equation is linear. Wilson's model describes that relation to be non-linear. While both models have their advantages and disadvantages, there have been no studies in which application of the two models have been compared.

Several different techniques are employed to estimate the erodibility parameters of these equations. Such techniques include flumes (Hanson 1990a), hole erosion tests (Wan and Fell, 2004), cohesive strength meter (Tollhurst et al, 1999), and submerged jet test (Hanson 1990b). The submerged jet test or the jet erosion test (JET) is a relatively new technique. It was primarily developed for in-situ testing. Since the development, the

JET has evolved in form and function. Recently, a miniature version of the JET called the mini-JET was developed and employed in several laboratory and field studies. It has proven to be advantageous over the original JET due it's small and light design. The mini-JET has a great potential to be a useful tool in studying fluvial erosion. However, absence of standard operating guidelines for the apparatus has caused confusion about appropriate procedures to conduct JETs. Users still lack information on optimum head setting, appropriate time interval for reading data and appropriate length of time for each test. This introduces uncertainty in values of estimated erodibility parameters due to user dependent choices of head setting, time interval and test length.

Large variability has been observed in the values of parameters of these equations when the mini-JET was used in field conditions (Daly et. al., 2013, 2015). This was attributed to variety of different factors such as soil moisture, presence of vegetation, macropores and heterogeneity of soil texture as well as complex interactions between these factors. Isolating variability caused by individual factors and quantifying their effect in terms of the value of erodibility parameters is a difficult prospect as these factors cannot be controlled in situ. Laboratory mini-JETs can be performed with controls on many of these factors in order to quantify variability of the JET and isolate the effect of specific factors.

The main objectives of this research are as follows:

1. To make recommendations about the standard operating procedure of the mini-JET by investigating the effect of pressure head, reading interval and test length of JETs on the erodibility parameters and to quantify the precision of

mini-JET device with respect to the erodibility parameters derived from different solution methodologies proposed in literature.

2. To investigate influence of moisture content on erodibility parameters derived from the mini-JETs under controlled laboratory conditions.
3. To investigate the effect of vegetation roots on the erodibility parameters derived from the mini-JETs under controlled laboratory conditions and relationship between the erodibility parameters and root properties.
4. To compare the performance of the linear and non-linear models by applying these models in a reach scale streambank stability study.

CHAPTER 2

VARIABILITY OF ERODIBILITY PARAMETERS FROM LABORATORY MINI JET EROSION TESTS[1]

Abstract

Application of jet erosion tests (JETs) to study in-situ erodibility is gaining popularity. New versions of the JET (original JET versus mini-JET) and new data analysis techniques have introduced questions regarding their operation and data collection procedures. One of the major issues regarding JETs is the high degree of variability of the erodibility parameters (i.e., erodibility coefficient, k_d, and critical shear stress, τ_c). This variability has been attributed to heterogeneity in different soil properties under natural field conditions, but limited research has quantified variability under controlled laboratory conditions, especially for the newer mini-JET. This study uniquely conducted 20 mini-JETs under controlled laboratory conditions on each of two soil types of contrasting texture. JETs were conducted in-situ on these same soils in previous research. The laboratory JETs predicted similar values of most parameters with much less variability than in the field. Three to five JETs conducted in the laboratory estimated

[1]Published as:

Khanal, A., Fox, G., Al-Madhhachi, A. T. (2015). "Variability of Erodibility parameters from Laboratory mini jet erosion tests". *Journal of HydrologicEngineering doi:10.1061/(ASCE)HE.1943-5584.0001401.*

erodibility parameters with a precision of 25% at a 95% confidence level. Laboratory JETs on disturbed, remolded samples provided baseline estimates of in-situ erodibility parameters. Additional JETs were conducted at three different head settings on the two soil types.

The influence of the head setting was dependent on the soil type, solution technique, and detachment model. In general, variability in derived erodibility parameters increased at larger head settings especially for the less erodible soil. Existing JET data were resampled to evaluate the effect of the initial time interval and termination time interval of data collection on derived erodibility parameters. Both initial and termination time intervals were most influential at larger head settings. An initial time interval of 30 s and a termination time interval of at least 300 s was recommended especially for less erodible soils.

Introduction

The quantification of soil detachment has remained a challenging prospect in the field of applied geomorphology. It is especially important in process-based modeling of streambank erosion. It is equally pertinent in studying and modeling fluvial features in non-riparian areas. As streambank erosion is identified as one of the main non-point sources of sediment pollution of natural streams, estimating streambank erosion rates is of significant importance. Therefore, quantifying sediment detachment is one of the most important problems for estimating watershed sediment loads.

Sediment detachment rates are most often estimated in the laboratory using various experimental techniques. These techniques include flumes, Rotating cylinder apparatus (Moore and Masch, 1962), hole erosion tests (HET) (Wan and Fell, 2004) and

jet erosion tests (JET) (Hanson and Hunt, 2007; Al-Madhhachi et al., 2013a, 2013b). Flumes and their variations are the most traditional techniques. Special flumes called the SEDflume were developed for measurement of the sediment detachment (McNeil et al., 1996). Erosion Function Apparatus is another example of flume modified for the purpose of measuring sediment scouring (Briaud et al., 2001). The HET and JET are relatively newer techniques. In all tests, a soil specimen of known properties (for example, texture and moisture content) is packed at a known density and subjected to shear forces by applying known pressure heads. The pressure heads exert a shear stress (τ) on the soil specimen inducing detachment of soil particles. The detachment is periodically measured in terms of depth of erosion or mass of detached sediment, which is converted into an erosion depth based on the bulk density. The observed erosion rate is then fit to a mathematical model, which relates the τ exerted by the applied pressure head to the rate of particle detachment (ε_r).

Jet Erosion Tests

The JET is a relatively novel technique used in studying the erosion properties of a soil specimen. It was developed by the USDA-ARS in Stillwater, OK (Hanson et al., 1990). A jet of water generated by a constant pressure impinges on a soil surface in submerged conditions. The jet exerts a certain shear force on the soil surface creating a scour hole. Two versions of JETs are in existence: the original JET and the mini-JET (Figure 2.1). Analytical procedures were derived for obtaining the erodibility parameters (i.e., erodibility coefficient, k_d, and critical shear stress, τ_c) based on the hydraulics of the submerged jet (Hanson and Cook, 1997; Hanson et al, 2002). The apparatus, general test

methodology and procedure to analyze the data for obtaining erodibility parameters of the excess shear stress equation are described in detail by Hanson and Cook (2004).

The mini-JET is a smaller version of the original JET apparatus. The use of mini-JET device was first described by Simon et al. (2010). The study presented a comparison of the erodibility parameters measured from the original and the mini-JET devices under field conditions and reported differences. A comparative study of the original JET and mini-JET devices in laboratory conditions was later conducted by Al-Madhhachi et al. (2013a). The study concluded that, with an adjustment to account for the differences in the size of the nozzles of the two JET devices, the original JET and the mini-JET provided equivalent measures of the erodibility coefficients. A corresponding study by Al-Madhhachi et al. (2013b) suggested no statistically significant differences for the erodibility parameters when estimated from flume tests and JET devices.

Estimation of Erodibility Parameters

The JET data can be fit to two different types of mathematical models to describe the erosion characteristics of a soil specimen: linear and nonlinear models. The linear model, also known as the excess shear stress equation (Partheniades, 1965), is the most frequently used sediment detachment model in the literature to date. The model states that the erosion rate is proportional to the difference between τ and the critical shear stress:

$$\varepsilon_r = k_d(\tau - \tau_c)^a \tag{2.1}$$

where ε_r is the detachment rate (m s^{-1}), k_d is the erodibility coefficient (m^3 N^{-1} s^{-1}), τ_c is the critical shear stress (Pa), and a is an exponent. The τ_c is the minimum τ required to initiate particle detachment. The k_d and τ_c are collectively called the erodibility

parameters of the excess shear stress equation. The value of the exponent (a) is usually assumed to be one (Hanson et al., 2002).

Currently, there are three approaches in analyzing data from JETs to estimate the erodibility parameters of the excess shear stress equation. The most popular method of analysis, called Blaisdell's solution (BL), was developed by Hanson and Cook (1997, 2004). The solution method was based on principles of fluid diffusion presented by Stein and Nett (1997) and a hyperbolic function modeling the depth progression of the scour hole developed by Blaisdell et al. (1981):

$$X^2 = (f - f_o)^2 - A^2 \tag{2.2}$$

where $X = \log\left(\frac{U_0 t}{d_0}\right)$, $f = \log\left(\frac{J}{d_0}\right) - \log\left(\frac{U_0 t}{d_0}\right)$, J is the depth of scour hole recorded at each time (t), d_0 is the diameter of jet orifice, and U_0 is the velocity of the jet at the origin. The function represents a rectangular hyperbola with A as both the semi-transverse and semi-conjugate and center at (0, f_0) in a Cartesian plane. The ordinate of the center of the hyperbola, $f_0 = \log\left(\frac{J_e}{d_0}\right)$, is used to predict the equilibrium depth (J_e) of the scour hole. The equilibrium depth is defined as the maximum depth of the scour hole beyond which the water jet cannot erode further. This solution method first determines the τ_c parameter based on the J_e of scour hole as predicted by Blaisdell's function as follows:

$$\tau_c = \tau_0 \left[\frac{J_p}{J_e}\right]^2 \tag{2.3}$$

where τ_o is the maximum boundary τ due to the jet velocity at the orifice, and J_p is the potential core length. The velocity at the jet centerline is equivalent to jet velocity at orifice through J_p (Hanson and Cook, 2004). The J_p is constant for the given JET

apparatus and τ_o is constant for a given head setting, h. The J_e depends on both the head setting and the fit of the observed data to the hyperbolic function. The k_d is then determined by solving for the least squared deviation between the observed scour time (t) and predicted time (t_m) as defined as follows:

$$t_m = T_r\left[0.5\ln\left(\frac{1+J^*}{1-J^*}\right) - J^* - 0.5\ln\left(\frac{1+J_i^*}{1-J_i^*}\right) + J_i^*\right] \tag{2.4}$$

where $T_r = \frac{J_e}{k_d \tau_c}$ is a reference time, $J^* = \frac{J}{J_e}$ is a dimensionless scour depth, and $J_i^* = \frac{J_i}{J_e}$ is a dimensionless measure of the initial distance between the jet orifice and soil surface.

Alternatives to Blaisdell's solution have been suggested recently (Simon et al., 2010; Daly et al., 2013). One of these solution methods is called the scour depth solution (SD). This method simultaneously searches for k_d and τ_c which provide the best fit of observed JET data on the scour depth versus time curve predicted by the excess shear stress equation. The other approach was presented by Simon et al. (2010), and referred to as the iterative solution (IT). This method is initialized using the values of erodibility parameters determined by Blaisdell's solution. The scour hole is assumed to reach the J_e at the end of each test. An upper bound on τ_c is fixed by substituting this J_e in equation (2.3). Then the values of τ_c and k_d which minimize the root mean square deviation between the observed t and predicted time (t_m) is searched for iteratively.

A nonlinear model describing detachment of soil particles or aggregates due to fluvial forces was proposed by Wilson (1993a, 1993b). The model is based on balance of all the forces and moments driving and resisting detachment of a two-dimensional representation of a particle or aggregate. The equation of the model is given as follows:

$$\varepsilon_r = \frac{b_0\sqrt{\tau}}{\rho_b}\left[1-\exp\left\{-\exp\left(3-\frac{b_1}{\tau}\right)\right\}\right] \qquad (2.5)$$

where ρ_b is the bulk density and Wilson's model has two parameters b_0 (g m^{-1} s^{-1} $N^{-0.5}$) and b_1 (Pa). These parameters, unlike parameters of the excess shear stress equation, are mechanistically defined. As seen from the equation, the relationship between ε_r and τ is nonlinear. Note that b_0 is similar to k_d but with a different magnitude and units.; b_1 is similar to τ_c.

Al-Madhhachi et al. (2013b) incorporated the hydraulics of both the original and mini-JET device in Wilson's model and demonstrated that the parameters of Wilson's model can also be determined from the experimental data obtained from the JETs. The observed particle detachment rate data is fitted to equation (2.5) by minimizing the sum of squared differences between the observed and modeled scour depth. Hence, the parameters of the model can be determined statistically from observed JET data similar to the linear model.

JET Procedures

Portability and in-situ testing capability are the main advantages of the JETs, making them ideally suitable for field studies (Hanson and Cook, 2004; Hanson and Simon, 2001; Simon et al., 2010; Daly et al., 2015b). The in-situ variability in these parameters has been attributed to heterogeneity in different intrinsic (soil texture) and extrinsic (moisture content, vegetation, macropores, and bio-chemical processes) factors. The variability can also be caused by complex interactions of these factors such that the effect of each of these factors is difficult to isolate. However, some degree of variability is to be expected due to the apparatus itself and the operation of the device. The precision

of the mini-JET apparatus has not been thoroughly established. The variability associated with the mini-JET apparatus itself can be a benchmark against which the variability observed at the field can be compared.

In absence of a standard procedure, the operation of the original JET and mini-JET can differ in many aspects from user to user. For example, different users can select different pressure head settings, which control the jet velocity and mechanics of the jet creating the scour hole, or choose to take readings at different time intervals including both how long to initiate the jet prior to the first set of readings (referred to herein as the initial time interval) and at what time interval to terminate the test when two or more subsequent readings are similar (referred to herein as the termination time interval). The effect of such user dependent variables on the estimation of parameters has also not been studied. Hanson and Cook (2004) recommended that the head setting be chosen so that the peak τ applied by the JET is similar to the peak τ in a natural open channel environment. This τ can be difficult to achieve during testing, and in some cases, such as erodible soils, can lead to tests that erode so quickly that quality measurements cannot be obtained. The gauge readings are taken following a protocol which starts out at a certain initial time interval. The initial time interval is kept small to be as conservative as possible and obtain high resolution early time data when the applied shear is highest and scouring is most rapid. This initial time interval is then increased periodically when two or three consecutive readings at the current interval are the same. The test is terminated when two or three consecutive readings are the same at a certain final or termination time interval. In absence of standard guidelines, the choices of the initial time interval at which the gauge readings are taken and termination time interval at which the test is completed

depends on the judgement and experience of the user. This may lead to discrepancies in derived erodibility parameters and make them incomparable from one test to another.

Objectives

JETs have evolved in form and function over last two decades. They have been adopted by researchers to investigate erodibility properties of natural features like streambanks as well as to aid in designs of artificial constructs like earthen embankments. A review of the literature shows that most of the studies have been focused on exploring the effect of soil properties on the erodibility parameters. There have been limited studies which have investigated the effect of user dependent factors such as applied pressure head and choices of initial time interval and termination time interval on derived erodibility parameters. This study hypothesized that the user dependent factors outlined above have a significant effect on the estimation of erodibility parameters from laboratory JETs performed on soil samples of the same texture, bulk density, and moisture content. The objectives of this study were as follows:

1. To estimate the precision of the mini-JET apparatus and variability in erodibility parameters (i.e., erodibility coefficient, k_d, and critical shear stress, τ_c) associated with the apparatus under controlled laboratory conditions and with respect to various solution methodologies proposed in the literature.
2. To investigate the effect of applied pressure head on the values of the erodibility parameters derived from three different solution methods for the linear excess shear stress model (BL, SD, and IT) and also for the Wilson model (WL).

3. To investigate the effect of the selected initial time interval and termination time intervals on the erodibility parameters derived from three different solution methods (BL, SD, and IT) for the linear excess shear stress model and the Wilson model (WL).

Methods and Materials

Mini-JETs were performed on remolded samples of two soils of contrasting texture. The construction and operation of the mini-JETs are described in detail in Al-Madhhachi et al. (2013a). The two soils utilized for the remolded samples were a sandy loam soil obtained from a streambank of Cow Creek in Stillwater, Oklahoma, and a clay loam soil obtained from the B horizon of a streambank of Five Mile Creek near Fort Cobb, Oklahoma. The particle size distribution of both soils was analyzed following ASTM standard D422. Liquid limit and plastic limit of the soils were performed following ASTM standard D4318. Standard compaction tests were performed on the soils using ASTM standard D698A. The characteristics of each soil are presented Table 2.1.

Each soil was air dried, sieved through a no. 4 sieve (4.75 mm), and mixed with water to achieve uniform water content. The sandy loam soil was mixed with water to obtain a water content of 10%; the clay loam soil was mixed with water to obtain water content of 16%. The water contents were chosen to be on the drier side of the optimum moisture content curve derived from the standard compaction test. The samples for the JETs were prepared by packing the soil in a standard mold.All the samples prepared with sandy loam soil was compacted to a dry density of 1.7 Mg m^{-3}, and the clay loam soil was compacted to dry density of 1.4 Mg m^{-3}. These densities were chosen to be closest to maximum dry density while being convenient enough to achieve the desired uniform dry

density. Attempts to achieve larger density, especially for clay loam soil resulted in non-uniform compaction. Total mass of the soil required to achieve the aforementioned dry density was calculated. The mass was divided in three equal portions. Each portion of soil was packed into separate layer consecutively to achieve a uniform dry density through the sample. Uniform packing was chosen to avoid layering effects as mentioned in Al-Madhhachi et al. (2013a).

Twenty mini-JETs were conducted on each of two soil types. The JETs on the more erodible sandy loam were conducted at a smaller head of 46 cm (H1); JETs on the less erodible clay loam soil were conducted at larger head of 109 cm (H3). This was done to mimic field mini-JETs as it is a common practice to conduct JETs at larger heads on more resistant soils. The JET data were analyzed to derive erodibility parameters for both linear and nonlinear models. The parameters of the linear model were estimated using three different solution techniques: Blaisdell's solution (BL), scour depth solution (SD), and iterative solution (IT) using the spreadsheet tool developed by Daly et al. (2013). The parameters of the Wilson model (WL) were also determined using the spreadsheet tool described by Al-Madhhachi et al. (2013b).

The estimated erodibility parameters were assumed to be either normally or log-normally distributed for the purpose of quantifying variability. This assumption was checked with an Anderson-Darling Test using MiniTab 16 (MiniTab, Inc.). The Anderson Darling test statistic (AD) and the P-value associated with the test were reported for each erodibility parameter. Smaller values of the AD statistic and P-values larger than the selected level of significance indicate normality. The AD statistics were

calculated with logarithms of the erodibility parameters to check the assumption of log normal distribution.

The variability of the normally distributed erodibility parameters were quantified first by calculating the sample size (n) required to estimate the given parameter within given precision level at a certain confidence level based on the standard deviation (S):

$$n = \left(\frac{ZS}{\Delta} \right)^2 \tag{2.6}$$

where Z is the normal deviate corresponding to the upper percentage point for a specified level of confidence. Here, it is assumed that S equals the population standard deviation. Also, it must be noted that the precision (Δ) is expressed in terms of the percentage deviation from the average (P). The variability of the log-normally distributed erodibility parameters were quantified by calculating the n required to estimate a true mean within a predetermined fraction and a given level of confidence is given as follows (Hale, 1972):

$$n = \left(\frac{ZS}{\ln(P+1)} \right)^2 \tag{2.7}$$

where S is the standard deviation of the logarithms of the observation and P is the fraction of the observed geometric mean by which it can deviated from the true mean. P expressed in terms of percentage in this study. Daly et al. (2015a) conducted a variability study of the erodibility parameters derived from mini-JETs; they conducted in the field on streambanks of Cow Creek in northern Oklahoma, which was the source of the sandy loam soil, and on a streambank of Five Mile Creek in southwestern Oklahoma, which was the source of clay loam soil. It was the intent to use this field measured data from Daly et al. (2015a) to compare to the laboratory mini-JETs since soils tested in the

laboratory were extracted from the same streambanks. Daly et al. (2015) observed variability of approximately three orders of magnitude in the erodibility parameters. Other researchers report similar findings with original JETs under in-situ conditions (Wynn et al., 2008; Karmaker and Dutta, 2011).

Five additional JETs were performed each at two different head settings of 79 cm (H2) and 109 cm (H3) on the sandy loam soil. Similarly, five additional JETs were performed each at two different head settings of 46 (H1) cm and 79 cm (H3) on the clay loam soil. For each test, the same mini-JET device was used and a strict protocol was applied to collect the data. As per the protocol, an initial reading was taken before wetting of the surface. Then, gauge readings were taken every 15 s. The reading time interval was increased to 30 s when two consecutive gauge readings had the same value. The reading interval was increased in a similar fashion to 60 s, 120 s, and 300 s. The test was terminated when the same value was recorded for two gauge readings at a 300 s interval (Figure 2.2a). The erodibility parameters were estimated from the additional JETs with the aforementioned techniques. Analysis of variance (ANOVA) was performed to quantify statistical difference across the three different head settings on the erodibility parameters. Pairwise comparison tests were performed on the erodibility parameters shown to be significantly different by ANOVA at a significance level of $\alpha = 0.05$.

In order to test the influence of the initial time interval, existing JET data conducted at the lowest (46 cm) and highest (109 cm) head settings were resampled at four different initial time intervals of 30 s, 60 s, 120 s, and 240 s. A shorter initial time interval results in collection of more early time data during the mini-JET when scouring

is most rapid (Figures 2.2a, 2.2b, and 2.2c). Resampling was accomplished by extracting a subset of original data in whichthe gauge readings recorded at each of these initial intervals were retained. For example, to resample the data at 60 s intervals, only the gauge readings recorded at intervals of 60 s or higher were retained in the resampled data (Figure 2.2b). Resampled data were analyzed using the spreadsheet tool and the erodibility parameters were estimated again. Similarly, in order to test the influence of the termination time interval at which the tests are completed, existing JET data conducted at lowest and highest head settings were resampled so that they were completed at three different intervals of 120 s, 60 s, and 30 s instead of the original 300 s. A shorter termination time corresponded to a shorter duration mini-JET and a shallower scour hole (Figures 2.2d, 2.2e, and 2.2f). This was accomplished by extracting a subset of original data which retained the data recorded before the recording interval reached each of these intervals. For example, to resample the data for termination interval of 60 s, only guage readings recorded before the collection interval reached 60s were retained and rest of the data was left out in the resampled data (Figure 2.2e). ANOVA was used to assess the statistical significance of these factors at $\alpha = 0.05$.

Results and Discussion

Variability of Erodibility Parameters

Mini-JET variability under controlled laboratory conditions was much smaller than reported in field studies on the same soils (Daly et al., 2015a). In general, the variability in the erodibility parameters for the clay loam soil was greater than the variability for the sandy loam soil for both the linear and nonlinear models (Figure 2.3a). The parameters of the non-linear model were more variable than the parameters of the

linear model (Figure 2.3b). Also similar to previous research findings, τ_c estimated from BL ($\tau_{c\text{-}BL}$) and k_d estimated from BL ($k_{d\text{-}BL}$) were two and one order of magnitude smaller than the corresponding parameters estimated by the SD and IT solutions, respectively (Figure 2.3a).

The AD tests suggested normal distributions for all but one of the derived erodibility parameters for sandy loam soil, and log normal distributions for most of the erodibility parameters for the clay loam soil (Table 2.2). Therefore, a normal distribution for sandy loam soil and log normal distributions for clay loam soil were assumed in calculating sample sizes required to appropriately characterize the erodibility parameters' distributions. The sample sizes required for deriving the erodibility parameters at a confidence level of 95% and precisions of 5%, 10% and 25% are provided in Table 2.3. Conducting three to five JETs to quantify the erodibility of a soil in the laboratory will typically provide a good estimate of the mean with 25% precision at a 95% confidence. Estimating erodibility parameters for the clay loam soil required larger sample sizes than for the sandy loam soil for both linear and nonlinear models. Using SD and IT solution techniques typically reduced the sample sizes, especially for τ_c.

Charanko et al. (2010) conducted 11 original JETs on a clay loam soil under laboratory conditions. They reported an average $\tau_{c\text{-}BL}$ of 0.48 Pa with precision of 59% and average $k_{d\text{-}BL}$ of 2.3 $cm^3N^{-1}s^{-1}$ with 19% precision. They concluded the original JETs in the laboratory to be repeatable with a smaller variation in comparison to field original JETs. It should be noted that the $\tau_{c\text{-}BL}$ estimated from the original JET in the Charanko et al. (2010) study on clay loam soils was one order of magnitude greater than that estimated from the mini-JETs on the clay loam soil in this study. Al-Madhhachi et al.

(2013a) made similar observations. They hypothesized that the difference in scales of the original JET and mini-JET was the reason for the difference and introduced an adjustment coefficient to match the $\tau_{c\text{-}BL}$. Recent research by Ghaneeized et al. (2015) on the original JET hypothesized that confinement may be an issue with the original JET assumptions. They developed a semi-empirical equation to predict the applied τ for the original JET and suggested the apparatus coefficients and equation to be reevaluated for the confined conditions of both the original and mini-JETs.

The laboratory mini-JETs reported herein showed much less variability than reported in field studies such as the Daly et al. (2015a) study. Daly et al. (2015) observed variability of approximately three orders of magnitude in the erodibility parameters. Other researchers report similar findings with original JETs under in-situ conditions (Wynn et al., 2008; Karmaker and Dutta, 2011). In fact, variability of the erodibility parameters estimated from the laboratory mini-JETs was two to three orders of magnitude less than those estimated from mini-JET field tests. The expected deviation in erodibility parameters from the mean value was much smaller for the laboratory mini-JETs (Table 2.4). The average values of k_d derived from the laboratory mini-JETs on disturbed and repacked soil samples and the in-situ field mini-JETs were remarkably similar. It should also be noted that Daly et al. (2015a) conducted the field mini-JETs at much larger head setting (244 cm) than the laboratory mini-JETs (106 cm). Factors like heterogeneity in soil texture, disturbance and repacking, moisture content, bulk density, and presence of roots along with the different head setting all contribute to the differences in estimation of erodibility parameters between the field and laboratory mini-JETs. However, the similarity in the average erodibility parameters and smaller variability

suggested that the laboratory mini-JETs were valuable for quantifying the expected erodibility properties.

Pressure Head Setting

The mini-JETs were carried out with three distinct head setting in this study. General properties of the jet hydraulics are given in Table 2.5. The influence of the head setting on J_e was statistically significant for both soil types and for all three solution techniques (P-values < 0.01). The average J_e increased consistently with increased head for both soil types and all solution techniques. The increase in J_e with respect to applied pressure head was larger for the BL technique. The sandy loam soil showed a larger increase in J_e with increase in head setting. The SD and IT techniques showed a similar increase in J_e with increase in head setting for both soils.

ANOVA showed $\tau_{c\text{-}BL}$, $\tau_{c\text{-}SD}$ and $\tau_{c\text{-}IT}$ parameters of the sandy loam soil were significantly different across different head settings (P-values < 0.01) (Figure 2.4). Pairwise comparison tests showed that $\tau_{c\text{-}BL}$ at H1 was significantly larger than $\tau_{c\text{-}BL}$ at H2 and H3. The $\tau_{c\text{-}SD}$ and $\tau_{c\text{-}IT}$ at H3 were significantly larger than the parameters at H1 and H2. The $\tau_{c\text{-}SD}$ and $\tau_{c\text{-}IT}$ of the sandy loam soil increased when using larger applied pressure heads.

No general pattern was observed relative to the influence of head setting on the erodibility parameters of the clay loam soil (Figure 2.5). This was probably due to the magnitude of variability in erodibility parameters observed during the laboratory mini-JETs. ANOVA showed $k_{d\text{-}SD}$, $k_{d\text{-}IT}$ and $\tau_{c\text{-}SD}$ parameters of the clay loam were significantly different across the head settings (P-values < 0.01) (Figure 2.5). Pairwise comparison tests showed $k_{d\text{-}SD}$ at H2 to be significantly larger than $k_{d\text{-}SD}$ at H3, but no significant

differences were observed between the other two pairs (H1-H2 and H1-H3). Similarly, $k_{d\text{-}IT}$ at H1 was significantly larger than $k_{d\text{-}IT}$ at H2 but no significant differences were observed between other pairs of head settings. The $\tau_{c\text{-}SD}$ at H2 was significantly larger than $\tau_{c\text{-}SD}$ at H3 but no significant differences were observed between the other two pairs of head settings (H1-H2 and H1-H3).

No general pattern was observed between the nonlinear erodibility parameters and the head setting (Figure 2.6). The b_1 of the sandy loam soil was significantly larger at H3 than at H1. No significant differences in b_1 were observed between other two pairs of head settings. Similarly, b_0 for the clay loam soil was significantly larger at H2 than at H1, but no significant differences were observed in b_1 between the other two pairs of head settings. The b_1 parameter of the clay loam soil was observed to be significantly larger at H2 and H3 (Figure 2.6). These observations are again influenced by the magnitude of variability in parameters of the nonlinear model, especially for the clay loam soil.

These analyses by themselves suggest that the head setting within the range used in this study do not make substantial difference in the values of estimated erodibility parameter and therefore may be appropriate for mini-JETs. Hanson et al. (1990) noted the need to conduct original JETs at a head setting that mimics the range of applied τ expected in the field, but this is not always possible for erodible soils typical of many streambanks expecting rapid erosion and migration. Furthermore, the estimation of the erodibility parameter is highly dependent on the quality and quantity of data itself. Hence, it is necessary to examine the interaction effect of head setting relative to the data collection intervals and length of the test.

Initial Time Interval

For the more erodible sandy loam soil, the initial time interval influenced the estimation of erodibility parameters (Figure 2.2a, 2.2b, and 2.2c). The average $\tau_{c\text{-}BL}$ increased with longer initial time intervals at H1, and this trend was observed to be more pronounced when using a larger applied pressure head, H3 (Figure 2.7). When a shorter initial time interval was used more early time data was available closer to the vertex of the hyperbolic function in equation (2.2). This shifted the asymptotes of the hyperbola away from the curve and increased the estimate of f_0, which in turn increased the estimated J_e. This effect ultimately resulted in smaller $\tau_{c\text{-}BL}$ at shorter initial time intervals. The range of $\tau_{c\text{-}BL}$ predicted with five mini-JETs differed significantly from the range of the parameter predicted with larger sample size of 20 mini-JETs when the initial time interval was greater than 30 s. The $k_{d\text{-}BL}$ decreased marginally with an increase in initial time interval, which was attributed to the fit of t versus t_m in equation (2.3). The average and range in $k_{d\text{-}SD}$ decreased significantly with longer initial time intervals for the more erodible sandy loam soil. This trend was observed at both smaller and larger head settings but was more prominent at the larger head setting, H3 (Figure 2.7). The scour depth method requires averaging of depths recorded at each interval in order to predict erosion rate. Averaging across smaller initial time intervals predicted greater erosion rates than averaging across larger initial time intervals. Hence, smaller erosion rates were estimated at the same τ when longer initial time intervals were used. This resulted in smaller estimated $k_{d\text{-}SD}$ values. The $k_{d\text{-}SD}$ values predicted with five mini-JETs in this analysis were significantly smaller than those values estimated from 20 mini-JETs when the initial time interval was increased to 30 s. The $\tau_{c\text{-}SD}$ was not significantly influenced by initial

time interval as the final scour depth did not change with the initial time interval for this analysis technique. The $\tau_{c\text{-}IT}$ decreased marginally with increased initial time intervals and stabilized at initial time intervals longer than 60 s. This was due to slight differences in the fit of the data as more data points were available at smaller initial time intervals. No significant influence of the initial time interval was observed on $k_{d\text{-}IT}$.

For the less erodible clay loam soil, the influence of the initial time interval was also dependent on the head setting. A significant influence of starting time interval was not observed at H1; however, at H3, $\tau_{c\text{-}BL}$ decreased significantly with longer initial time intervals (Figure 2.8). This was attributed to more data points on the vertex end of the hyperbola at smaller initial time intervals. Unlike the sandy loam soil, the greater number of data points closer to the vertex end of the hyperbola shifted the asymptotes closer to the vertex decreasing the value of $f_{0.}$ This also decreased the value of estimated J_e and ultimately increased the estimated $\tau_{c\text{-}BL}$ at smaller initial time intervals. The $k_{d\text{-}BL}$ was not influenced by the initial time interval as the fit of t versus t_m in equation (2.3) remained same across the initial time intervals. The fit between t and t_m was significantly better for the clay loam soil than the sandy loam soil. The $k_{d\text{-}SD}$ and $\tau_{c\text{-}SD}$ decreased slightly, especially at longest time intervals of 120 s and 240 s. The effect on $k_{d\text{-}SD}$ was attributed to less available data when resampled at time intervals of 120 s and 240 s. The $k_{d\text{-}IT}$ and $\tau_{c\text{-}IT}$ were equivalent at all initial time intervals as the final scour depth of the tests did not change with the initial time intervals.

For the nonlinear detachment model, the b_0 decreased with longer initial time intervals for both the more erodible sandy loam and less erodible clay loam soils at both H1 and H3 (Figure 2.9). The b_1 for the clay loam soil decreased with longer initial time

intervals only at H3. Both b_0 and $k_{d\text{-}SD}$ decreased with increased initial time interval; note that both the SD solution and Wilson model were based on same solution concept, and therefore the reasons for the observed changes in the Wilson Model parameters were equivalent to those previously described for the SD solution.

Termination Time Interval

For the sandy loam soil, the termination time interval highly influenced the variation in the erodibility parameters derived using the BL solution ($\tau_{c\text{-}BL}$ and $k_{d\text{-}BL}$) and was most pronounced for H3, as shown in Figure 2.10. The $k_{d\text{-}BL}$ decreased with longer termination intervals, and $\tau_{c\text{-}BL}$ increased with longer termination intervals. Longer termination intervals added data on the hyperbola towards its extremity which shifted the asymptotes towards the curve and decreased the value of f_0. This decreased the estimated J_e and consequently increased the $\tau_{c\text{-}BL}$. The range of $\tau_{c\text{-}BL}$ predicted with five mini-JETs was observed to be closest to the range of $\tau_{c\text{-}BL}$ predicted from sample size of 20 mini-JETs when the termination time interval was 300 s. Running mini-JETs to termination intervals of 300 s was necessary for obtaining the most precise estimates of $\tau_{c\text{-}BL}$ on these soils. The $k_{d\text{-}BL}$ decreased marginally with increased termination time intervals, which was attributed to the fit of t versus t_m in equation (2.3). Most of the scouring of the sandy loam soil occurred early and erosion rates became insignificant as the termination interval increased. There was no significant difference in the scour depth at later times. This caused the $\tau_{c\text{-}SD}$ to vary marginally with the termination time interval. The variability of $\tau_{c\text{-}SD}$ was smaller with an increase in termination time interval (Figure 2.10e). The termination time interval had no influence on the estimated $k_{d\text{-}SD.}$ Therefore, if early time data are available and indicate the general trend between scour depth and time, the

termination time interval will have less influence on the derived parameters of more erodible soils for the SD solution technique.

The influence of the termination time interval was more pronounced for the less erodible clay loam soil. The $k_{d\text{-}BL}$ decreased rapidly with longer termination time intervals at both H1 and H3, and the $\tau_{c\text{-}BL}$ showed similar trends at H3 (Figure 2.11). At a larger head, the scouring of the sample continued for a longer time. This added more data points on the hyperbola towards its extremity. Unlike in case of the sandy loam soil, this shifted the asymptotes away from the curve increasing the f_0 ordinate. Consequently, the J_e values increased and the $\tau_{c\text{-}BL}$ decreased. At smaller heads, this effect was not strong enough to significantly decrease the value of $\tau_{c\text{-}BL}$, but the variability in estimation of $\tau_{c\text{-}BL}$ did decrease at longer termination intervals. The $k_{d\text{-}SD}$ and $\tau_{c\text{-}SD}$ decreased significantly with longer termination time intervals at H1. This was attributed to the fact that the depth of the scour hole continued to increase at longer termination times. This increased the concentration of data points at smaller τ and smaller erosion rates, which consequently decreased the slope as well as the x-intercept of the linear model. The $k_{d\text{-}IT}$ and $\tau_{c\text{-}IT}$ were strongly influenced by termination interval both at H1 and H3, rapidly decreasing at longer termination time intervals. This was expected as the final depth of the scour hole, which was assumed as J_e by the IT method, continued to increase with the duration of the test. This significantly decreased the $\tau_{c\text{-}IT}$. The fit of t versus t_m was also observed to change with the termination time interval. The deviation between t and t_m increased with longer termination time intervals decreasing the $k_{d\text{-}IT}$ values.

For the nonlinear model, most of the erodibility parameters for the two soils were significantly impacted by termination time interval based on statistical tests (Figure 2.12),

but with much less noticeable effects compared to the linear model. At H3, both b_0 and b_1 for the clay loam soil decreased with longer termination time intervals while the b_1 for the sandy loam soil changed nominally (Figure 2.12). The nonlinear model uses the same solution procedure as the scour depth model. The smaller b_0 and b_1 values of the clay loam soil can be explained by the concentration of data points at smaller τ and smaller erosion rates.

Summary and Conclusions

Mini-JETs were performed on remolded samples of two distinct soil types under controlled laboratory conditions to quantify the variability of erodibility parameters of linear and nonlinear detachment models. The tests controlled for soil texture, compaction density, moisture content, applied pressure, and data collection protocol. The tests revealed that the erodibility parameters of the more erodible sandy loam soil were much less variable than the less erodible clay loam soil. In general, the erodibility parameters of the linear model were estimated with the least variability when using the SD solution technique. The b_0 parameter of the nonlinear model was more variable than the corresponding k_d in the linear excess shear stress model, with similar variability between b_1 and τ_c. A comparison to previously published field tests showed that the average values of the parameters of the linear model, especially k_d, from laboratory tests were remarkably similar to those predicted from in-situ mini-JETs in the field. Laboratory mini-JETs on disturbed and repacked soil samples may be used to establish benchmark values of the erodibility parameters. Variability of the erodibility parameters estimated from the laboratory tests was two to three orders of magnitude less than those estimated from the field tests. Conducting three to five mini-JETs to quantify the erodibility of a

soil in the laboratory will typically provide a good estimate of the mean with 25% precision at a 95% confidence. No specific patterns were observed in terms of the influence of the selected applied pressure head and the derived erodibility parameters. However, when the effect of the applied head setting was coupled with the initial time interval and termination time interval of data collection during the mini-JET, certain patterns emerged. For example, selection of the initial and termination time intervals were most influential at larger applied pressure heads. An initial time interval of at least 30 s is recommended for mini-JETs for easily erodible sandy soils; on less erodible soils, a time interval of 30 s may yield no scour and therefore longer time intervals will need to be used. A smaller applied head is preferred to a larger applied head from a data analysis perspective; however, one must also ensure that the applied head is representative of the expected applied shear stress to be modeled or predicted with the derived erodibility parameters. Hence, a termination time interval of 300 s is recommended for less erodible soils if circumstances require the use of larger applied pressure heads.

Acknowledgements

The authors acknowledge the financial support of the Buchanan Family Trust through the Buchanan Endowed Chair and the Oklahoma Agricultural Experiment Station at Oklahoma State University. This project was also supported by Agriculture and Food Research Initiative Competitive Grant no. 2013-51130-21484 from the USDA National Institute of Food and Agriculture and through a FY 2012 319(h) Special Project #C9-00F56701.

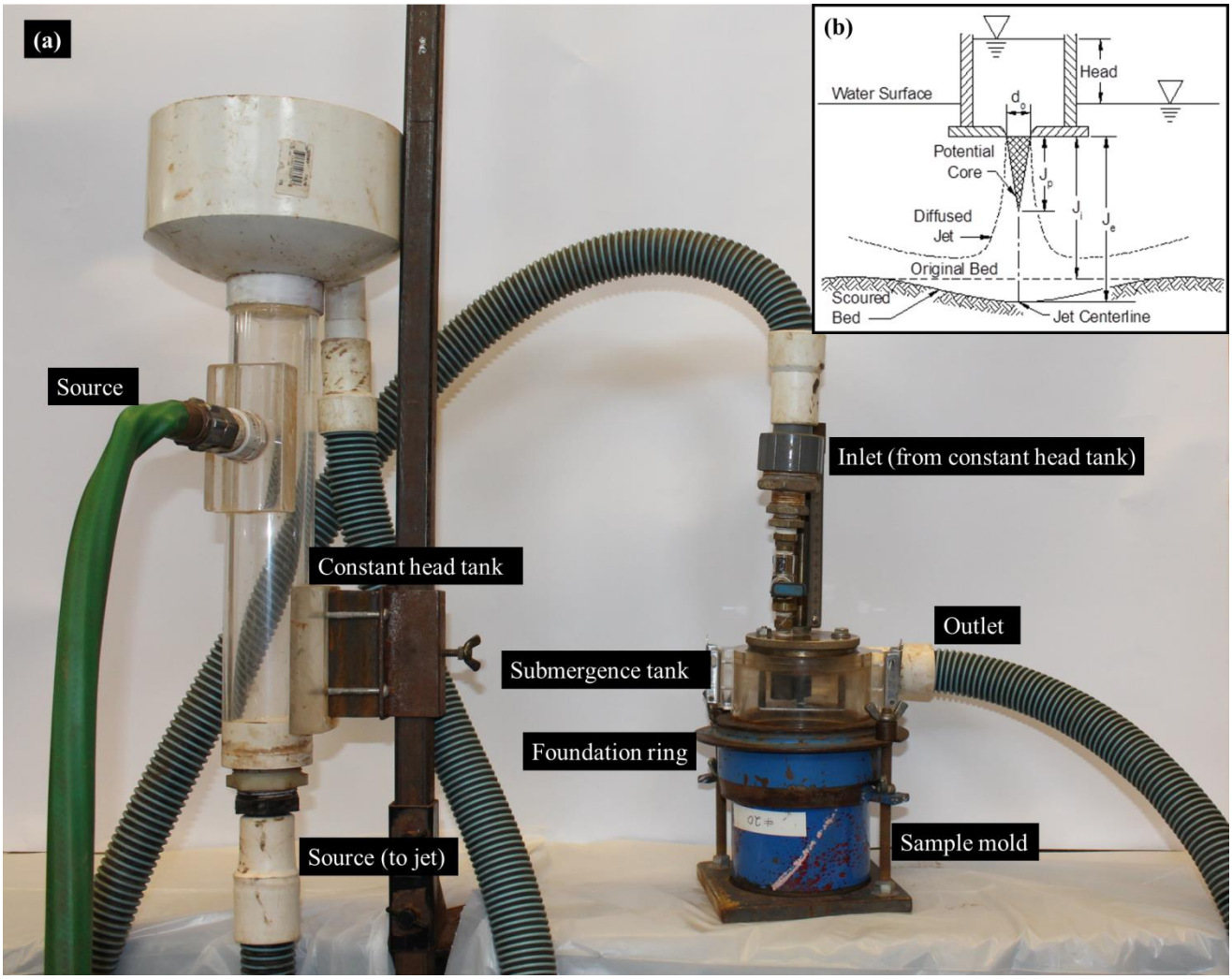

Figure 2.1. (a) Illustration of submerged JET setup and (b) water jet and scour depth parameters used by Hanson and Cook (2004).

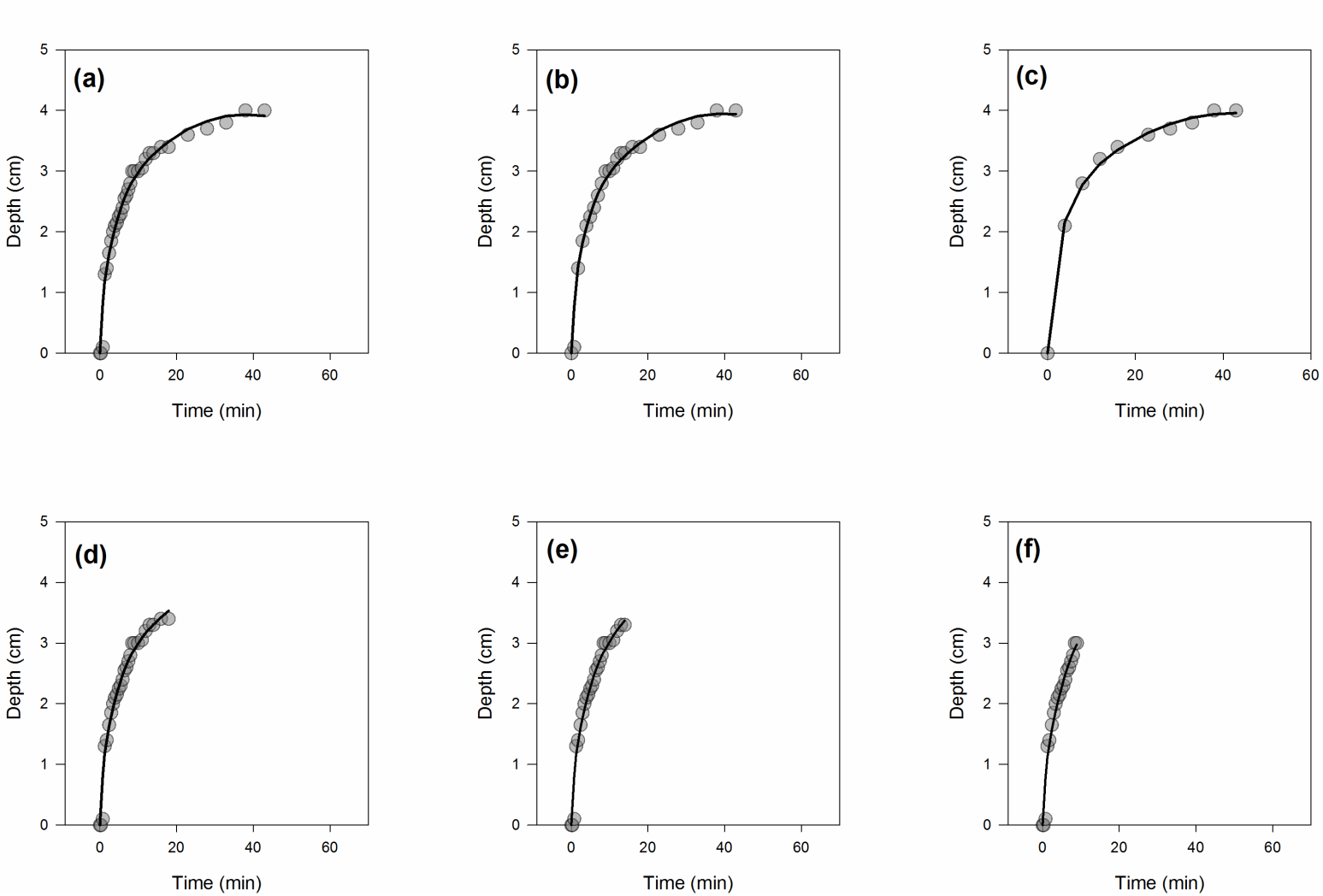

Figure 2.2. Sample data collected for clay loam soil at (a) original initial time interval of 15 s and termination time interval of 300 s and resampled data at (b) initial time interval of 60 s, (c) initial time interval of 240 s, (d) termination time interval of 120 s, (e) termination time interval of 60 s, and (f) termination time interval of 30 s; solid lines depicts the predicted scour depth using the scour depth method.

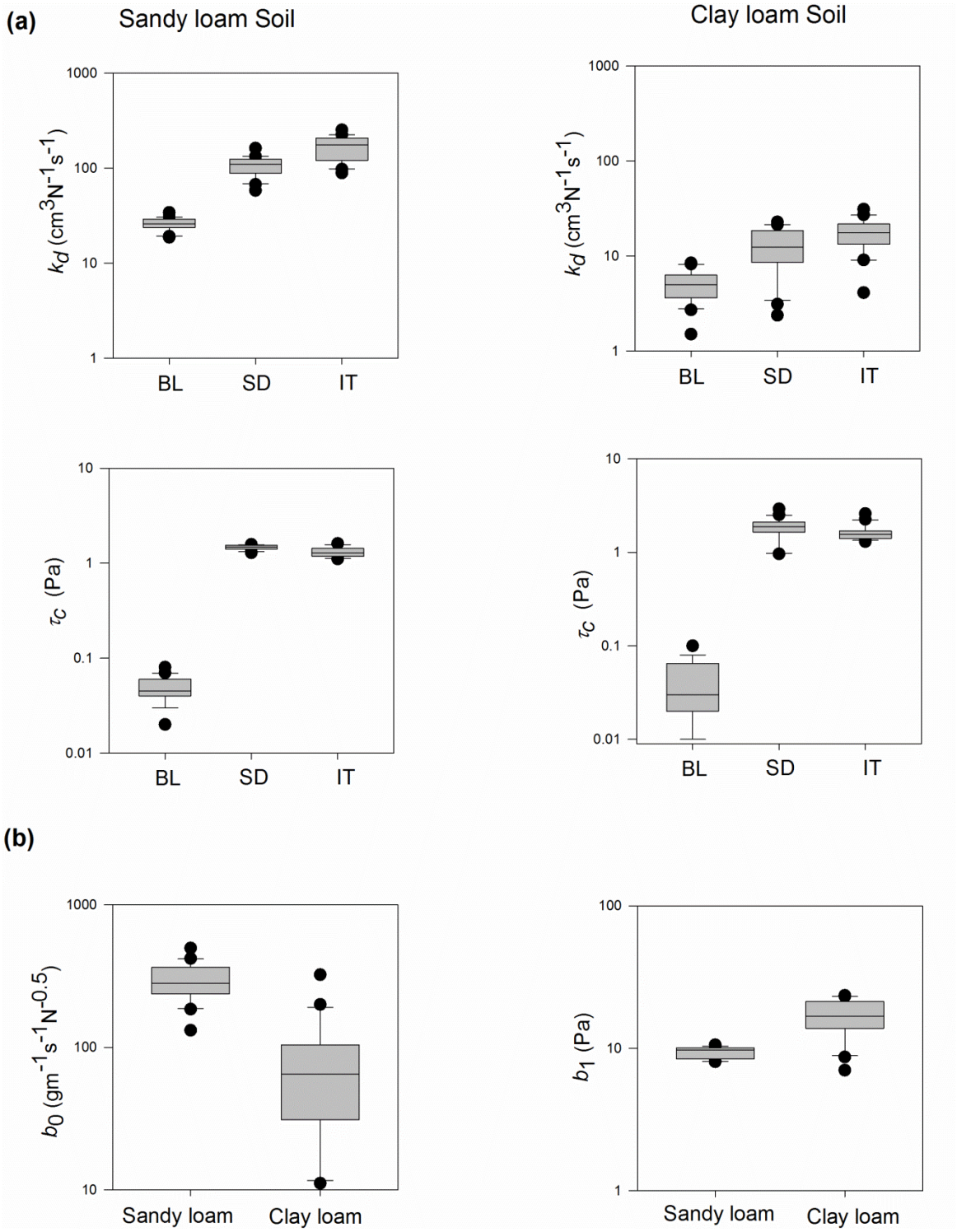

Figure 2.3. Derived erodibility parameters from laboratory mini-JETS for the (a) linear detachment model (τ_c is the critical shear stress and k_d is the erodibility coefficient) and (b) nonlinear detachment model (b_0 and b_1 are nonlinear detachment model parameters). BL = Blaisdell, SD = scour depth, and IT = iterative solution

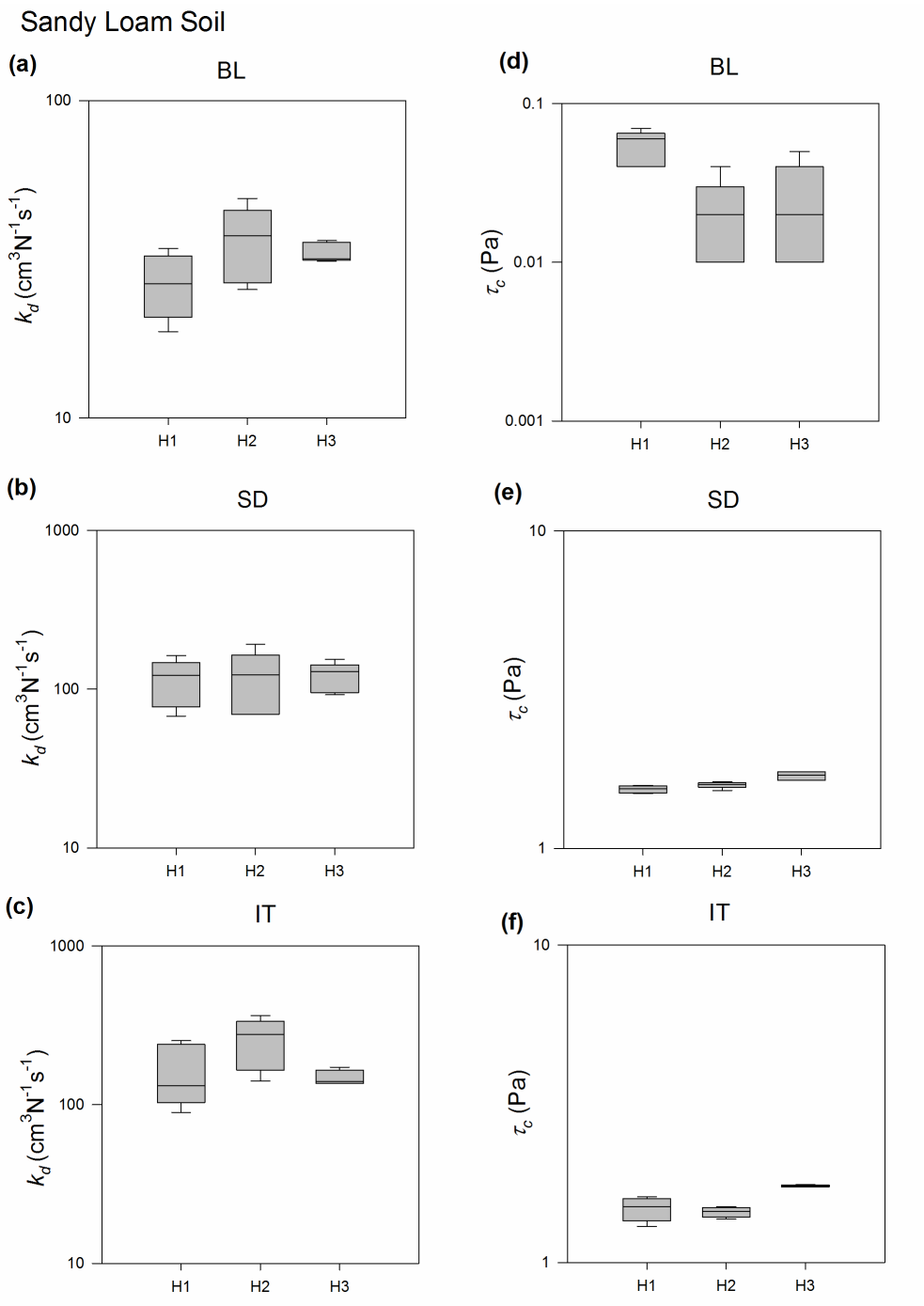

Figure 2.4. Linear detachment model erodibility parameters (τ_c is the critical shear stress and k_d is the erodibility coefficient) derived from mini JETs at head settings of H1 (46 cm), H2 (79 cm), and H3 (109 cm) for sandy loam soil. BL = Blaisdell solution, SD = scour depth solution, and IT = iterative solution. Note that (a), (b) and (c) depict same variable but vertical scales of (b) and (c) are different from (a). The same applies for (d), (e) and (f). This was necessary as BL derived erodibility parameters were typically one order of magnitude lower than SD and IT derived parameters.

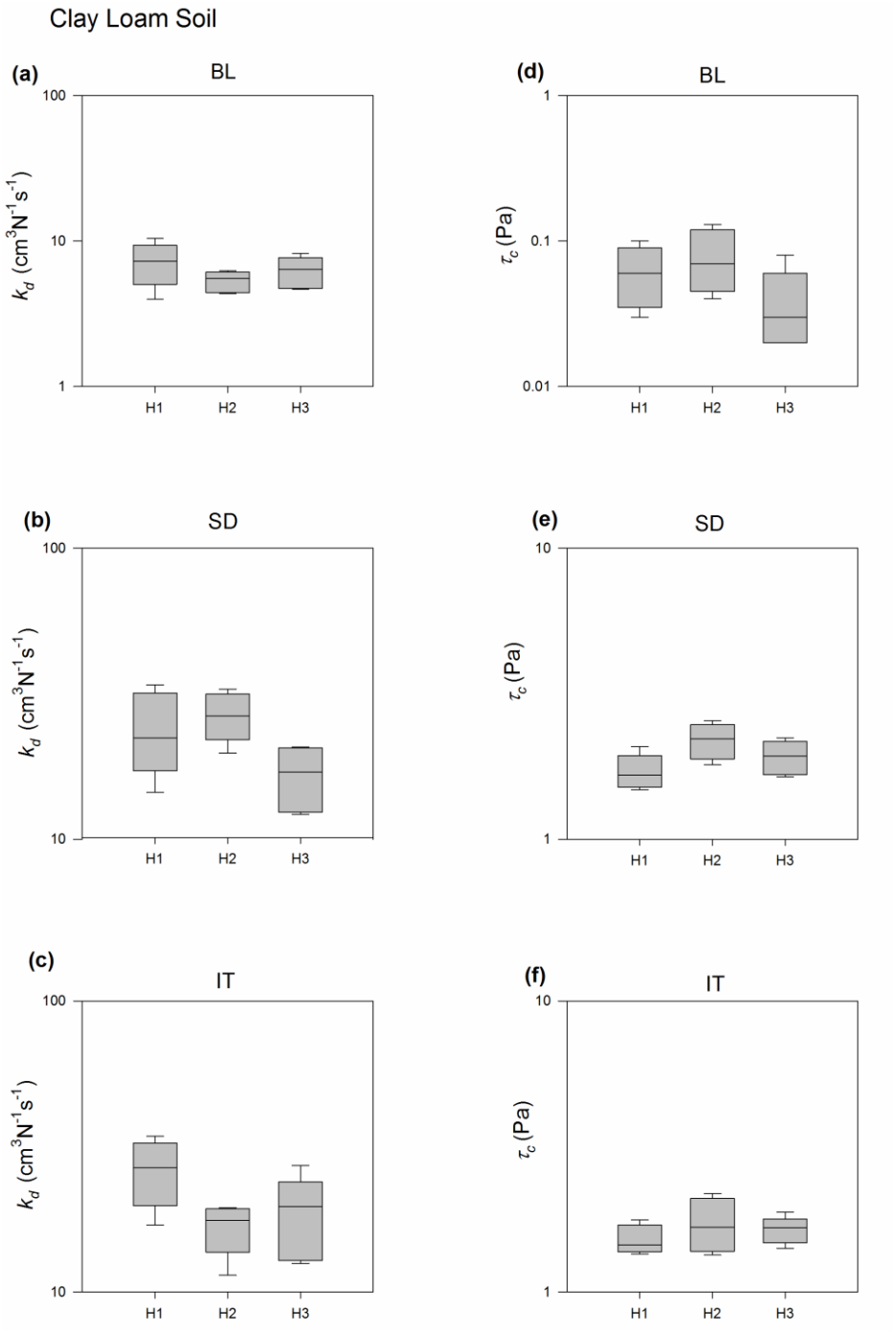

Figure 2.5. Linear detachment model erodibility parameters (τ_c is the critical shear stress and k_d is the erodibility coefficient) derived from mini JET at head settings of H1 (46 cm), H2 (79 cm), and H3 (109 cm) for the clay loam soil. BL = Blaisdell solution, SD = scour depth solution, and IT = iterative solution. . Note that (a), (b) and (c) depict same variable but vertical scales of (b) and (c) are different from (a). The same applies for (d), (e) and (f). This was necessary as BL derived erodibility parameters were typically one order of magnitude lower than SD and IT derived parameters

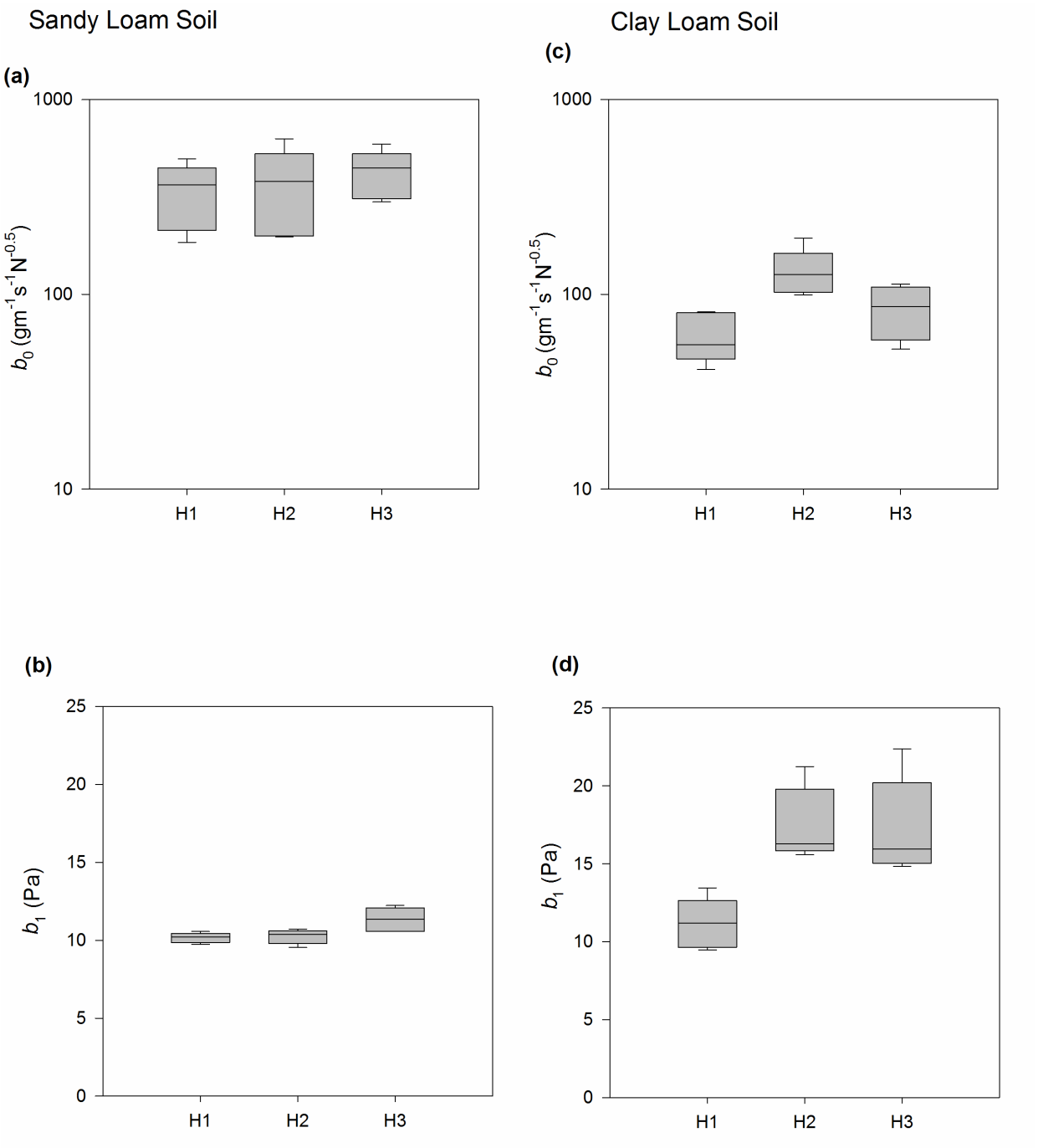

Figure 2.6. Nonlinear detachment model erodibility parameters (b_0 and b_1) derived from mini JETs at head settings of H1 (46 cm), H2 (79 cm), and H3 (109 cm).

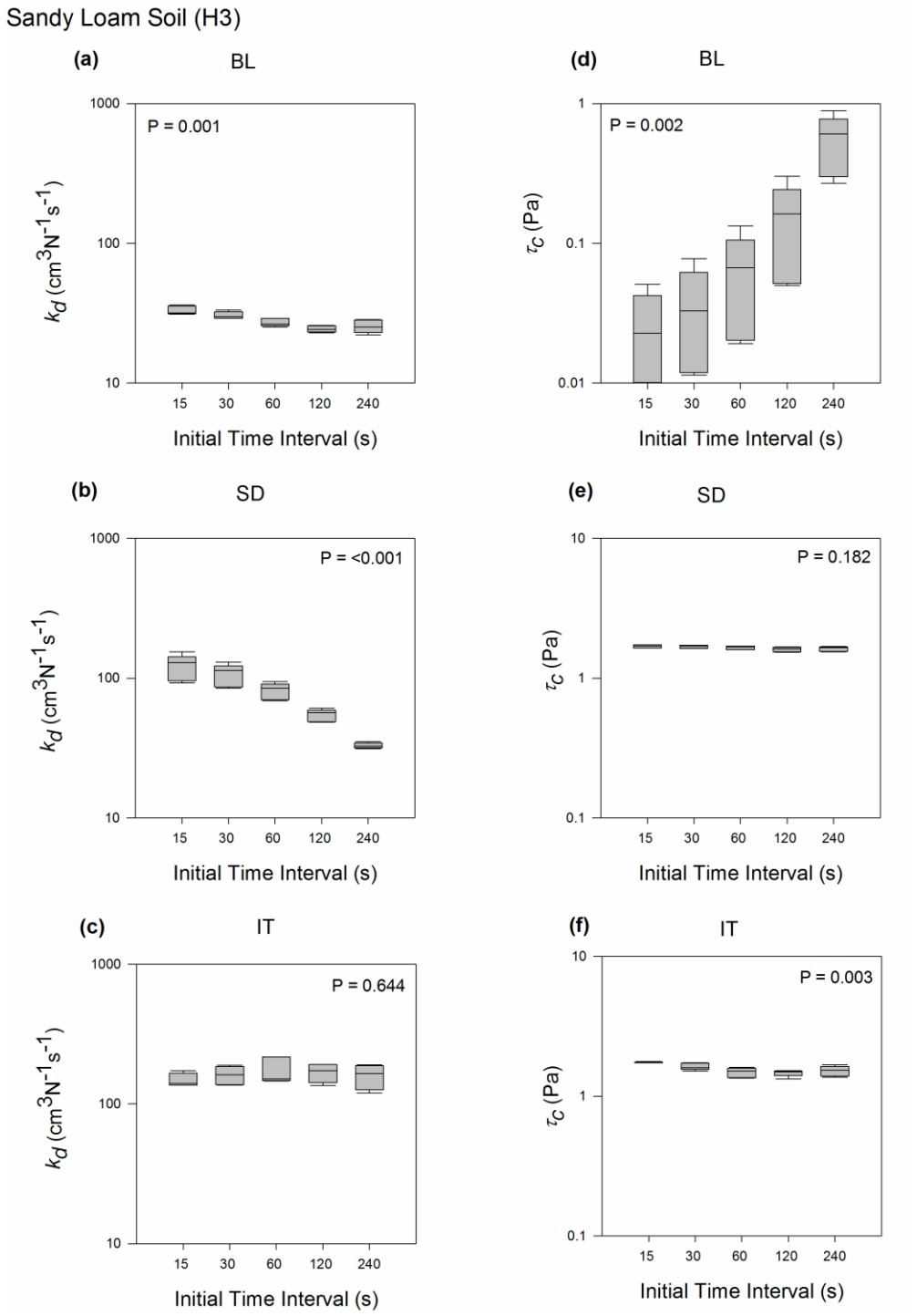

Figure 2.7. Influence of initial time interval of data collection on linear detachment model erodibility parameters (τ_c is the critical shear stress and k_d is the erodibility coefficient) derived from mini JETs for sandy loam soil at H3 (109 cm). BL = Blaisdell solution, SD = scour depth solution, and IT = iterative solution. Note that (d), (e) and (f) depict same variable but vertical scales of (b) and (c) are different from (a). This was necessary as $\tau_{c\text{-BL}}$ was typically one order of magnitude lower than $\tau_{c\text{-SD}}$ and $\tau_{c\text{-IT}}$.

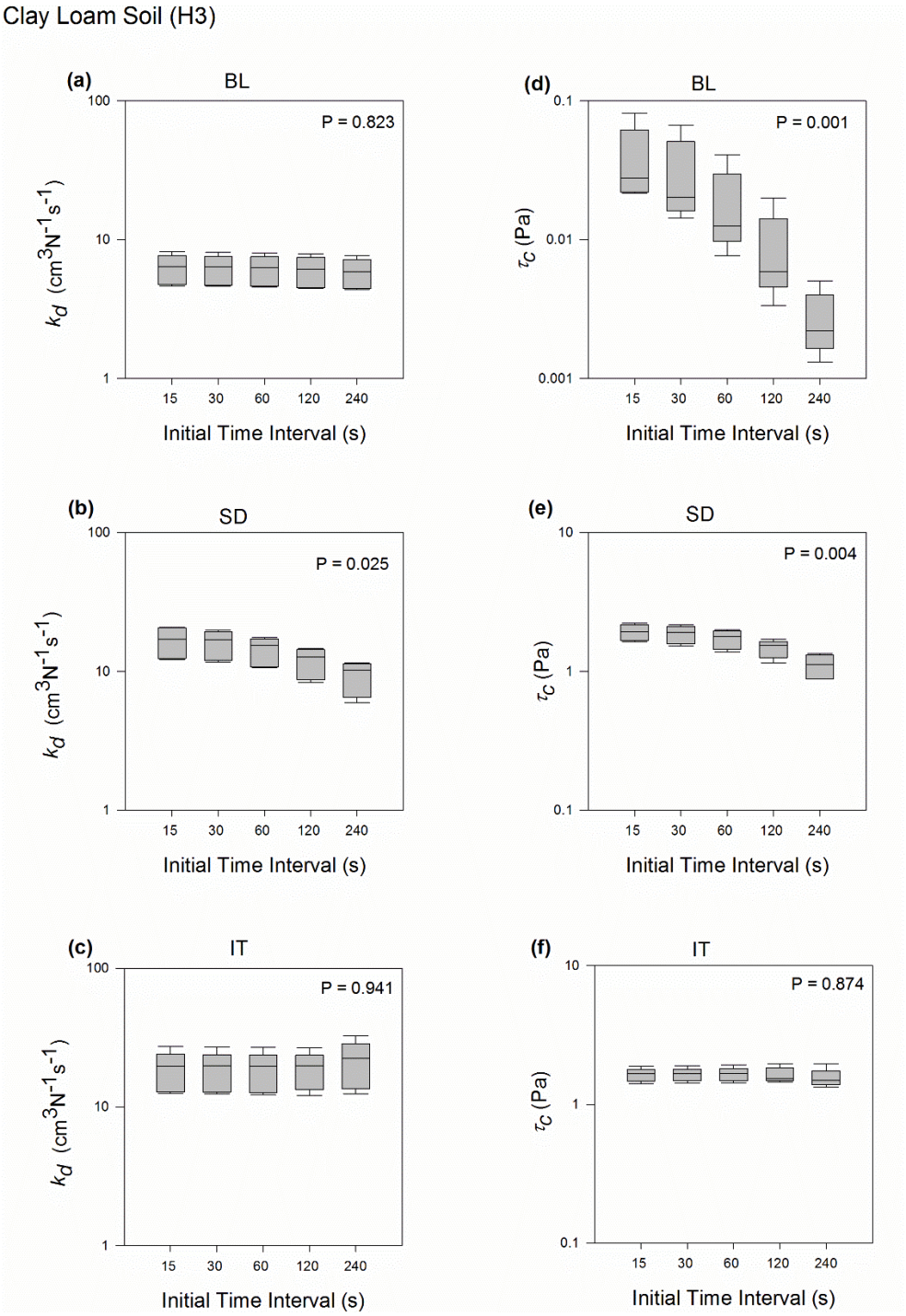

Figure 2.8. Influence of initial time interval of data collection on linear detachment model erodibility parameters (τ_c is the critical shear stress and k_d is the erodibility coefficient) derived from mini JETs for clay loam soil at H3 (109 cm). BL = Blaisdell solution, SD = scour depth solution, and IT = iterative solution. Note that (d), (e) and (f) depict same variable but vertical scales of (b) and (c) are different from (a). This was necessary as $\tau_{c\text{-BL}}$ was typically one order of magnitude lower than $\tau_{c\text{-SD}}$ and $\tau_{c\text{-IT}}$.

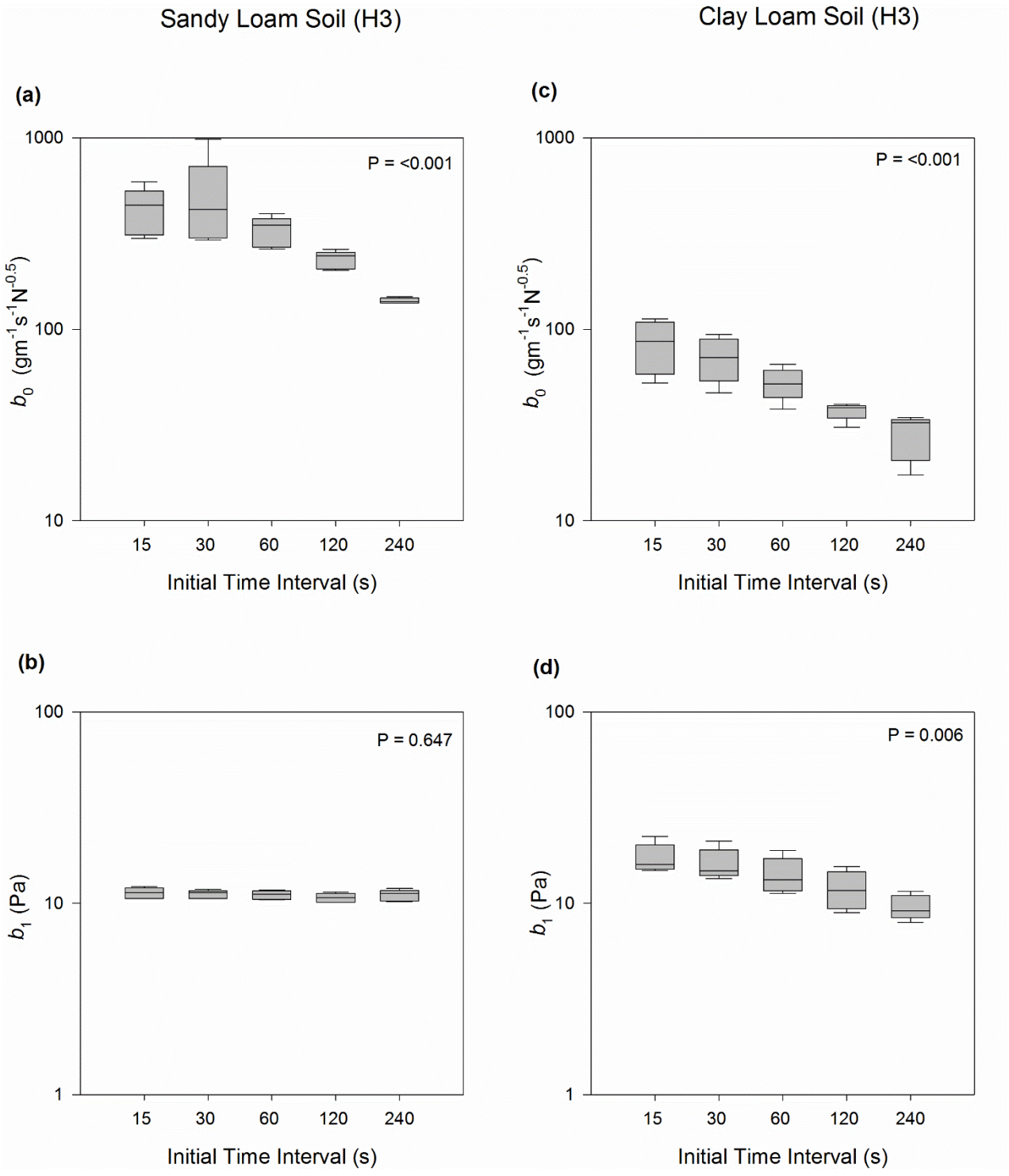

Figure 2.9. Influence of initial time interval of data collection on nonlinear detachment model erodibility parameters (b_0 and b_1) derived from mini JETs for the sandy loam and clay loam soils at H3 (109 cm).

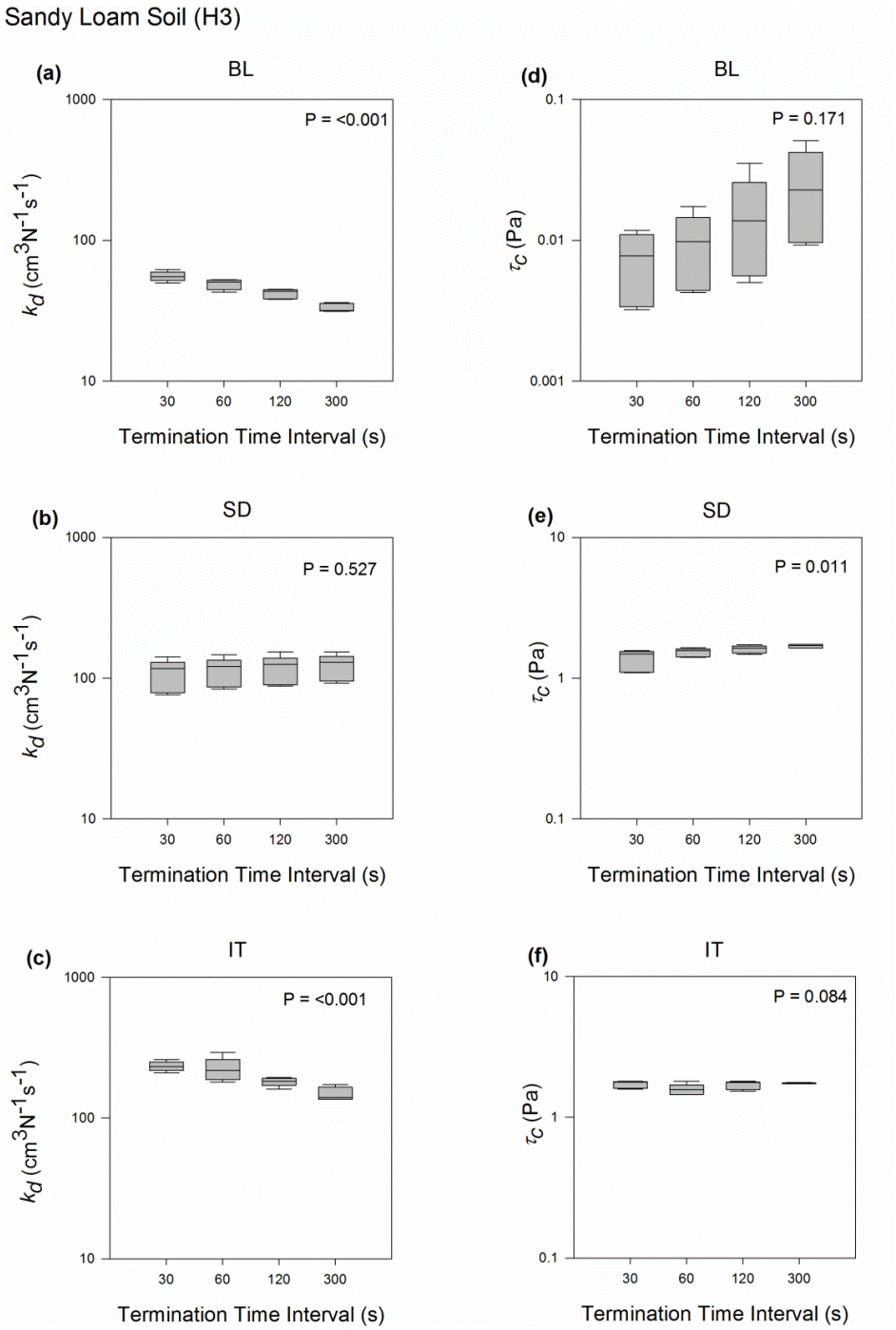

Figure 2.10. Influence of termination time interval of data collection on linear detachment model erodibility parameters (τ_c is the critical shear stress and k_d is the erodibility coefficient) derived from mini JETs for the sandy loam soil at H3 (109 cm). BL = Blaisdell solution, SD = scour depth solution, and IT = iterative solution. Note that (d), (e) and (f) depict same variable but vertical scales of (b) and (c) are different from (a). This was necessary as $\tau_{c\text{-BL}}$ was typically one order of magnitude lower than $\tau_{c\text{-SD}}$ and $\tau_{c\text{-IT}}$.

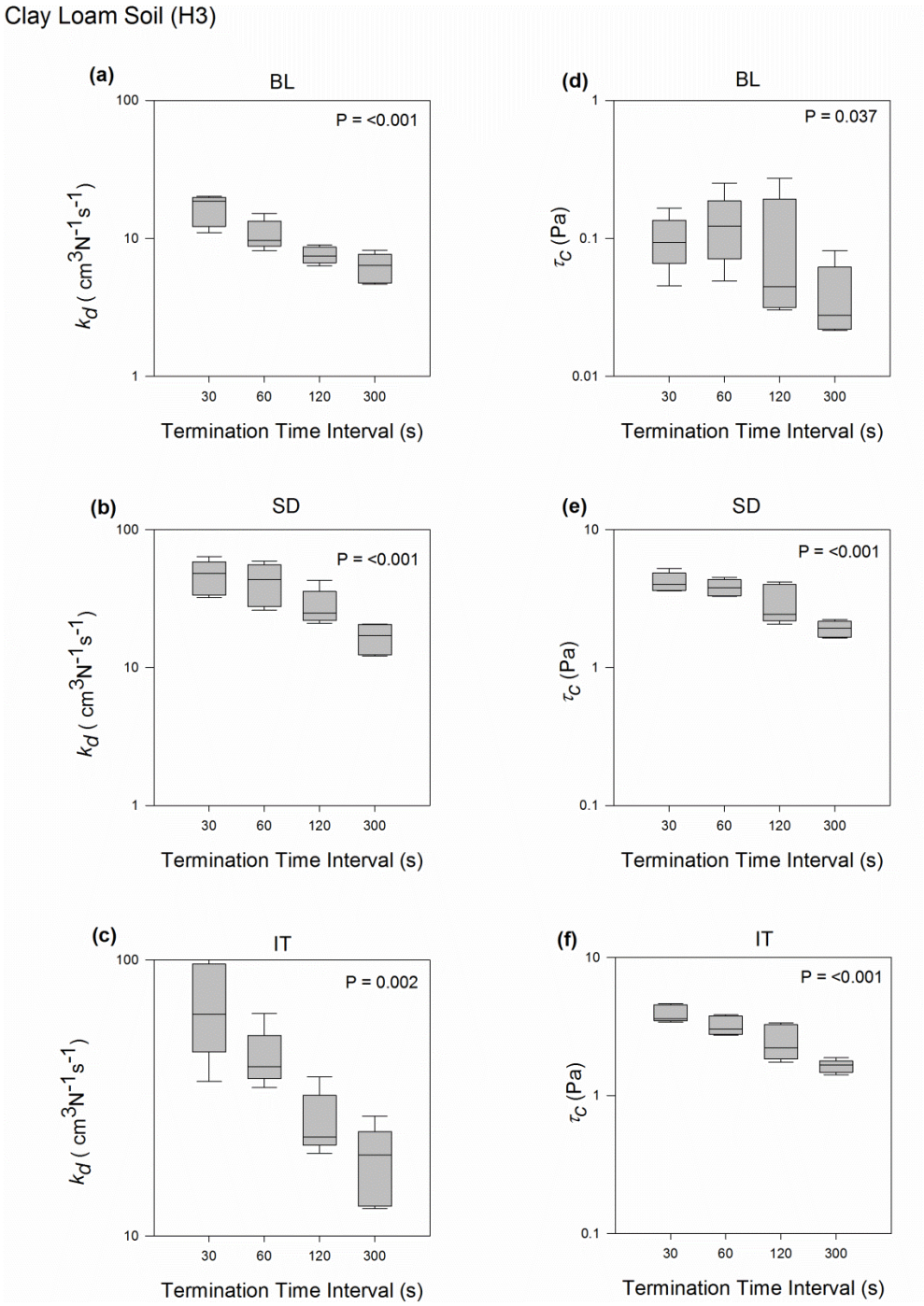

Figure 2.11. Influence of termination time interval of data collection on linear detachment model erodibility parameters (τ_c is the critical shear stress and k_d is the erodibility coefficient) derived from mini JETs for the clay loam soil at H3 (109 cm). BL = Blaisdell solution, SD = scour depth solution, and IT = iterative solution. Note that (d), (e) and (f) depict same variable but vertical scales of (b) and (c) are different from (a). This was necessary as $\tau_{c\text{-BL}}$ was typically one order of magnitude lower than $\tau_{c\text{-SD}}$ and $\tau_{c\text{-IT}}$.

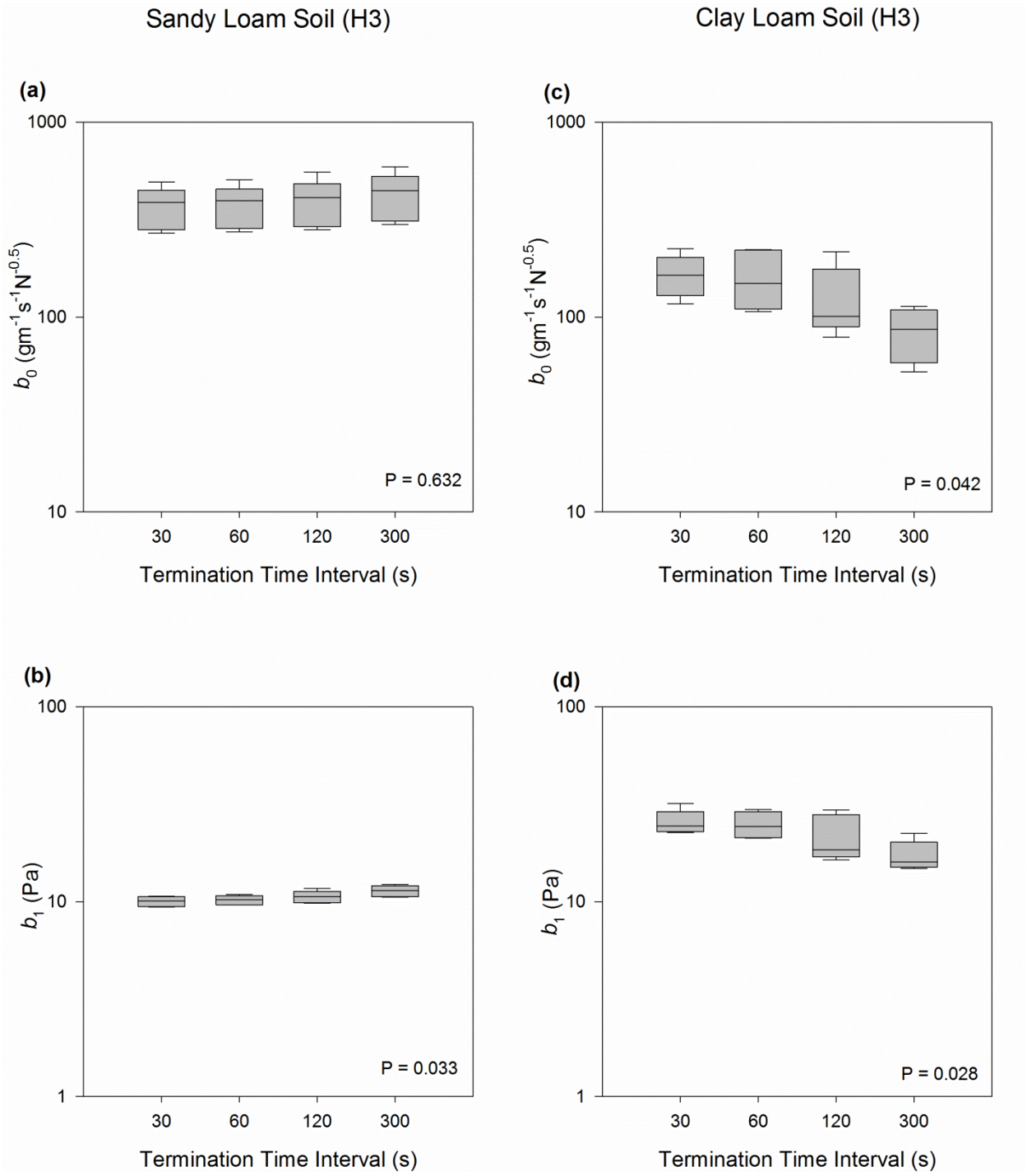

Figure 2.12. Influence of initial time interval of data collection on nonlinear detachment model erodibility parameters (b_0 and b_1) derived from mini JETs for the sandy loam and clay loam soils at H3 (109 cm).

Table 2.1. Properties of soils used for the JETs.

		Soil texture				Standard Compaction	
Source	USCS classification	Sand (%)	Silt (%)	Clay (%)	Plasticity Index	Maximum Density	Optimum water content (%)
Cow Creek	Sandy loam	54	38	8	Non-plastic	1.78	15
Five Mile Creek	Clay loam	30	33	36	6	1.61	20

Table 2.2. Anderson-Darling test statistic (AD) and respective P-values for the erodibility parameters (n =20). P-values > 0.05 indicate acceptable distribution fit.

	Erodibility Parameters*							
	$\tau_{c\text{-}BL}$ (Pa)	$\tau_{c\text{-}SD}$ (Pa)	$\tau_{c\text{-}IT}$ (Pa)	$k_{d\text{-}BL}$ ($cm^3N^{-1}s^{-1}$)	$k_{d\text{-}SD}$ ($cm^3N^{-1}s^{-1}$)	$k_{d\text{-}IT}$ ($cm^3N^{-1}s^{-1}$)	b_0 ($gm^{-1}s^{-1}N^{-0.5}$)	b_1 (Pa)
Sandy loam								
Normal								
AD	0.47	0.50	0.59	0.18	0.30	0.38	0.19	0.92
P-value	0.23	0.19	0.11	0.90	0.55	0.38	0.89	<0.05
Log-normal								
AD	0.48	0.55	0.46	0.28	0.51	0.58	0.21	1.01
P-value	0.20	0.13	0.24	0.58	0.17	0.11	0.84	<0.05
Clay loam								
Normal								
AD	1.03	0.80	1.34	0.15	0.21	0.15	1.32	0.28
P-value	<0.05	0.03	<0.05	0.95	0.83	0.95	< 0.05	0.58
Log-normal								
AD	0.47	0.64	0.85	0.35	0.73	0.59	0.37	0.60
P-value	0.21	0.08	<0.05	0.43	<0.05	0.10	0.37	0.10

* τ_c is the critical shear stress, k_d is the erodibility coefficient, and b_0 and b_1 are nonlinear detachment model parameters; BL is the Blaisdell solution, SD is the scour depth solution, and IT is the iterative solution of the linear detachment model.

Table 2.3. Sample size required to estimate erodibility parameters within given error percentage of the mean at a 95% confidence level (Z = 1.645).

		*kd (cm-3N-1s-1)**		*τc (Pa)*		*b0 (gm-1s-1N-0.5)*		*b1 (Pa)*	
Error		Sandy loam	Clay loam	Sandy Loam	Clay loam	Sandy Loam	Clay loam	Sandy Loam	Clay loam
5%									
	BL*	25	278	109	836	96	871	9	90
	SD	56	613	4	106				
	IT	88	338	16	48				
10%									
	BL	7	73	28	219	24	340	3	46
	SD	14	161	1	28				
	IT	22	89	4	13				
25%									
	BL	1	13	5	40	4	62	1	8
	SD	3	29	1	5				
	IT	4	16	1	2				

* τ_c is the critical shear stress, k_d is the erodibility coefficient, and b_0 and b_1 are nonlinear detachment model parameters; BL is the Blaisdell solution, SD is the scour depth solution, and IT is the iterative solution of the linear detachment model.

Table 2.4. Comparison between field and laboratory data of mean estimated erodibility parameters and percentage deviation from the mean obtained with a sample size of five JETs.

	Laboratory – Sandy Loam		In-Situ Tests – Cow Creek (Daly et.al., 2015a)		Laboratory – Clay Loam		In-Situ Tests – Five Mile Creek (Daly et.al., 2015a)	
Parameter*	Mean	P %	Mean	P %	Mean	P %	Mean	P %
$\tau_{c\text{-}BL}$ (Pa)	0.05	28	0.1	120	0.04	88	3.81	551
$\tau_{c\text{-}SD}$ (Pa)	1.47	5	1.05	23	1.78	25	11.3	60
$\tau_{c\text{-}IT}$ (Pa)	1.31	10	0.95	28	1.62	16	8.03	42
$k_{d\text{-}BL}$ ($cm^3N^{-1}s^{-1}$)	26.02	13	39.5	75	5.13	44	2.9	86
$k_{d\text{-}SD}$ ($cm^3N^{-1}s^{-1}$)	108.39	20	245	107	13.14	72	19.2	88
$k_{d\text{-}IT}$ ($cm^3N^{-1}s^{-1}$)	169.54	25	170	81	17.47	49	17.3	57

* τ_c is the critical shear stress, k_d is the erodibility coefficient; BL is the Blaisdell solution, SD is the scour depth solution, and IT is the iterative solution of the linear detachment model.

Table 2.5. General properties of jet hydraulics where *H* is head setting, d_0 is the nozzle diameter, *C* is coefficient of discharge, *U* is jet velocity and *Re* is the jet Reynolds number.

H (m)	d_0 (mm)	*C*	*U* ($m\ s^{-1}$)	*Re*
0.46	3.18	0.74	3.37	7768
0.79	3.18	0.74	2.91	10180
1.09	3.18	0.74	2.27	11923

CHAPTER 3

EFFECT OF MOISTURE CONTENT ON ERODIBILITY PARAMETERS DERIVED FROM MINI-JETS

Abstract

Soil moisture has been identified as one of the major factors influencing the erodibility of soil. Interaction of the soil moisture with other soil properties has complicated predicting the erosion of cohesive soil. This study conducted mini-JETs on two soils of contrasting texture; sandy loam and clay loam. The tests were controlled for the applied pressure head, texture and packing density and the moisture content profiles of the test samples were varied uniformly after compaction. Mini-JETs were conducted on the remolded samples with two moisture content profiles different from the compaction moisture content. The parameters of a linear excess shear stress equation derived from Blaisdell, Scour Depth and Iterative methods and a non-linear detachment equation were compared. The soil moisture influenced the parameters of each soil type differently. The influence of moisture content also varied according the solution methodology, suggesting that results of the JETs should be interpreted relative to the solution method used to derive the parameters. In general, the k_d parameter increased by one order of magnitude with moisture content for both soil types. The b_0 parameter increased by up to two orders of magnitude with moisture content for the clay loam soil.

Interestingly, simultaneous increases in τ_c and b_1 were also observed at higher moisture content. This may be due to changes in the internal structure of the soil.

Introduction

Soil moisture has been noted to influence various properties of soil including shear strength, aggregation, infiltration capacity, and inter-particle cohesion. Soil erodibility depends on various factors, one of them being moisture content. The role of antecedent moisture in various erosion processes such as rain-splash erosion and rill erosion have been established (Govers et.al., 1993), especially in the case of cohesive soils with high clay content. The rain-splash erosion was shown to increase exponentially with antecedent soil moisture in a field study carried out with a rainfall simulator (Luk, 1985). In a rill erosion test, the sediment detachment was shown to decrease four to 15 times when the rill was pre-wetted before applying the flow. Higher moisture contents are linked with increased cohesion between particles, decreased infiltration into the soil mass, increased aggregation, and crust formation which increase the resistance to erosion. It should be noted that these studies were carried out in field and water was applied to initially dry soil well short of saturation.

The effect of moisture content on erodibility is also highly dependent on its interaction with other soil properties and atmospheric conditions. Bissonnais et al (1995) report increased erodibility on wet plots in comparison to dry plots but decreased erodibility on re-wetted plots. The authors also point out that soil with highest clay content had the lowest erosion rate when rewetted and soil with highest organic carbon content had the lowest erosion rate when rewetted. Hence, the complexity of predicting erodibility of soil is further complicated by interaction of moisture content and other soil

properties. Isolating the influences of moisture content from other factors would provide an invaluable insight.

Typically, the erosion rate of a cohesive soil is predicted using a model which relates soil erodibility to a measure of hydraulic forces on the soil. The most common model is known as the excess shear stress equation:

$$\varepsilon_r = k_d(\tau - \tau_c)^a \tag{3.1}$$

where ε_r is the detachment rate (m s^{-1}), k_d is the erodibility coefficient (m^3 N^{-1} s^{-1}), τ_c is the critical shear stress (Pa), and a is an exponent. The τ_c is the minimum τ required to initiate particle detachment (Partheniades, 1965). The k_d and τ_c are collectively called the erodibility parameters of the excess shear stress equation. The value of the exponent (a) is usually assumed to be one (Hanson et al., 2002).

Currently, there are three approaches in analyzing data from JETs to estimate the erodibility parameters of the excess shear stress equation. The most popular method of analysis, called Blaisdell's solution (BL), was developed by Hanson and Cook (1997, 2004). The solution method was based on principles of fluid diffusion presented by Stein and Nett (1997) and a hyperbolic function modeling the depth progression of the scour hole developed by Blaisdell et al. (1981):

$$X^2 = (f - f_o)^2 - A^2 \tag{3.2}$$

where $X = \log\left(\frac{U_0 t}{d_0}\right)$, $f = \log\left(\frac{J}{d_0}\right) - \log\left(\frac{U_0 t}{d_0}\right)$, J is the depth of scour hole recorded at each time (t), d_0 is the diameter of jet orifice, and U_0 is the velocity of the jet at the origin. The function represents a rectangular hyperbola with A as both the semi-transverse and semi-conjugate and center at (0, f_0) in a Cartesian plane. The ordinate of the center of the

hyperbola, $f_0 = \log\left(\frac{J_e}{d_0}\right)$, is used to predict the equilibrium depth (J_e) of the scour hole. The equilibrium depth is defined as the maximum depth of the scour hole beyond which the water jet cannot erode further. This solution method first determines the τ_c parameter based on the J_e of scour hole as predicted by Blaisdell's function as follows:

$$\tau_c = \tau_0 \left[\frac{J_p}{J_e}\right]^2 \tag{3.3}$$

where τ_o is the maximum boundary τ due to the jet velocity at the orifice, and J_p is the potential core length. The velocity at the jet centerline is equivalent to jet velocity at orifice through J_p (Hanson and Cook, 2004). The J_p is constant for the given JET apparatus and τ_o is constant for a given head setting, h. The J_e depends on both the head setting and the fit of the observed data to the hyperbolic function. The k_d is then determined by solving for the least squared deviation between the observed scour time (t) and predicted time (t_m) as defined as follows:

$$t_m = T_r\left[0.5\ln\left(\frac{1+J^*}{1-J^*}\right) - J^* - 0.5\ln\left(\frac{1+J_i^*}{1-J_i^*}\right) + J_i^*\right] \tag{3.4}$$

where $T_r = \frac{J_e}{k_d \tau_c}$ is a reference time, $J^* = \frac{J}{J_e}$ is a dimensionless scour depth, and $J_i^* = \frac{J_i}{J_e}$ is a dimensionless measure of the initial distance between the jet orifice and soil surface.

Alternatives to Blaisdell's solution have been suggested recently (Simon et al., 2010; Daly et al., 2013). One of these solution methods is called the scour depth solution (SD). This method simultaneously searches for k_d and τ_c which provide the best fit of observed JET data on the scour depth versus time curve predicted by the excess shear stress equation. The other approach was presented by Simon et al. (2010), and referred to

as the iterative solution (IT). This method is initialized using the values of erodibility parameters determined by Blaisdell's solution. The scour hole is assumed to reach the J_e at the end of each test. An upper bound on τ_c is fixed by substituting this J_e in equation (3.3). Then the values of τ_c and k_d which minimize the root mean square deviation between the observed t and predicted time (t_m) is searched for iteratively.

An alternative to the excess shear stress model is the Wilson mode1 (1993a, 1993b). The model is based on balance of all the forces and moments driving and resisting detachment of a two-dimensional representation of a particle or aggregate. The equation of the model is given as follows:

$$\varepsilon_r = \frac{b_0\sqrt{\tau}}{\rho_b}\left[1-\exp\left\{-\exp\left(3-\frac{b_1}{\tau}\right)\right\}\right] \tag{3.5}$$

where ρ_b is the bulk density and Wilson's model has two parameters: b_0 (g m^{-1} s^{-1} $N^{-0.5}$) and b_1 (Pa). These parameters, unlike parameters of the excess shear stress equation, are mechanistically defined, but several variables are unknown. As seen from the equation, the relationship between ε_r and τ is nonlinear. Note that b_0 is similar to k_d but with a different magnitude and units; b_1 is similar to τ_c.

Al-Madhhachi et al. (2013a, b) incorporated the hydraulics of both the original and mini-JET device in Wilson's model and demonstrated that the parameters of Wilson's model can also be determined from the experimental data obtained from the JETs. The observed particle detachment rate data is fit to equation (3.5) by minimizing the sum of squared differences between the observed and modeled scour depth. Hence, the parameters of the model can be determined statistically from observed JET data similar to the linear model.

The model parameters k_d, τ_c, b_0, b_1 can be estimated experimentally using various techniques like flumes, hole erosion tests and jet erosions tests (JETs). JETs were initially designed and have been extensively used in investigating the erosion properties of soil *in situ.* They also have been employed in laboratory settings on remolded samples to investigate the effects of soil properties on soil erodibility. Hanson and Hunt (2007) employed original JETs on remolded samples of two different types of soil. They packed the soil at different compaction efforts and moisture contents to achieve the range of dry density and moisture content that described the compaction curve of the soils. They compared the results of the JET test with the results of a large-scale embankment breach testing. The results of this study showed that the k_d parameter decreased by as much as two orders of magnitude when the samples were packed at the optimum moisture content (OMC). The k_d values also increased slightly when samples were packed above the OMC. The authors concluded that compaction water content played a major role in determining erodibility. However, it should be noted that this study was carried out to determine the acceptable specifications of compaction efforts and moisture content for designing and constructing earthen embankments. The erosion process active in an earthen embankment can be widely different than the erosion processes active in a natural setting. The compaction of soil in construction of the embankments and also remolding of the samples changes the internal structure of the soil particles. Cetin et al. (2007) conducted a study to investigate the changes in internal structure and physical properties of remolded samples when compacted at a range of dry densities and moisture contents encompassing both dry side and wet side of the OMC. They used samples prepared by mixing natural clay with 33.1% muscovite mica sand. The authors found that the

randomness in orientation of soil particles decreased and the inter-particle contact increased as the dry density and moisture content approached the peak of OMC. Beyond the OMC, the internal structure of soil was characterized by increased inter-particle contact and long strings and packets of particles with random orientation.

Remolding samples at different moisture contents is not an appropriate approach to test the effect of moisture content on erodibility of soil. In natural settings, the moisture content of soil usually increases by processes of infiltration and/or capillary rise of subsurface water. In this study we hypothesize that changing the moisture content of a remolded sample after compaction influences the erodibility of the soil and that the mini-JETs can detect the influences. We assume that allowing water to enter the soil mass without disturbing the soil changes the cohesion between soil particles and that in turn decreases the soil erodibility. The objectives of this study were to conduct mini-JETs on two soils of contrasting texture in controlled laboratory conditions to derive the erodibility parameters of soil samples that have been wetted after compaction. The erodibility parameters will be compared against erodibility parameters of dry remolded samples and saturated remolded samples.

Methods and Materials

Remolded samples were prepared from the sandy loam soil obtained from surface of streambank of Cow Creek in Stillwater, Oklahoma and clay loam soil obtained from B horizons of the streambank of Five Mile Creek near Fort Cobb, Oklahoma. The particle size distribution of both soils was analyzed following ASTM standard D422. Liquid limit and plastic limit of the soils were performed following ASTM standard D4318. Standard

compaction test were performed on the soils using ASTM standard D698A (ASTM, 2006). The properties of each soil are presented Table 3.1.

Each soil sample was air dried, sieved through no 4 sieve (4.75 mm) and mixed with water to achieve uniform water content. The sandy loam soil was mixed with water to water content of 10% and the clay loam soil was mixed with water to water content of 16%. The water contents were chosen to be on the drier side of the OMC. The samples for the JETs were prepared by packing the soil in a standard mold. Packing was done in three equal layers to achieve uniform dry density through the sample. Uniform packing was chosen to avoid layering effects as mentioned in Al-Madhhachi et al. (2013a). Sandy loam soil was compacted to dry density of 1.7 Mg/m^3 and clay loam was compacted to dry density of 1.4 Mg/m^3. These densities were chosen to be closest to maximum dry density while being convenient enough to achieve the desired uniform dry density. Attempts to achieve a higher dry density, especially for the clay loam soil resulted in non-uniform compaction. The moisture content profiles of the remolded samples were assumed to be uniform through the depth of the mold. The moisture content profiles are denoted as M1S for the sandy loam soil and as M1C for the clay loam soil in Figure 3.1a and 3.1b, respectively.

In order to increase the moisture content of the packed samples, the molds were encased in an apparatus as shown in Figure 3.2. The apparatus held a porous plate at one end and geo-textile at other end. This end was connected to water inlet. The porous plate ensured even contact with the soil surface and uniform flow through the cross section of soil sample. The geo-textile ensured flow of water out of the soil sample. The water was allowed to flow into the mold steadily under small hydrostatic pressure. This uniformly

changed the moisture content profile inside the mold. The mold was taken out of the apparatus after the water fully penetrated through the mold and water was observed at the other end. A core was driven through the mold and a sample of wetted soil was obtained. The core sample was cut into segments of 2 cm length and moisture content of each segment was measured using the gravimetric method. The average moisture content profiles of soil samples subjected to this procedure are shown as M2S for the sandy loam soil and M2C for the clay loam soil in Figure 3.1a and 3.1b. The average moisture content of sandy loam soil was raised to 17% and that of clay loam soil was raised to 27%.

The moisture content of the sandy loam soil was further raised by subjecting the remolded samples to a seepage column. The seepage column apparatus is described in Al-Madhhachi et al. (2013). The seepage was stopped after the sample was thoroughly saturated and ponding of water was observed on the surface. A core was driven through the mold and a sample of wetted soil was obtained. The core sample was cut into four equal segments and moisture content of each segment was measured using the gravimetric method. The average moisture content profiles of soil samples subjected to this procedure are shown as M3S in Figure 3.1a. The average moisture content of the remolded sample was 20%.

The moisture content of the clay loam soil was further increased by simply immersing the remolded samples in water for 5 to 7 days. Then the samples were taken out, wrapped in plastic foil and stored in an ice-box for 24 hours. This was done to let the moisture concentration profile inside the soil mass to equilibrate to obtain as uniform moisture content profile as possible. Then a core was driven through the molds and a

sample of wet soil was obtained. The core sample was cut into five equal samples and moisture content of each segment was obtained using the gravimetric method. The average moisture content profiles of soil samples subjected to this procedure are shown as M3C in Figure 3.1b. The average moisture content of the remolded sample was 30%.

Additional remolded samples were prepared for conducting the mini-JETs. Twenty mini-Jets were performed on the remolded samples with moisture profile M1S. Five mini-JETs were performed on the remolded samples with moisture profile M2S and M3S each. Five mini-JETs were performed on the remolded samples of clay loam soil with moisture content profiles M1C, M2C and M3C.

The data obtained from each tests were analyzed to estimate the parameters of the linear excess shear stress equation and non-linear Wilson model equation. The parameters of the excess shear stress were estimated from three different solutions methods, the BL, SD and IT solutions using the spreadsheet tool developed by Daly et al (2013). Analysis of variance (ANOVA) was performed to identify difference between the erodibility parameters estimated at the three different moisture contents and pair-wise Tukey tests were performed to identify differences between erodibility parameters of each pair of moisture content profiles.

Results

Sandy Loam Soil

Significant differences were observed between the erodibility parameters of the sandy loam estimated at three different moisture content profiles (Figure 3.3). The only exception was the k_d estimated from IT solution $k_{d\text{-}IT}$. A non-linear trend with increase in moisture content was observed for the k_d estimated from the BL ($k_{d\text{-}BL}$) and the $k_{d\text{-}IT}$ as the

average of both parameters increased at M2S and decreased at M3S. The average k_d estimated from the SD method ($k_{d\text{-}SD}$) and the average b_0 increased linearly with increased moisture content. A Nonlinear trend was observed in the average τ_c estimated by all the solution techniques and b_1, as these parameters decreased at M2S and increased at M3S (Figures 3.3 and 3.5).

Clay Loam Soil

Significant differences were observed between the erodibility parameters of the clay loam soil estimated at the three different moisture content profiles (Figure 3.4). The average $k_{d\text{-}BL}$ and $k_{d\text{-}IT}$ decreased at M2C and increased at M3C (Figure 3.4a). The average $k_{d\text{-}SD}$ increased linearly with the moisture content and most noticeably it increased by about three times at M3C as compared to M1C (Figure 3.4c). The average b_0 increased two times from M1C to M2C and six times from M2C to M3C. The variability in b_0 also increased at M3C. The average τ_c estimated from all the solution techniques increased linearly with increase in moisture content (Figure 3.4). Average b_1 also increased with increased moisture content (Figure 3.5d).

Discussion

The influence of the moisture content on the erodibility parameter depended on the soil type, the solution technique, and the erodibility parameter. The BL and IT predicted similar effects of the moisture content on k_d on the same soil type. The effect predicted by SD was different from these two other solution techniques. The effect of the moisture content on τ_c was uniform across the solution techniques.

A significant increase in $\tau_{c\text{-}BL}$ for both soil types at the highest moisture content was counter intuitive. The sandy loam soil was saturated and more fluid at M3S; the clay loam was also softer at M3C. Both soils were expected to have a lower threshold of τ for initiating particle detachment. Most previous studies predicted a negative correlation between $k_{d\text{-}BL}$ and $\tau_{c\text{-}BL}$; in fact Hanson and Hunt (2007) limited their discussion to the influence of the water content on $k_{d\text{-}BL}$ assuming $\tau_{c\text{-}BL}$ to be function of $k_{d\text{-}BL}$. The BL method estimated $\tau_{c\text{-}BL}$ as a function of J_e which in turn was modeled by a hyperbolic function (equation 3.2). The J_e estimated by the hyperbolic function was directly proportional to the final depth of scour hole, and the $\tau_{c\text{-}BL}$ was inversely proportional to the square of the estimated J_e. On closer examination, it can be observed that the average final scour depth of JETs conducted at M3S (2.87 cm) was significantly lower than those conducted at M1S (4.01 cm) or M2S (4.75 cm). Similarly, the average final scour depths of JETs conducted at M3C (2.74 cm), M2C (3.07 cm) and M1C (3.56 cm) were in ascending order. ANOVA on the average of final scour depths of JETs showed that the final depths at each moisture content profiles were significantly different at $\alpha = 0.05$. Hence, the slightly deeper scour holes of the JETs at M2S translated to lower $\tau_{c\text{-}BL}$ and shallow scour holes at M3S translated to higher $\tau_{c\text{-}BL.}$ The ascending order of the scour depths translated to ascending order of the $\tau_{c\text{-}BL}$ for the clay loam as well. Similar increase in $\tau_{c\text{-}BL}$ with moisture content estimated from submerged JETs with moisture content was also observed by Hanson and Cook (2002). However, the authors also observed that the $k_{d\text{-}BL}$ decreased uniformly with the moisture content. It should be noted that the moisture content of samples in the Hanson and Cook (2002) study was increased before compaction.

The $k_{d\text{-}BL}$ was estimated by solving for the least squared deviation between the observed scour time (t) and predicted time (t_m) as defined in equation 3.4. The t_m is a function of the parameters ($k_{d\text{-}BL}$, $\tau_{c\text{-}BL}$), the J_e and the dimensionless scour depth. This translates to strong positive correlation between the $k_{d\text{-}BL}$ and overall rate of the scouring in a particular JET. The overall rate was defined as the ratio of total scour depth to total time of test. In the case of sandy loam soil, the overall rates at M1S, M2S and M3S were 0.16 cm/min, 0.20 cm/min and 0.13 cm/min respectively. In case of the clay loam soil, the overall rates conducted at M1C, M2C and M3C were 0.07 cm/min, 0.06 cm/min and 0.08 cm/min, respectively. Regazzoni et al. (2010) performed JETs on remolded samples of highly plastic and clayey soil and compared the estimated $k_{d\text{-}BL}$ and $\tau_{c\text{-}BL}$ with the same estimated for remolded samples which were saturated after the compaction. The authors reported higher $k_{d\text{-}BL}$ and $\tau_{c\text{-}BL}$ for the saturated samples in comparison to the unsaturated samples. These results are consistent with the results in this study. However, the authors did not present any evidence of the saturation and uniformity of the moisture content profiles.

The $\tau_{c\text{-}SD}$ was estimated as the measure of the τ at which the erosion rate was zero and $k_{d\text{-}SD}$ was the rate of change of the erosion rate with the applied τ (Figure 3.6). Hence, the final depth of the scour holes was also most influential in estimation of the $\tau_{c\text{-}SD}$ and this fact is observed in the average values of $\tau_{c\text{-}SD}$ estimated at M1S, M2S and M3S as well as those estimated at M1C, M2C and M3C. The $\tau_{c\text{-}SD}$ did not depend on the square of a equilibrium depth and hence the variability of $\tau_{c\text{-}SD}$ was significantly less than the variability of $\tau_{c\text{-}BL}$ (Figure 3.3d and Figure 3.4d). The $k_{d\text{-}SD}$ was mostly influenced by the data points recorded early in the test when the erosion rate was most rapid (Figure 3.6).

The trend of $\tau_{c\text{-}IT}$ closely resembled the trend of $\tau_{c\text{-}SD}$. Estimation of $\tau_{c\text{-}IT}$ also depended on the final depth of the scour hole at the end of the each JET as the IT assumes the final depth of the scour hole to be the equilibrium depth and sets an upper limit on the τ_c . Both $k_{d\text{-}IT}$ and the $\tau_{c\text{-}IT}$ were then estimated by solving for the least squared deviation between the observed scour time (t) and predicted time (t_m) as defined in equation 3.4. This procedure produces estimated $\tau_{c\text{-}IT}$ higher than $\tau_{c\text{-}SD.}$ The procedure is also responsible for the trend of $k_{d\text{-}IT}$ which resembles the trend of the $k_{d\text{-}BL}$. Hence, the $k_{d\text{-}IT}$ of both the sandy loam and clay loam soil were dependent on the overall rates of the JETs. However, the $k_{d\text{-}IT}$ was a magnitude higher than the $k_{d\text{-}BL}$ as IT did not predict the J_e based on the hyperbolic function.

The final depth of scour and the rate of erosion at high applied τ are most influential in determining the b_1 and b_0 for both soils (Figure 3.7). The nonlinear model predicted the sandy soil to be slightly more erodible at M2S. At M3S, increase in b_0 suggested the increase in erodibility of soil, but simultaneous increase in b_1 also suggested a higher threshold for initiating detachment. The simultaneous increases in b_0 and b_1 parameters for the clay loam soil also suggested a similar influence of moisture content on the more cohesive soil.

The increase in erodibility of the sandy soil at M2S was predicted by all the solution techniques of the linear model as well as the non-linear model. This prediction was consistent with observation by Hanson and Hunt (2007) where the values of sandy soil increased when packed at water contents above the OMC. The can be attributed to an increase in pore water pressure decreasing the inter particle cohesion. At M3S, the pore water pressure further increased and inter-particle cohesion decreased. The rate of erosion

increased but there was also simultaneous increase in entrainment of particles in the fluid flow. This decreased the eroding capacity of water. The resettlement of heavier sand particles also increased as the applied τ decreased towards the end of the tests. Although the initial erosion rates were greater than that M1S or M2S, the overall rate of erosion decreased due to shallow scour holes. This caused the BL and IT solution to predict lower k_d at M3S. The scour depth and the nonlinear model, however, reflected the increase in the initial rate of erosion, when the applied τ was highest, in their higher values of the k_d (Figure 3.6).

The decreased erodibility of the clay loam soil at M2C compared to that at M1C and predicted by BL and IT solutions can be attributed to small increase in cohesion between the soil particles. The increase in cohesion was discernible at low τ towards the end of the test. At M3C, however, the clay soil becomes more plastic and more deformable. Increase in τ_c at M3C can be attributed to increase in plasticity. Simultaneous increase in pore water pressure increased the k_d as well. The SD method and non-linear model both predicted higher k_d at M3C as the estimation of these parameters was most influenced by high erosion rates predicted at high τ at this moisture content.

It is also interesting to observe the disparity between the increase in water contents and magnitude of changes in the erodibility parameter. For example, the average water content of sandy loam soil increased by 7% from M1S to M2S and about 3% from M2S to M3S. However, larger and significant differences in the erodibility parameters were observed between M2S and M3S. Similarly, the average water content of clay loam soil increased by 9% from M1C to M2C and by 3% from M2C and M3C, but more significant differences in the magnitudes of the erodibility parameters were observed

between M2C and M3C. This can be attributed to changes in soil structure at the highest water contents. The sandy loam soil was subjected to steady water flow at small positive pressure in a confined space to raise its water content to M2S but seepage force was applied to raise its water content to that of M3S. The seepage force can be expected to break down the internal soil structure more than that of a slow steady infiltration. Similarly, the clay loam soil was also subjected to slow steady flow in a confined space under small positive pressure in raising its water content to M2C. No swelling was observed in the remolded sample due to this treatment. However, when moisture content was raised to M3C, it was simply left to saturate under higher positive pressure in an unconfined space. This allowed the clay loam soil to swell. Swelling most likely changed the internal structure of the soil making it more erodible.

The results presented in this study allow us make an comparison of the solution techniques used to derive the parameters of the linear equation. As it has been discussed, the BL and IT iterate to find the least squared deviation between the time to reach the equilibrium depth, and the SD solution iterates to find the least squared deviation between the erosion rates to estimate the parameters. Hence, the $k_{d\text{-}SD}$ is most influenced by the data collected at high applied τ. However, the $k_{d\text{-}BL}$ and $k_{d\text{-}IT}$ take into account more data collected at low τ (Figure 3.7). This might be more helpful in discerning the subtle influences on erodibility, especially of more cohesive soils, when there are subtle changes in moisture content as seen Figures 3.4a and 3.4e. The SD does not possess this capability.

This suggests that there might not be one most appropriate solution technique and the choice of solution technique should depend on the application. Many researchers have

concluded that BL severely under predicted the τ_c (Simon et al, 2010; Cossette et al, 2012; Daly et al, 2013) and SD and IT methods were developed as alternatives to BL method. The choice between SD and IT technique however does not seem to be so clear. The SD technique follows the literal definition of the excess shear stress equation and might be more suitable when comparisons have be made with the parameters derived from other experimental techniques such as the flume and the HET. The BL and IT techniques have their advantages as well.

Conclusions

Moisture content is broadly identified as one of the major influencing factors in the erodibility of cohesive soil. However, few studies have been able to isolate the effect of moisture content on the erodibility. This study conducted mini-JETs under controlled laboratory conditions on two soil types of contrasting texture. A set of controlled mini-JETs were conducted by packing sandy soil and clay loam soil at varying initial moisture content profiles. The moisture content profiles of packed samples of each soil were raised from the initial packing moisture content to higher moisture content profiles by allowing a steady flow of water under moderate positive pressure. The moisture content of the packed sandy loam soil was increased further by subjecting it to seepage force and the moisture content of the clay loam soil samples were increased further by simply allowing them soak in water for over a week. Mini-JETs were performed on the soil samples. The data from the mini-JETs were analyzed to derive the parameters of linear model using three different solution techniques and also to derive the parameters of the non-linear model. The estimation of the parameters varied with soil type and the solution technique. The BL and IT solution techniques reflected the change in overall erosion rate

due to changes in the moisture content in their estimation of the k_d parameter. The $k_{d\text{-}BL}$ and $k_{d\text{-}IT}$ of the sandy loam increased at M2S and decreased at M3S. Hence, the sandy loam soil was predicted to be less erodible at the highest moisture content. The $k_{d\text{-}BL}$ and $k_{d\text{-}IT}$ of the clay loam soil decreased at M2C and then increased at M3C. The BL and IT solution methods predicted a decrease in the erodibility of the clay loam soil with increased moisture content alone. The SD solution reflected the changes in erosion rate at high values of τ in the estimation of the k_d parameter and predicted both the soil to be more erodible with increased moisture content. The non-linear model also made similar predictions as the SD solution. The τ_c and b_1 increased significantly at the highest moisture contents of both soil types. This was attributed to shallower scour holes of the JETs conducted at those moisture content profiles. The shallow scour holes were caused by increased resettlement of the particles in case of the sandy loam soil and increased plasticity in case of the clay loam soil. The change in internal structure of sandy loam soil at M3S and swelling of clay loam soil at M3C caused significant increases in b_0 and $k_{d\text{-}SD}$. Increasing moisture content of packed soil influences the erodibility of the soil and the influence can be detected in the estimated of the parameters of the linear and non-linear models. The detection of the influence of moisture content also varied with the solution techniques used to derive the parameters of the linear model. Hence the change in parameters of linear model should be interpreted according to the solution technique. This study attributed this phenomenon to a change in the internal soil structure at those moisture contents.

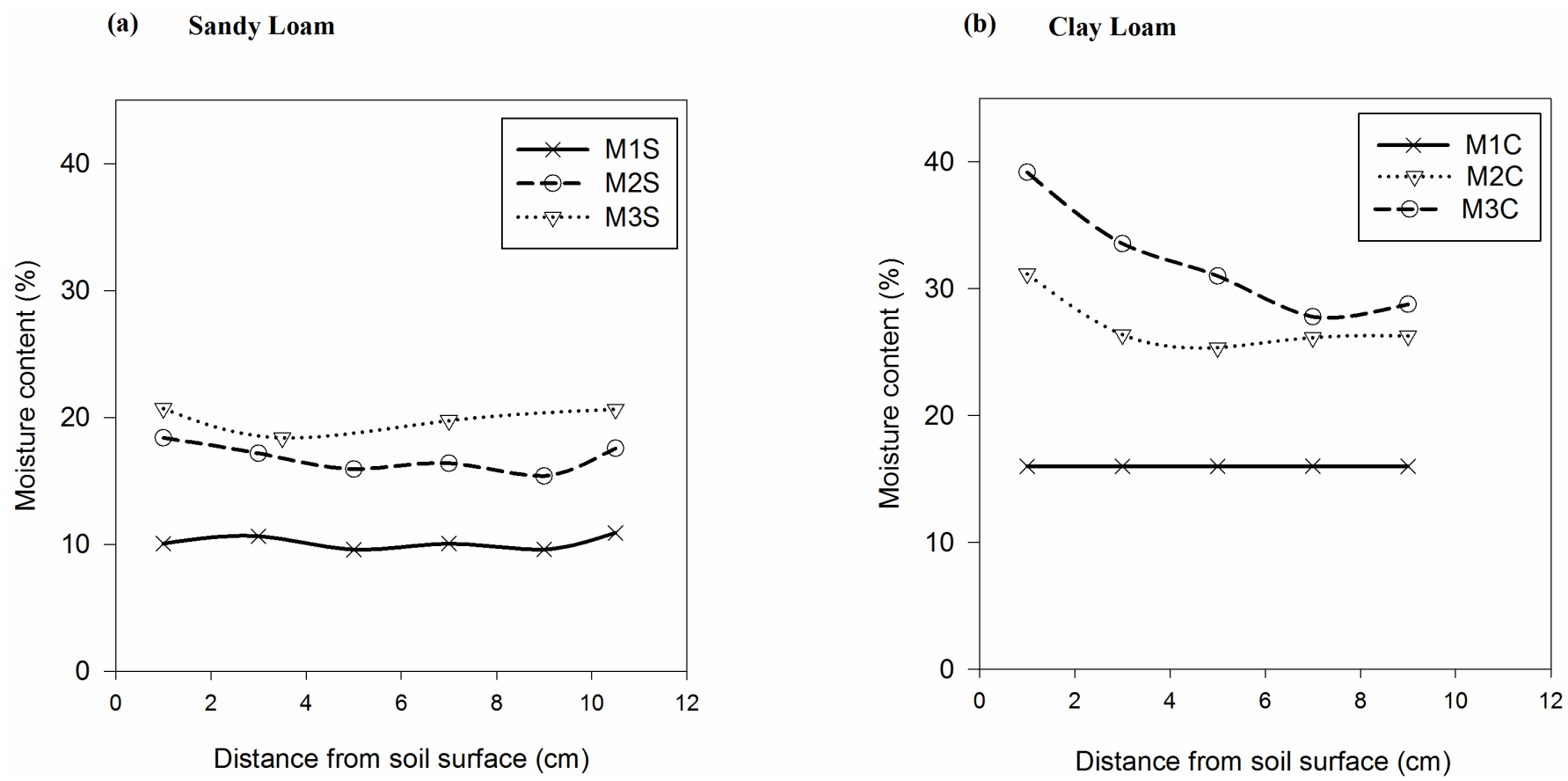

Figure 3.1. Moisture content profiles of the soil samples used for the mini-JETs

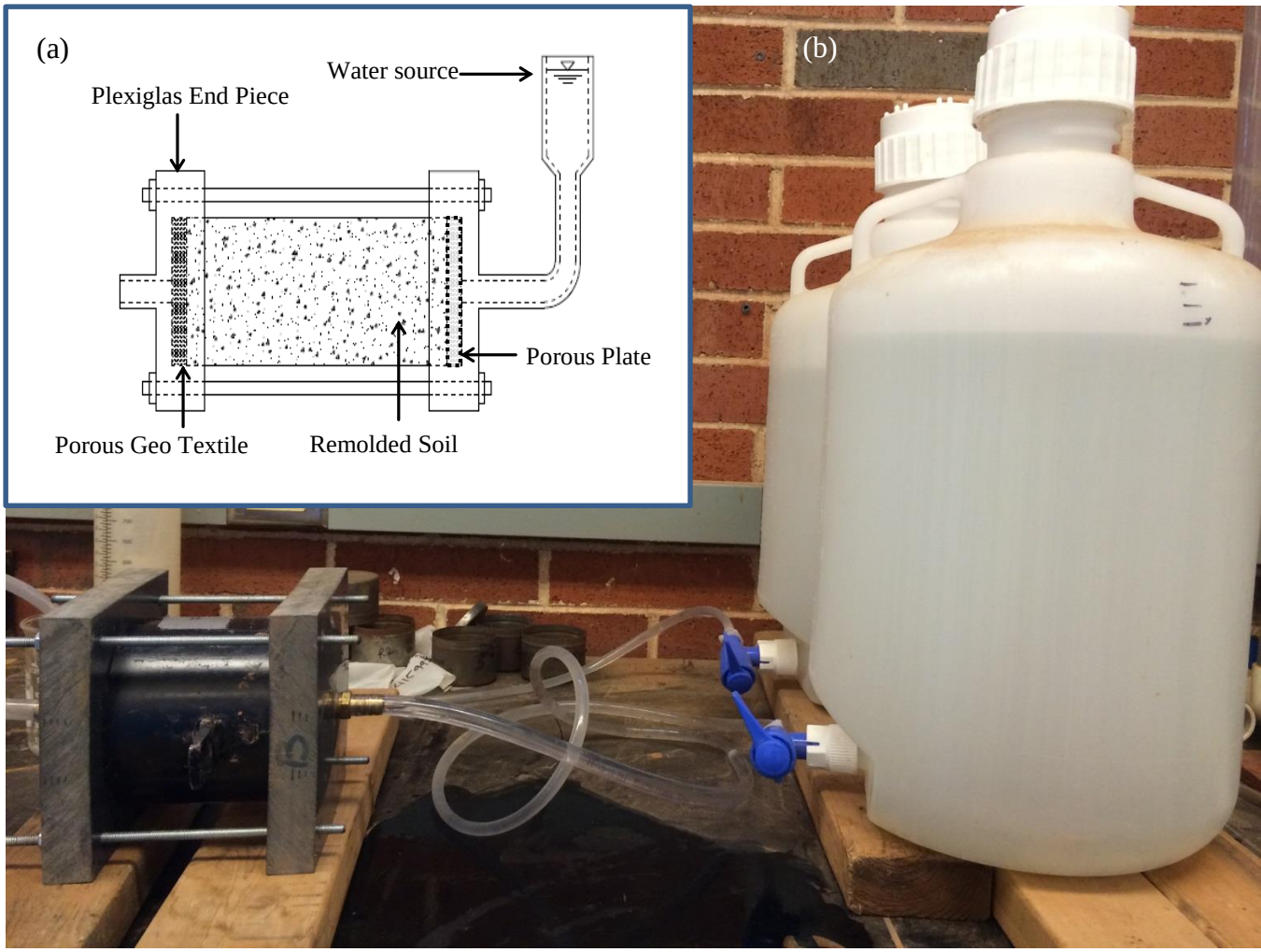

Figure 3.2. (a) Schematic of the apparatus used for raising the moisture content of the remolded soil samples to M2S and M2C. (b) Photograph of the apparatus setup.

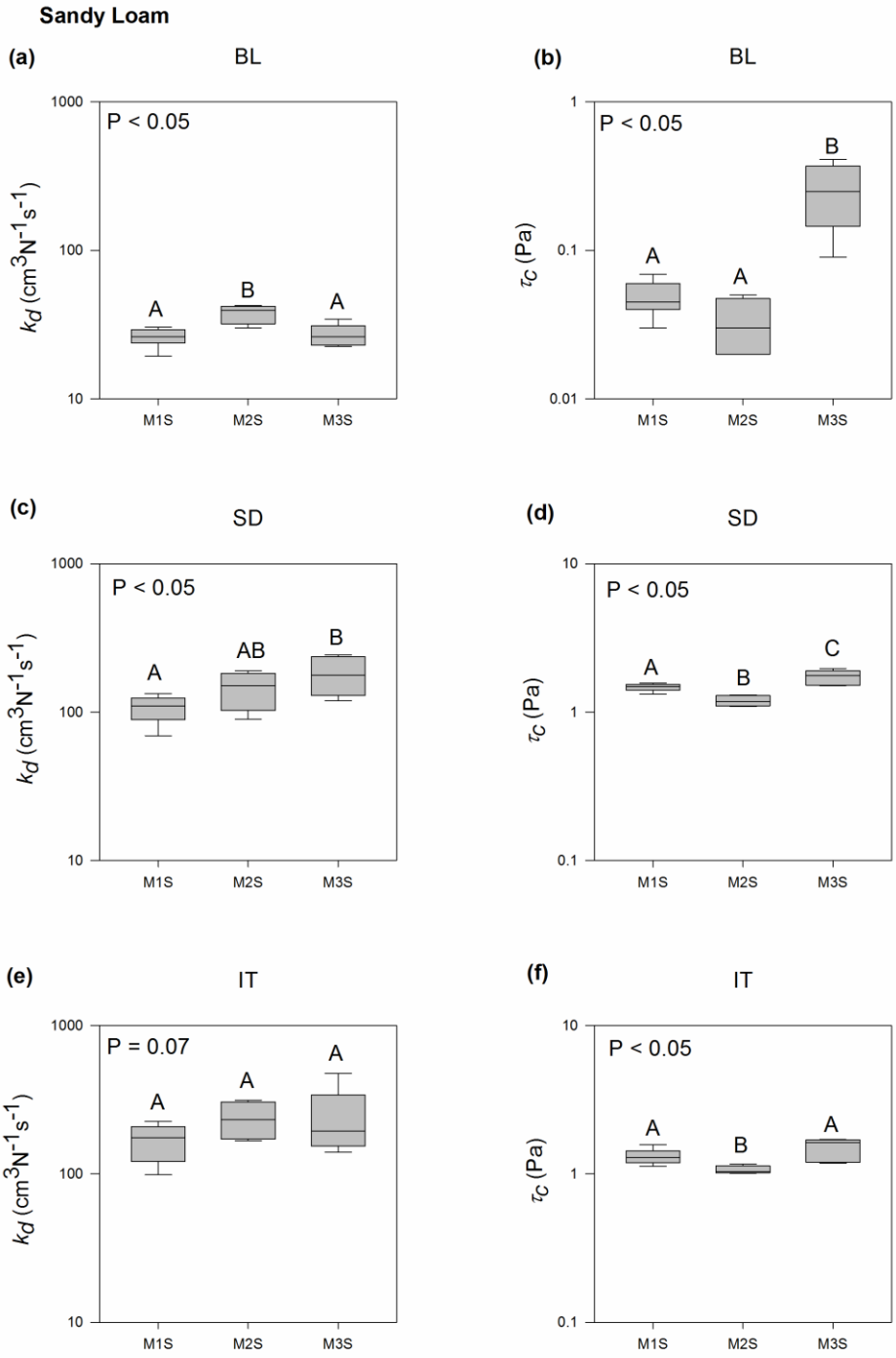

Figure 3.3. ANOVA and Pair-wide Tukey tests performed on erodibility parameters of the linear model for the sandy loam soil derived from mini-JETs conducted at three different moisture contents (M1S, M2S and M3S as defined in Figure 1). Presence of same alphabet (A, B and C) on top of the box plots denotes lack of significant difference between each pair of moisture contents. BL= Blaisdell solution, SD = Scour Depth Solution and IT = Iterative solution.

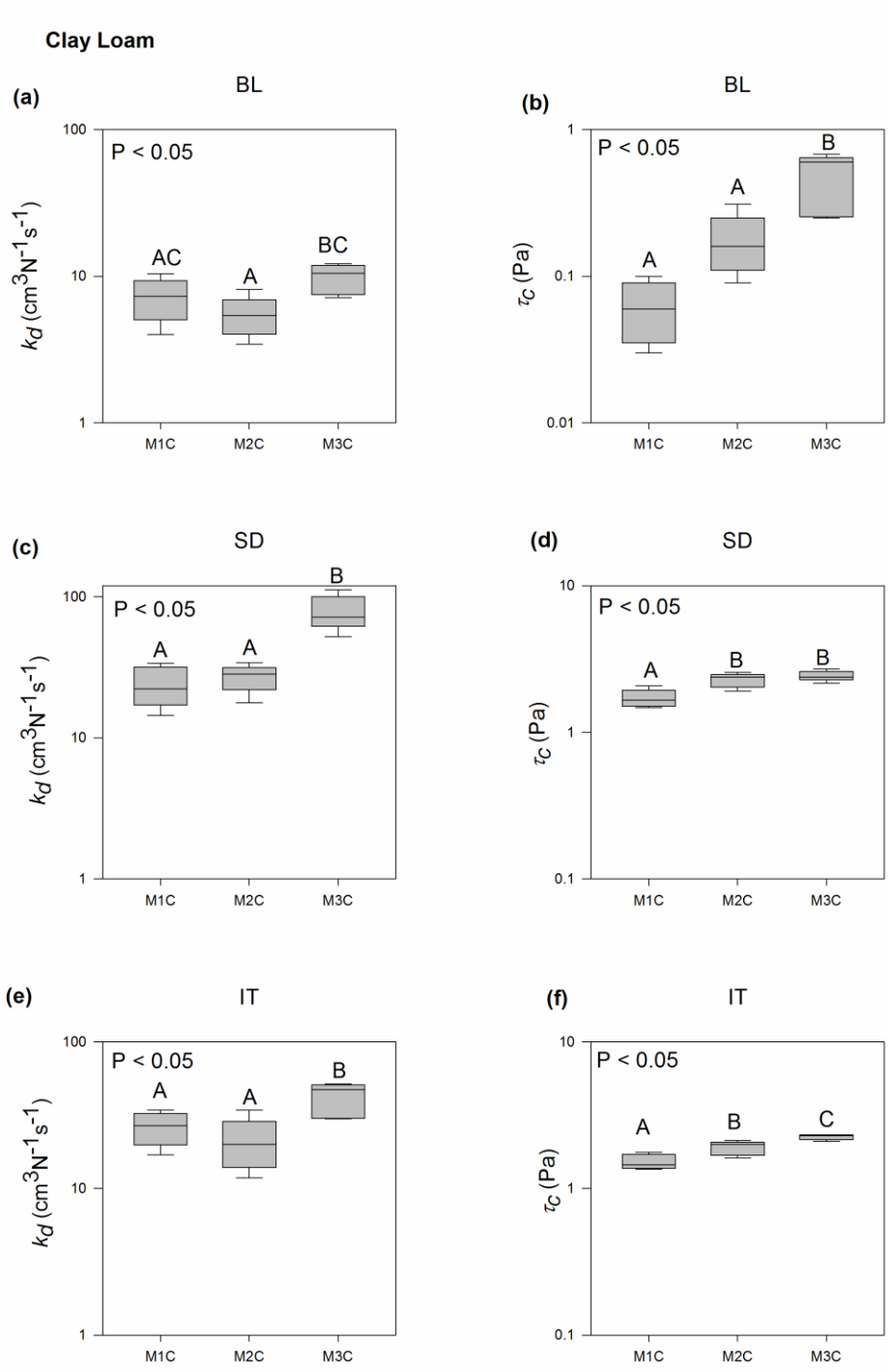

Figure 3.4. ANOVA and Pair-wide Tukey tests performed on erodibility parameters of the linear model for the clay loam soil derived from mini-JETs conducted at three different moisture contents (M1S, M2S and M3S as defined in Figure 1). Presence of same alphabet (A, B and C) on top of the box plots denotes lack of significant in difference between each pair of moisture contents. BL= Blaisdell solution, SD = Scour Depth Solution and IT = Iterative solution.

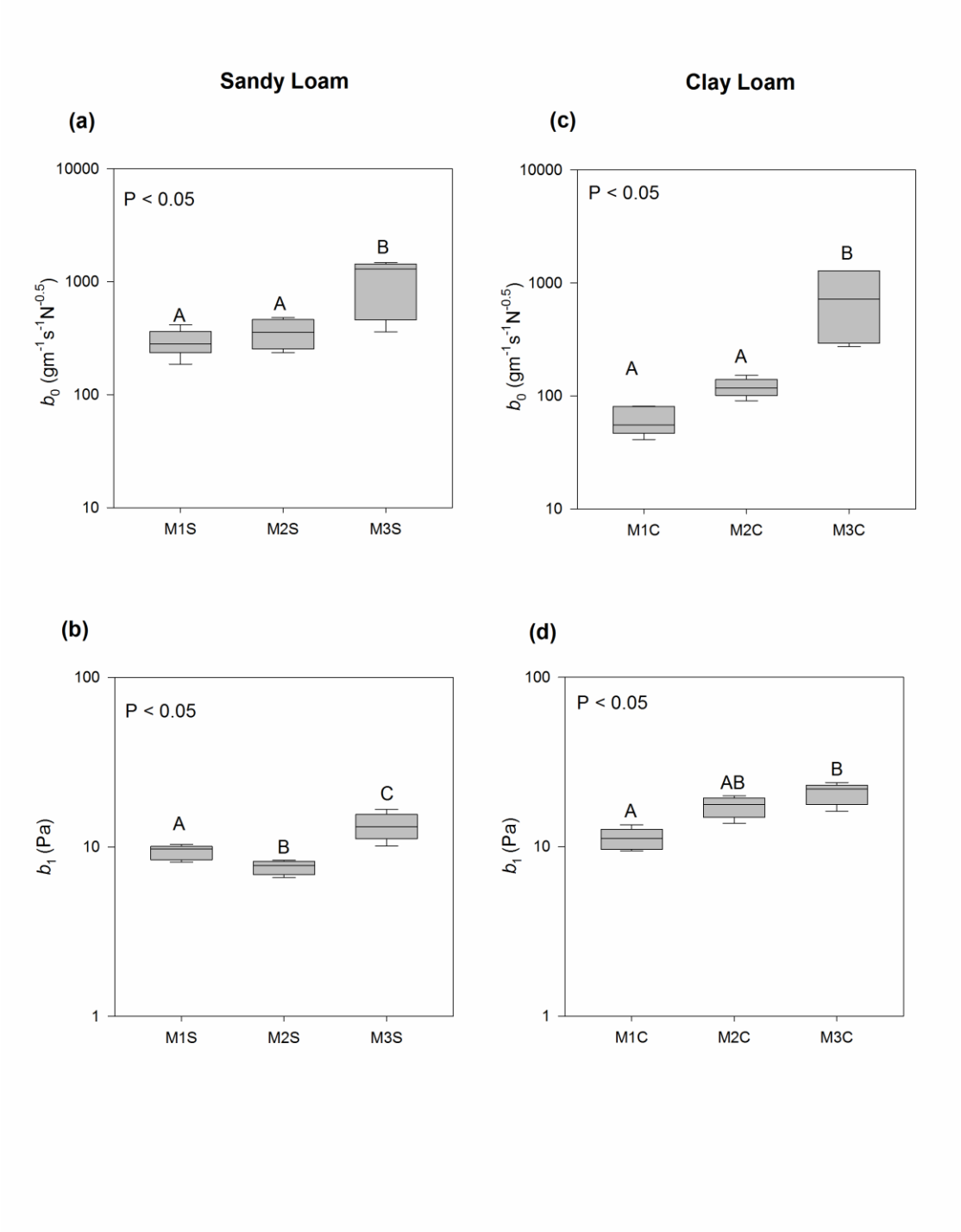

Figure 3.5. ANOVA and Pair-wide Tukey tests performed on erodibility parameters of the nonlinear model for the sandy loam soil and clay loam soil derived from mini-JETs conducted at three different moisture contents (M1S, M2S and M3S as defined in Figure 1). Presence of same alphabet (A, B and C) on top of the box plots denotes lack of significant difference between each pair of moisture contents. BL= Blaisdell solution, SD = Scour Depth Solution and IT = Iterative solution.

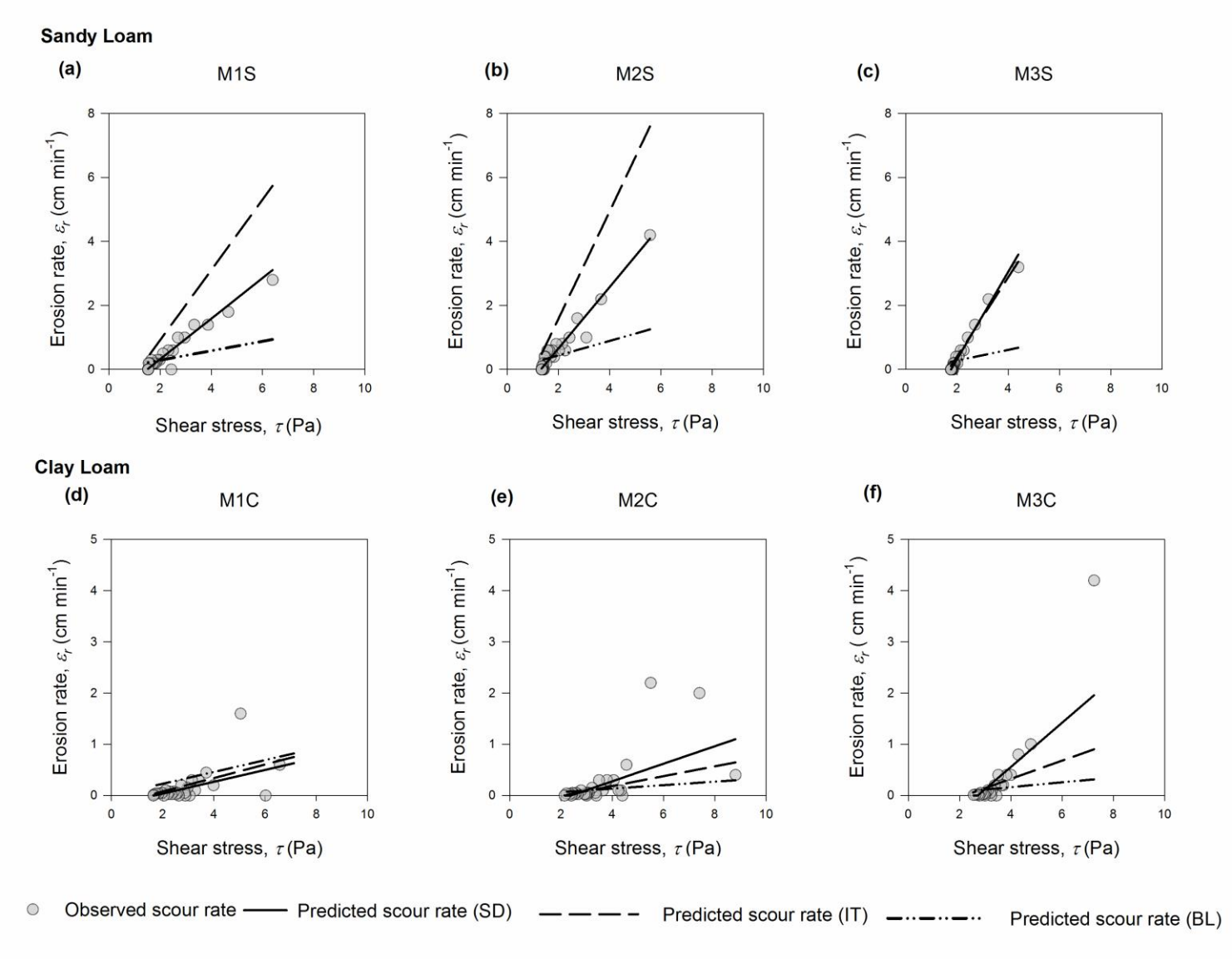

Figure 3.6. Influence of the moisture content profiles (M1S, M2S and M3S as defined in Figure 1) on the fit of the observed data to the linear model. BL= Blaisdell solution, SD = Scour Depth solution, and IT = Iterative solution.

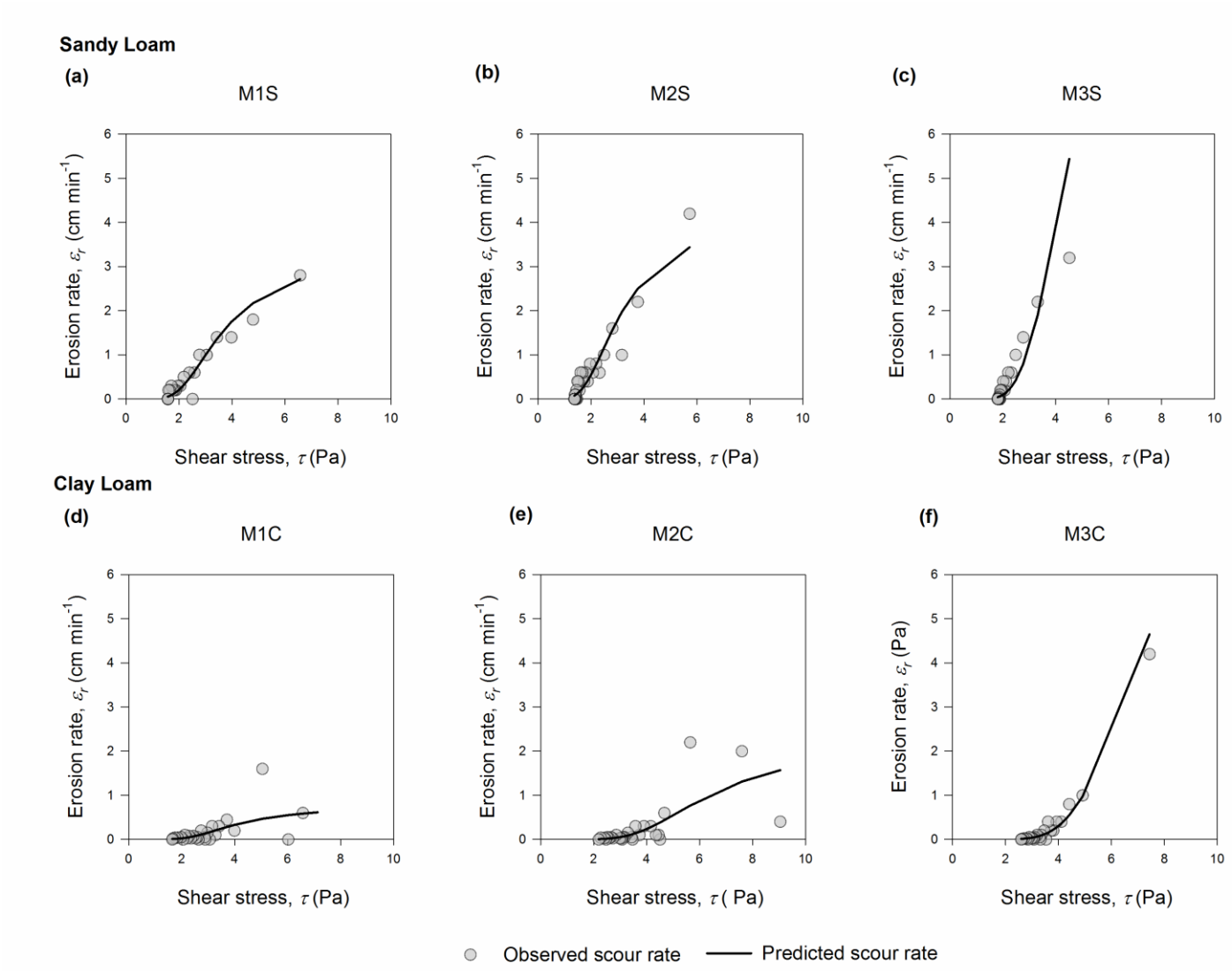

Figure 3.7. Iinfluence of the moisture content profiles (M1S, M2S and M3S as defined in Figure 1) on the fit of the observed data on the non-linear model.

Table 3.1. Properties of soils used for the JETs.

		Soil texture				Standard Compaction	
Source	USCS classification	Sand (%)	Silt (%)	Clay (%)	Plasticity Index	Maximum Density (Mg m^{-3})	Optimum water content (%)
Cow Creek	Sandy loam	54	38	8	Non-plastic	1.78	15
Five Mile Creek	Clay loam	30	33	36	6	1.61	20

CHAPTER 4

INVESTIGATION OF DETACHMENT CHARACTERISTICS OF VEGETATED SOIL USING LABORATORY MINI-JETS

Abstract

The influence of vegetation on flow and sediment dynamics at various spatial and temporal scales has been well documented. Vegetation has been proven as one of the most effective measures in streambank stabilization. Traditionally, research on the influence of vegetation roots on streambank stabilization has focused on mechanical reinforcement and reduced applied shear stress due to above ground biomass. Few studies have investigated the effect of roots on fluvial detachment of sediment. This study conducted 36 mini-JETs on bare soil samples and 29 mini-JETs on vegetated soil samples and estimated the parameters of the linear excess shear stress model and a nonlinear detachment model (Wilson model). This study also investigated the correlations between parameters of the two models and root characteristics. The root traits were found to be highly correlated to each other. This is indicative of interaction effect of different root traits. The τ_c and b_1 parameters were on average higher for the vegetated samples than the bare soil samples. The b_0 and k_d parameters were negatively related to root diameter through power functions. Significant correlations were observed among the parameters of the excess shear stress model and the nonlinear detachment

model; especially high correlation was observed between τ_c and b_1 for the vegetated samples. Mini-JETs can be a useful method to study detachment characteristics of vegetated soils and should be expanded to other soil types and vegetation.

Introduction

A delicate feedback exists between riparian vegetation and fluvial systems which determines the form and function of the fluvial environment (Reinhardt et al., 2010; Darby, 2010; Gurnell, 2013). The influence of vegetation on flow and sediment dynamics at various spatial and temporal scales has been well documented (Curran and Hession, 2013). The influence of vegetation on the sediment dynamics of a river determines the stability of the banks and supply of sediment load in the river (Lawler 2008, Wynn and Mostaghimi, 2006). Streambank erosion, a natural process (Florsheim et al., 2008) can be intensified by various anthropogenic activities (Goodwin et al., 1997; Trimble, 1997; Belsky et al., 1999). This can lead to significant impairment of natural river channels (Simon et al., 2000; Fox and Wilson, 2010). Recent restoration efforts have focused on bank stabilization to mitigate such detrimental effects (Bernhardt et al., 2005; Palmer et al. 2005).

Vegetation has been proven as one of the most effective measures in streambank stabilization (Thorne, 1982; Simon and Darby, 1999). The above ground biomass intercepts the precipitation and protects the soil from detachment on impact (Osborn, 1954), adds to the roughness and resistance against flow, and alters the velocity profile and shear stress patterns (Curran and Hession, 2013). Loss of soil due to splash and rill erosion has been observed to decrease exponentially with percentage of vegetation cover (Poesen et al., 1994). Vegetation roots are known to have a wide range of influence on

various intrinsic properties of soil such as bulk density (Lipiec, 1990), aggregate stability (Amezketa, 1999), infiltration capacity, and shear strength (Gary and Sotir, 1996). These intrinsic properties are important factors which contribute to bank stability. Traditionally, the focus of utilizing vegetation in streambank stabilization has been on bio-mechanical reinforcement of the roots. As roots are strong in tension, roots act similar to steel reinforcement in concrete structures and provide resistance against shear (Waldron, 1977; Wu et al., 1979; Andersen and Richards, 1987; Gray and Leiser, 1987; Simon and Collison, 2002).

The bio-mechanical reinforcement provided by the roots was initially modeled as added shear strength in a modified form of the Coulomb equation (Waldron, 1977). It was assumed that that all the roots extended vertically and provided resistance against shearing in a horizontal plane. The Coulomb equation was modified to following form:

$$S = c + \Delta S + \sigma_N \tan\phi \tag{4.1}$$

$$\Delta S = T_r(\sin\theta + \cos\theta \tan\phi)(\frac{A_r}{A}) \tag{4.2}$$

where S is the shearing resistance of the soil, c is the cohesion, σ_N is the normal stress applied on shear plane, ϕ is the internal angle of friction, T_r is the tensile strength of the roots and A_r/A is the ratio of root area and area of the shear plane. Gray (1974) carried out a sensitivity analysis and demonstrated that the term ($sin\theta+cos\theta tan\phi$) varied from 1.0 to 1.3 for normal values of the angles. Wu et al. (1979) adopted value of 1.2 to simplify equation (4.2). The final form of the simple perpendicular model for root reinforcement was as follows:

$$\Delta S = 1.2T_r \frac{A_r}{A} \tag{4.3}$$

Waldron and Dakessian (1981) suggested this equation overestimated the reinforcement provided by the roots as it assumes that all the roots in shear plane are mobilized to their maximum strength during shearing. This hypothesis of overestimation was verified by various field and laboratory tests carried out by Pollen et al. (2004). The authors pointed to the fact that the full tensile strength of the roots is mobilized only at high displacement of soil mass and full tensile strength of roots is not utilized before the failure of the soil mass. Pollen and Simon (2005) suggested using a fiber bundle model called RipRoot which assumes that roots with in soil mass have different tensile strength and the load is redistributed among the remaining intact roots. This model accounts for progressive failure of roots and was found to be more accurate than the perpendicular model suggested by Wu et al. (1979). Other processes like straightening of the roots to overcome their tortuosity also take place within the root permeated soil mass. These processes mobilize the energy to frictional bonds between the root and soil mass. In order to account for such processes, Pollen (2007) recognized two basic modes of root failure: root breaking and root pullout. The author measured the pullout forces as a function of the shear strength of the soil matrix. The study showed soil moisture conditions, root diameter and shear strength of soil matrix determined whether the tensile strength of roots were mobilized or they simply pulled out without contributing to streambank stabilization.

Most of the research on the influence of vegetation roots on streambank stabilization have been focused on mechanical reinforcement and estimation of ΔS (Simon and Collison, 2002; Fan and Su, 2008; Adhikari et al., 2013). Some studies have incorporated the Riproot model in bank stabilization models like Bank Stability and Toe

Erosion Model (BSTEM) to investigate the contribution of roots to the factor of safety (Pollen-Bankhead and Simon, 2009; Polvi et al., 2014). However, all of these studies have ignored the effect of roots on hydrologic and hydraulic processes that play an important role in stability of the streambank. Roots exert significant control on the subsurface moisture condition of the streambanks, create and maintain macropores and determine seasonal variations in pore water pressure and matric suction of soil (Pollen-Bankhead and Simon, 2010). The hydraulic forces in a channel first act on the toe and undercut the banks which leads to instability. The mass failure of banks is caused by the initial fluvial erosion of the bank materials (Carson and Kirby, 1972; Thorne, 1982). Vegetation roots have been successfully employed to protect the bank toe and reduce erosion of the exposed bank face. However, quantification of the erosion reduction has proven to be difficult (Pollen-Bankhead and Simon, 2010).

Most of the research how roots on influence fluvial erosion have focused on deriving statistical relationships between the particle detachment rate with few specific roots traits. Gyssels et al. (2005) provided a list of studies which tried to incorporate the effect of roots by expressing erodibility coefficients or changes in the erodibility coefficient as function of mean root diameter and/or root length density. In this review study, Gyssels et al. (2005) also pointed to a few studies on concentrated flow erosion, which observed the effect of root diameter, root length density and root type (tap root or fibrous) on erodibility coefficients. However, these studies failed to develop any statistical or predictive models. Flume experiments have been conducted to quantify the effect of roots on fluvial erosion. Da Baets et al. (2010) report results of a flume experiment carried out on 192 bare and 192 root permeated topsoil samples. The authors

measured the absolute sediment detachment rate using an excess shear stress type equation which had an erodibility coefficient (k_c). They developed several regression models which predicted the k_c coefficient as function of root diameter, soil bulk density and soil moisture. The authors defined a relative sediment detachment rate as the ratio of absolute detachment rates of bare soil and root permeated soil. They performed multiple regression analysis and developed statistical models which predicted relative sediment detachment rates as function of root diameter and root density along with other soil and flow properties. The authors also observed differences in erosion reducing effects for tap root systems versus fibrous root systems. The authors concluded that model validation contained unexplained variance and called for a process-based model.

A similar study carried out by Burylo et al. (2012) focused on roots of two grass species and one tree species. They also used relative sediment detachment rate as a measure of the erosion reducing effect of roots. The authors of this study investigated a larger set of root variables which influenced the soil erosion rates. These root traits included root to shoot biomass ratio, root density, root volume, root mean diameter, root length density, root surface area, specific root length, root tissue density, percentage of fine roots and root tensile strength. One way analysis of variance and analysis of co-variance was used to investigate variance in relative sediment detachment rate and the root traits. The authors also performed a principle component analysis (PCA) on all different root traits of the three species. The study identified mean root diameter and percentage of fine roots (percentage of root lengths with diameters less than 0.5 mm) to be most influential in relative sediment detachment rate. The study concluded that relative sediment detachment rate increased with increased mean root diameter and

decreased with an increase in percentages of finer roots. This also implied that grass species with smaller mean root diameters and a higher percentage of finer roots were better at resisting erosion.

Most of these studies have called for a more mechanistic and process-based approach to quantify the detachment reducing effects of roots (De Baetes and Poesen., 2010; Burlyo et al., 2012). Fluvial erosion was quantified with empirical models like the excess shear stress model. The application of these models is limited as they are specific to particular vegetation and site conditions.

Erodibility equations provide process-based approach to estimate soil detachment rates. The most frequently used erodibility model is known as the excess shear stress equation (Partheniades, 1965). This model states that the erosion rate is proportional to the difference between the applied shear stress and the critical shear stress:

$$\varepsilon_r = k_d(\tau - \tau_c)^a \qquad (4.4)$$

where ε_r is the detachment rate (cms^{-1}), k_d is the coefficient of erodibility ($cm^3N^{-1}s^{-1}$), τ is the applied shear stress (Pa), τ_c is the critical shear stress (Pa), and a is an exponent. The τ_c is the minimum pressure head required to initiate particle detachment. The k_d and τ_c are collectively called the erodibility parameters of the excess shear stress equation. The value of the exponent (a) is usually assumed to be one (Hanson et al., 2002)

The model parameters (k_d, τ_c) can be estimated experimentally using various techniques like flumes, hole erosion tests and jet erosions tests (JETs). The JET is a relatively novel technique used in studying the erosion properties of a soil specimen. It was developed by the USDA-ARS in Stillwater, OK (Hanson et al., 1990). The apparatus, general test methodology and procedure to analyze the data for obtaining

erodibility parameters of the excess shear stress equation is described in detail by Hanson and Cook (2004). A jet of water generated by a constant pressure impinges on a soil surface in submerged conditions. The JET exerts a certain shear force on the soil surface creating a scour hole. The depth of the scour hole is measured periodically and recorded. This observed data is then fit to equation (4.4) to estimate the respective erodibility parameters. There are three approaches in analyzing data from JETs to estimate the erodibility parameters of the excess shear stress equation. The most popular method of analysis, called Blaisdell's solution (BL), was developed by Hanson and Cook (1997) and Hanson (2004). The solution method was based on principles of fluid diffusion presented by Stein and Nett (1997) and a hyperbolic-logarithmic function modeling progression of depth of scour hole developed by Blaisdell et al. (1981). Alternatives to Blaisdell's solution have been suggested recently (Simon et al., 2010; Daly et al., 2013). One of these solution methods is called scour depth solution (SD). This method simultaneously searches for k_d and τ_c which provide the best fit of observed JET data on the scour depth versus time curve predicted by the excess shear stress equation. The other approach was presented by Simon et al. (2010), and referred to as the iterative solution (IT). This method is initialized using the values of erodibility parameters determined by Blaisdell's solution. An upper bound on τ_c is fixed to prevent it from exceeding the value corresponding to equilibrium depth. Then the values of τ_c and k_d which minimize the root mean square deviation between measured and predicted dimensionless times is searched for iteratively.

Two versions of JETs are in existence: the original JET and the mini-JET. The mini-JET is the miniaturized version of the original JET apparatus. The use of mini-JET

device was first described by Simon et al. (2010). A comparative study of the original JET and mini-JET devices in laboratory conditions was later conducted by Al-Madhhachi et.al. (2013a). The study concluded that, with certain adjustment coefficient to account for the difference in size of the nozzles of the two JET devices, original JETs and mini-JETs provided equivalent measures of the erodibility coefficients.

Another approach to estimate the sediment detachment rate is a mechanistic model called Wilson's model (Wilson, 1993a, 1993b). Wilson's model was developed to predict detachment of cohesive soil particles or aggregates on the basis of balance of forces and moments which drive and resist detachment. The mathematical expression for the model is as follows:

$$\varepsilon_r = b_0\sqrt{\tau}\left[1-\exp\{-\exp(3-\frac{b_1}{\tau})\}\right] \qquad (4.5)$$

where ε_r is the particle detachment rate (cms^{-1}), τ is the applied shear (Pa), and Wilson's model has two parameters: b_0 ($gm^{-1}s^{-1}N^{-0.5}$) and b_1 (Pa). These parameters, unlike parameters of the excess shear stress equation, are mechanistically defined. The model was found to predict detachment as well as or better than the excess shear stress model.

Al-Madhhachi et al. (2013b) incorporated the hydraulics of both the original and mini-JET device into Wilson's model and demonstrated that the parameters of Wilson's model can also be determined from the experimental data obtained from the JETs. The observed particle detachment rate data was fit to equation (4.5) by minimizing the sum of squared differences between observed and predicted scour depth.

Mini-Jets have proven to be popular for investigating the erosion properties of soil *in situ*. They also have been employed in laboratory settings on remolded samples to

investigate the effects of soil properties such as packing moisture content and packing density. However, there are limited studies which have conducted JETs on root permeated soils. Pollen-Bankhead and Simon (2010) carried out 20 JETs on root permeated soil in a switch grass plot using the original JET device. The authors reported linear power relationships between the volume of the scour hole and root volume, root length density and root biomass. The results of this study showed that the JETs can be used to show the influence of roots on the scouring. However, they did not present any findings on the parameters of the erodibility equations and their correlation with the root properties. This limits the possibility of using the JET derived parameters for modeling the detachment of root-permeated soil over certain range of the applied shear stress.

The main hypothesis of the study was that the erosion characteristics of root permeated soils could be distinguished from bare soil in terms of parameters of the erodibility equations. These parameters can be derived from mini-JETs conducted in controlled laboratory settings. The objectives of the study were as follows:

1. To demonstrate significant differences in the erodibility coefficients of root permeated soil versus bare soil.
2. To investigate the correlations between erodibility coefficients of two different sediment detachment models.
3. To investigate the correlations between root characteristics and erodibility coefficients.

Methods and materials

Mini-JETs were conducted in the laboratory to estimate erodibility coefficients. Soil was obtained in bulk from banks of Cow Creek in Stillwater, Oklahoma. It was air

dried and sieved through a no. 4 sieve (4.75 mm). The particle size distribution of the soil was analyzed following ASTM standard D422. Liquid limit and plastic limit of the soil were performed following ASTM standard D4318. Standard compaction tests were performed on the soils using ASTM standard D698A (ASTM, 2006). The basic soil properties are outlined in Table 4.1.

Samples were prepared by compacting the soil in standard proctor molds at constant moisture content of 10% and dry density of 1.5 Mg m^{-3}. The samples were tested in four batches. In each batch, a few molds were left bare and remaining molds were vegetated with seeds of Sprangletop grass (*Leptochola dubia*). Sprangletop is grass species native to Oklahoma and has been extensively used in streambank restoration projects (Lovern et al., 2013). The seeds were sown in the periphery of the samples as the middle was left bare at the surface for conducting JETs. Different numbers of seeds were sown in each vegetated sample in various patterns to achieve variable root densities (Figure 4.1). The samples were then placed in a greenhouse to allow the grass to grow. The bare samples were placed alongside the vegetated samples so that they were subjected to the same environmental conditions as the vegetated samples.

The vegetated samples were kept in the green house until the roots penetrated through the bottom of the molds. The above-ground biomass was then cutoff at the soil surface in order to not disturb the hydraulics of the submerged JETs. The roots were recovered from the vegetated samples by washing and sieving after the JETs. The recovered roots were scanned using WinRHIZO^{TM} (Regents Instruments Inc.,2014) software to determine average root diameter *(D)*, total root length *(L)*, root surface area *(SA)* and root volume *(RV)*. The percentages of total length *(FL)*, surface area *(FSA)* and

volume *(FV)* of roots with less than 0.5 mm diameter were determined as fine root traits. Examples of the scans are shown in Figure 4.2. Then three of the most developed root fibers were chosen from each sample and the peak load required to break the individual fiber was measured using an INSTRON universal testing machine. The median of these three values were recorded as the peak load *(PKL)*. The tensile strength *(TS)* of the root was calculated by dividing the PKL by the average cross sectional area of the roots. The measured root characteristics are presented in Table 4.2. The data from the JETs were analyzed using a spreadsheet tool developed by Daly et al (2013). The model parameters derived from Blaisdell solution were reported as $k_{d\text{-}BL}$ and $\tau_{c\text{-}BL}$, and model parameters derived from Scour depth solution were reported as $k_{d\text{-}SD}$ and $\tau_{c\text{-}SD}$. The parameter values derived from iterative method were not reported as they were found to be similar to parameters derived from scour depth method in magnitude.

ANOVA was performed to test the significant differences in the erodibility parameters estimated between the batches. The parameters of the erodibility equations derived from all the JETs were not normally distributed. The non-parametric Mann-Whitney rank sum tests were performed to determine the statistical differences in the model parameters between the bare and vegetated samples. The Mann-Whitney rank sum test was performed on each batch of samples as well as the compiled data. The median values of each model parameter along with the interquartile range were reported. Pearson's correlation coefficients (r) were calculated to investigate correlations among the erodibility parameters as well as the correlations between erodibility parameters and root traits.

Results and Discussion

The erodibility parameters of the samples in different batches differed significantly. Although the samples were prepared in similar conditions, the season and time period in which they were in the greenhouse differed. Although the efforts were made to maintain consistency in watering and tending of the samples, the samples are bound to develop differently. The difference in the batches can be attributed to difference in evolution of internal structure of soil samples in response to factors like water absorption, temperature and seasonality. Hence, the Mann-Whitney rank sum test was performed on the results obtained from each batch separately (Table 4.3). However, the differences between the batches also illustrate the influence of extrinsic factors in generating high degree of variability in the erodibility characteristics of soil. The role of these factors can be expected to be even more dominant in natural conditions. Mann-Whitney rank sum test was also performed on the combined data set to test the effect of the vegetation while taking the inherent variability into consideration (Table 4.3).

The τ_c and b_1 values were higher for the root permeated samples in most batches and in the combined data set (Table 4.3). The k_d and b_0 values were lower for the vegetated soil in all batches except batch 3 in which the $k_{d\text{-}SD}$ and b_0 values increased significantly ($p = 0.05$) for the vegetated soil. This was an anomalous observation. The combined data set did show decreased k_d values for the vegetated samples. The b_0, however, increased for the combined data set. This observation was counter-intuitive. However, variability in b_0 was observed to be higher than any other parameter. Such variability in b_0 was consistent with observations of other studies (Daly et al 2015; Khanal et al 2016).

The $k_{d\text{-}BL}$ and $k_{d\text{-}SD}$ were positively correlated with each other as well as to the b_0 with p-values less than 0.01 (Table 4.4). The $\tau_{c\text{-}BL}$ and $\tau_{c\text{-}SD}$ were also found to be highly correlated with each other (r = 0.9) and with the b_1 parameter (r = 0.9) and significant ($p < 0.01$). The k_d and τ_c estimated from each solution routine were negatively correlated (r = 0.46, 0.49) and significant ($p < 0.01$). This is comparable to correlation trends reported by Simon et.al. (2010) and Al-Madhhachi et al (2013a). The parameters of the Wilson's equation (b_0 and b_1) were not found to be significantly correlated (Table 4.4).

The $k_{d\text{-}BL}$ and $k_{d\text{–}SD}$ were negatively correlated to *D*, *L*, *RV* and (Table 4.5). The correlation coefficients were observed to range from -0.2 to -0.49. The correlations ($p <0.01$) between $k_{d\text{-}BL}$ and *D* and between $k_{d\text{-}BL}$ and *SA* ($p < 0.03$) were statistically significant. The $k_{d\text{-}BL}$ and $k_{d\text{-}SD}$ were found to be positively and strongly correlated to percentage of finer root traits with p-values less than 0.01. The b_0 was negatively correlated with *D* ($p < 0.05$). Exploring the correlations further revealed that relationships between b_0 and *D*, $k_{d\text{-}BL}$ and *D* and $k_{d\text{-}SD}$ and *D* were best explained by linear power functions. This is consistent with other studies which have correlated soil detachment rates and scour volumes with root diameters (De Baets et al., 2006; Pollen-Bankhead and Simon, 2010). The relationships between erodibility parameters and *D* can be especially useful in simulating the effect of roots on fluvial erosion in process based models as these relationships express such effects in more quantitative terms.

The τ_c and b_1 parameters were not significantly correlated to any of the root traits. However, as noted earlier, these parameters were consistently higher for the root permeated soil and the most easily distinguishing factor between the bare and vegetated samples. This could be either due to the higher compaction of the vegetated samples or

improvements in soil structure due to vegetation. Unfortunately, we could not test the vegetated samples for the compaction or the structural stability without destroying the samples in this study. Nevertheless, this sets one of many directions towards which this study can be expanded.

The b_0 had significant positive correlation with the percentage of finer root traits with r = 0.4 and p-values less than 0.05 (Table 4.5). Burlyo et al (2012) reported negative correlation between the relative detachment rate and percentage of finer roots and concluded that a higher percentage of fine roots contributed significantly to reducing soil detachment. This contradicts the observations made in this study as a positive correlation between k_d and b_0 parameters and percentage of fine root traits was observed. However, the variability in k_d and b_0 parameters in this study also must be noted.

It is interesting to note that there was no significant correlation observed between the *TS* of the roots and the erodibility parameters of both models. In root reinforcement models, the cohesion provided by the roots is a function of *TS* (Wu et al., 1979; Pollen, 2007). Tensile strength of the roots has been the most prominently measured root trait in studying mass stabilization due to roots. However, this study shows that *TS* of the roots may not be significant in adding resistance against particle detachment due to fluvial forces.

The root traits were highly correlated with each other (Table 4.6). Correlations coefficients between *D*, *L*, *SA* and *RV* were observed to be range from 0.70 to 0.95 and all the correlations were statistically significant ($p < 0.01$). A linear power relation was observed between the *TS* and *D* (Figure 4.4). This observation is in agreement with observations made by most of similar studies (Adhikari et al, 2013; Burlyo et al 2012).

The fine root traits *(FL, FSA, FV)* were found to be negatively correlated with *D, L* and *SA.* All of these correlations were statistically significant. This is indicative of the fact that the percentage of the finer root decreases as the roots get more developed. This explains the positive correlations between b_0 and k_d and the fine root traits. Such correlations exist because a high percentage of fine roots were indicative of less developed roots and hence higher erodibility coefficients of the soil samples.

This study has limitations of scale. The vegetation was grown in molds of 10 cm diameter. This imposed restrictions on the growth and development of the roots limiting their scale. Hence, the ranges of root traits (*L*, *D*, *SA*) are limited in comparison to the natural environment. Similarly, the mini-JETs were conducted in controlled laboratory settings. Translating the findings of laboratory studies to the natural field conditions is challenging. However, a recent study has observed that JETs conducted in controlled laboratory conditions can serve as useful guides for the field tests (Khanal et al., 2016).

This scope of this study was also limited to the influence of the roots. However, there are other hydrologic and hydraulic processes active in the soil matrix which may cause the soil to erode differently (Pollen-Bankhead and Simon, 2010). These processes can explain some of the anomalous observations made in this study. In this study we did not monitor the hydrologic changes such as matric suction and pore-water pressure in samples. Future studies should consider the hydrologic changes and develop ways to monitor aforementioned factors.

Conclusions

This study conducted 36 mini-JETs on bare soil samples and 29 mini-JETs on vegetated soil samples and estimated the parameters of the excess shear stress model and

Wilson model. The results showed that the mini-JETs conducted in controlled laboratory conditions can be useful in detecting and quantifying the influence of the roots on erodibility parameters of vegetated soil. This study also investigated the correlations between parameters of two different models and correlations between different root traits and these parameters. Significant correlations were observed among the parameters of the excess shear stress model and the Wilson's model; especially high correlation was observed between τ_c and b_1 parameters for the vegetated samples. Root traits like average diameter, length and surface area were negatively correlated with the k_d and b_0 parameters. The percentage of finer roots was positively correlated with these parameters. Linear power relationships between the k_d and root traits, especially with root diameter, were observed. Despite some limitations, results obtained in this can prove to be useful in simulating the erodibility of root permeated soil in process based models as the parameters of the erodibility models can be adjusted in relation to the root properties. Current practice of neglecting the effect of roots on particle detachment and considering only mass stability ignores one of the most important processes and introduces considerable uncertainty in design and analysis of streambank erosion. Findings of this study are important as first steps towards incorporating the effect of roots in process-based models of fluvial erosion. Continuing this study with different vegetation and soil types in larger samples may alleviate the limitations of scale. A vegetation type which can develop roots faster in limited time will be beneficial.

Figure 4.1. Samples prepared for JETs. Bare samples were used as controls

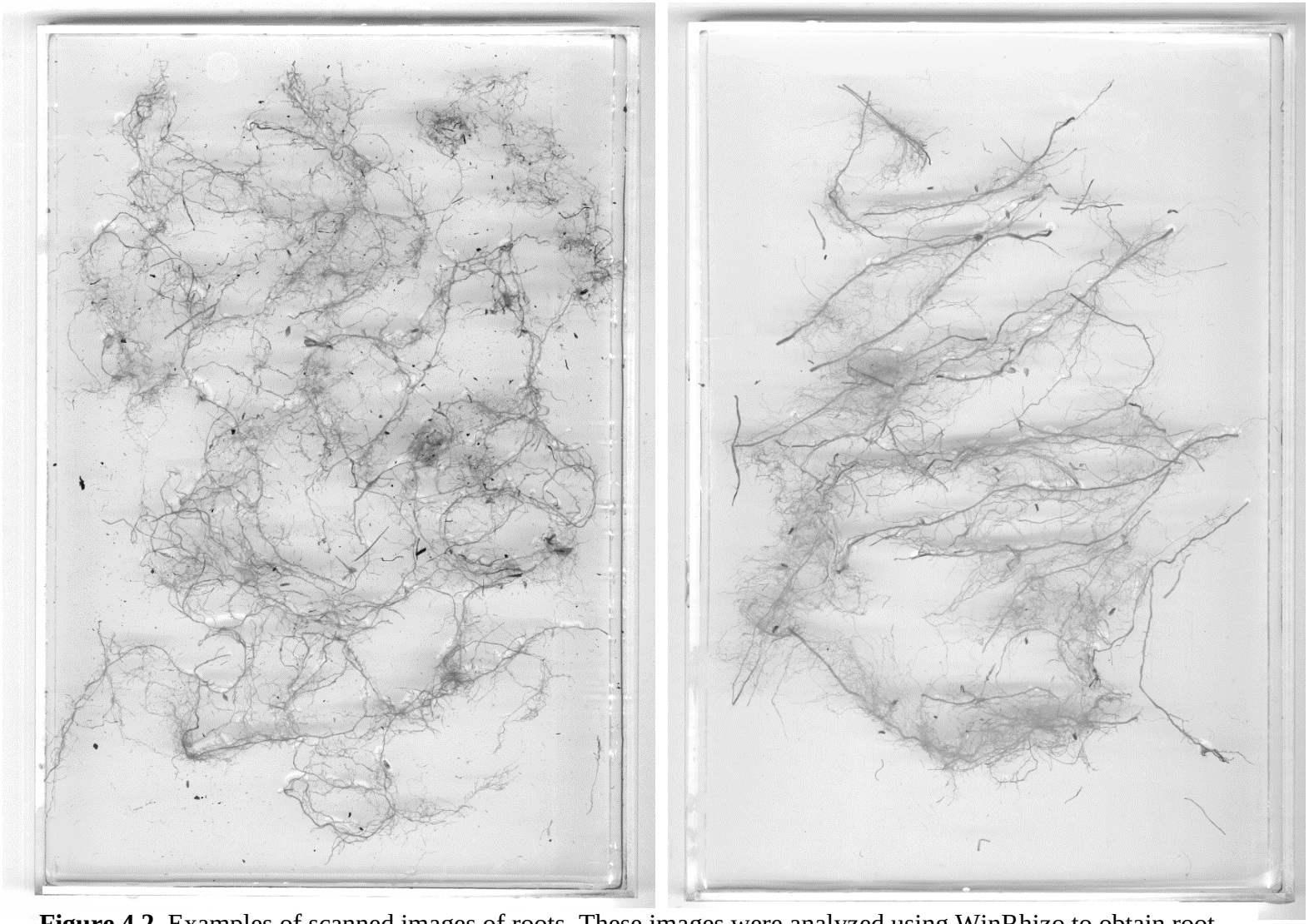

Figure 4.2. Examples of scanned images of roots. These images were analyzed using WinRhizo to obtain root characteristics

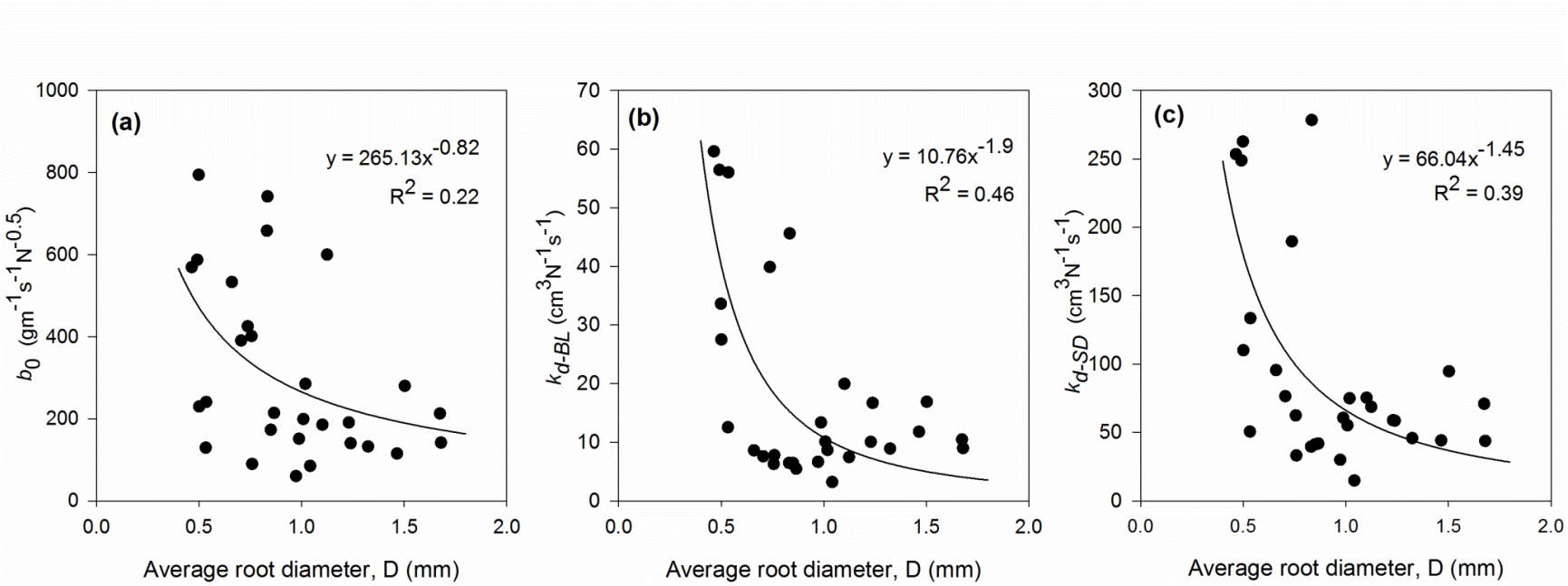

Figure 4.3. Non-linear relationship between the root diameter and (a) b_0, a parameter of Wilson's model, (b) k_d of excess shear stress equation derived from the blaisdell's solution and (c) k_d of excess shear stress equation derived from the scour depth solution.

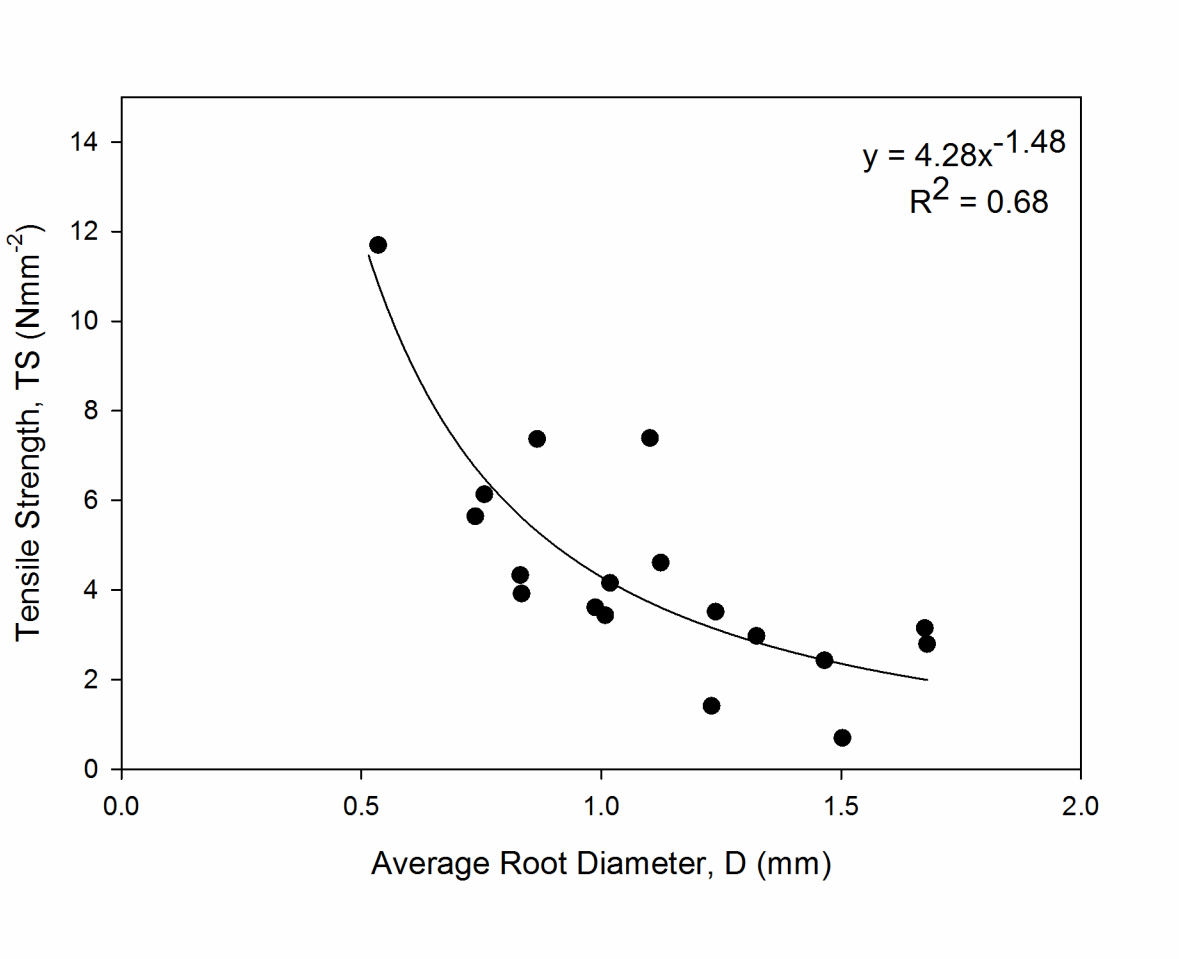

Figure 4.4. Non-linear relationship between the root diameter and tensile strength of the roots.

Table 4.1. Soil properties used for preparing the JET samples

		Soil texture				Standard Compaction	
Source	USCS classification	Sand (%)	Silt (%)	Clay (%)	Plasticity Index	Maximum Density (Mg/m^3)	Optimum Moisture Content (%)
Cow Creek	Sandy loam	54	38	8	Non-plastic	1.78	15

Table 4.2. Root properties obtained from the JET samples and measured by WinRHIZO

SN	D	L	SA	RV	FL	FSA	FV	PKL	TS
	mm	cm	cm^2	cm^3	%	%	%	N	N mm^{-2}
1	0.7	340.2	71.2	1.2	60.4	26.3	5.1		
2	0.8	226.5	54.1	1.0	55.0	22.2	4.5		
3	0.7	351.0	77.8	1.4	58.1	25.3	5.7		
4	1.0	1318.1	431.4	11.2	49.7	14.0	1.0		
5	0.9	1082.4	289.0	6.1	50.3	17.6	2.4		
6	1.0	1674.9	511.8	12.4	46.4	13.9	1.6		
7	0.5	636.5	99.7	1.2	72.6	47.4	20.5	0.4	1.9
8	0.5	80.0	11.7	0.1	80.3	60.7	34.1	0.3	2.0
9	0.5	97.4	16.4	0.2	62.8	39.8	16.7	2.6	11.7
10	0.5	615.5	95.0	1.2	74.0	49.3	22.0	0.4	2.0
11	0.5	670.5	105.5	1.3	73.2	46.3	17.0	0.4	1.9
12	0.8	1632.4	427.5	8.9	54.2	19.9	2.6	2.1	3.9
13	0.7	1530.8	354.6	6.5	57.5	23.8	3.0	2.4	5.6
14	0.8	1378.7	360.0	7.3	52.2	18.1	2.7	2.3	4.3
15	0.9	1627.1	442.7	9.6	52.6	18.1	1.9	4.3	7.4
16	1.0	1295.5	410.4	10.3	51.5	15.7	1.2	2.7	3.4
17	1.1	1889.8	667.3	18.8	48.3	12.7	0.8	4.6	4.6
18	1.0	1157.1	370.3	9.4	51.3	15.5	1.3	3.4	4.1
19	0.8	777.8	184.8	3.5	56.9	22.2	3.6	2.8	6.1
20	1.2	903.0	348.9	10.7	48.7	11.8	0.7	1.7	1.4
21	1.2	955.5	371.8	11.5	47.6	11.7	0.6	4.2	3.5
22	1.1	1230.6	425.9	11.7	50.3	13.4	1.0	7.0	7.4
23	0.5	132.0	22.1	0.3	71.3	45.8	17.3	0.1	0.5
24	1.0	889.3	275.9	6.8	49.0	14.6	1.3	2.8	3.6
25	1.3	1276.2	530.7	17.6	46.4	11.8	0.6	4.1	3.0
26	1.7	1806.0	950.0	39.8	42.9	7.9	0.3	6.9	3.1
27	1.7	1361.5	718.3	30.2	50.2	11.2	3.0	6.2	2.8
28	1.5	1684.6	775.4	28.4	44.4	9.9	0.4	4.1	2.4
29	1.5	1460.9	689.8	25.9	49.5	10.9	0.4	1.2	0.7

SN = Test Number D = Average diameter, L = Total length, SA = Surface area, RV = Root volume, FL = Length of fine root, FSA = Surface area of fine root, FV = volume of fine root, PKL = Peak load, TS = Tensile strength

Table 4.3. Results of Mann-Whitney rank sum tests for differences in median k_d ($cm^3N^{-1}s^{-1}$), τ_c (Pa), b_0 ($gm^{-1}s^{-1}N^{-0.5}$) and b_1 (Pa) parameters between the bare soil samples and vegetated samples at $\alpha = 0.05$. BL = Blaisdell Solution and SD = Scour Depth Solution technique for estimation of parameters of the excess shear stress equation; IQR = interquartile range, defined as the difference between 25th and 75th percentile.

Batch No.	Parameter	Bare soil	Vegetated soil	
		Median values (IQR)		p-value
1 ($n_{bare} = 6$) ($n_{vegetated} = 6$)	$k_{d\text{-}BL}$	16.7 (11.1)	7.1 (2.3)	0.06
	$\tau_{c\text{-}BL}$	0.1 (0.01)	0.3 (0.3)	0.01*
	$k_{d\text{-}SD}$	81.4 (56.6)	37.0 (55.0)	0.24
	$\tau_{c\text{-}SD}$	1.7 (0.8)	2.1(0.6)	0.02*
	b_0	197.6 (67.3)	131.0 (347.4)	0.69
	b_1	11.5 (5.0)	16.7 (8.4)	0.01*
2 ($n_{bare} = 8$) ($n_{vegetated} = 7$)	$k_{d\text{-}BL}$	55.5 (21.2)	45.6 (22.8)	0.15
	$\tau_{c\text{-}BL}$	0.03 (0.04)	0.04 (0.07)	0.46
	$k_{d\text{-}SD}$	256.5 (124.2)	248.8 (129.3)	0.23
	$\tau_{c\text{-}SD}$	0.9 (0.1)	1.1 (0.18)	0.02*
	b_0	593.2(283.8)	569.4 (501.6)	0.78
	b_1	6.4 (1.2)	7.9 (2.0)	0.04*
3 ($n_{bare} = 5$) ($n_{vegetated} = 5$)	$k_{d\text{-}BL}$	6.5 (0.9)	6.9 (2.9)	0.79
	$\tau_{c\text{-}BL}$	0.2 (0.1)	0.3 (0.2)	0.43
	$k_{d\text{-}SD}$	36.7 (13.9)	58.6 (28.9)	0.05*
	$\tau_{c\text{-}SD}$	1.9 (0.4)	2.1 (0.3)	0.12
	b_0	197.9 (88.5)	342.6 (404.6)	0.05*
	b_1	16.1 (3.5)	18.7 (4.4)	0.17
4 ($n_{bare} = 17$) ($n_{vegetated} = 10$)	$k_{d\text{-}BL}$	13.8 (6.5)	12.1 (6.9)	0.20
	$\tau_{c\text{-}BL}$	0.03 (0.03)	0.03 (0.02)	0.43
	$k_{d\text{-}SD}$	65.5 (25.5)	58.6 (26.6)	0.27
	$\tau_{c\text{-}SD}$	1.2 (0.3)	1.3 (0.1)	0.28
	b_0	195.6 (74.0)	146.0 (14.8)	0.20
	b_1	8.2 (3.5)	9.15 (1.7)	0.40
Combined ($n_{bare} = 36$) ($n_{vegetated} = 29$)	$k_{d\text{-}BL}$	15.3 (30.1)	10.1 (16.2)	0.09
	$\tau_{c\text{-}BL}$	0.04 (0.04)	0.05 (0.2)	0.02*
	$k_{d\text{-}SD}$	70.4 (66.7)	62.2 (58.8)	0.44
	$\tau_{c\text{-}SD}$	1.2 (0.7)	1.3 (0.9)	0.01*
	b_0	205.8 (137.4)	213.6 (338.1)	0.90
	b_1	8.3 (5.1)	9.7 (9.3)	0.01*

Table 4.4. Pearson's correlation coefficients (p-values) between parameters of the Wilson model (b_0 and b_1), Excess shear stress equation estimated from Blaisdell's solution ($k_{d\text{-}BL}$ and $\tau_{c\text{-}BL}$) and from scour depth solution ($k_{d\text{-}SD}$ and $\tau_{c\text{-}SD}$)

	b_0	b_1	$k_{d\text{-}BL}$	$k_{d\text{-}SD}$	$\tau_{c\text{-}BL}$	$\tau_{c\text{-}SD}$
b_0	1.0	-	-	-	-	-
b_1	0.1 (0.5)	1.0	-	-	-	-
$k_{d\text{-}BL}$	0.5 (0.01)	-0.6 (<0.01)	1.0	-	-	-
$k_{d\text{-}SD}$	0.7 (<0.01)	-0.4 (0.02)	0.9 (< 0.01)	1.0	-	-
$\tau_{c\text{-}BL}$	0.2 (0.4)	0.9 (<0.01)	-0.5 (0.01)	-0.3 (0.1)	1.0	-
$\tau_{c\text{-}SD}$	-0.1 (0.7)	0.9 (<0.01)	-0.6 (< 0.01)	-0.5 (0.01)	0.9 (< 0.01)	1.0

Table 4.5. Pearson's correlation coefficients (p-values) between parameters of the Wilson model (b_0 and b_1), Excess shear stress equation estimated from Blaisdell's solution ($k_{d\text{-}BL}$ and $\tau_{c\text{-}BL}$) and from Scour Depth solution ($k_{d\text{-}SD}$ and $\tau_{c\text{-}SD}$) and measured root traits.

	b_0	b_1	$k_{d\text{-}BL}$	$k_{d\text{-}SD}$	$\tau_{c\text{-}BL}$	$\tau_{c\text{-}SD}$
D	-0.5 (0.01)	-0.1 (0.7)	-0.5 (0.01)	-0.5 (0.01)	-0.1 (0.5)	-0.07 (0.7)
L	-0.1 (0.7)	0.2 (0.3)	-0.3 (0.06)	-0.2 (0.21)	0.2 (0.4)	0.1 (0.5)
SA	-0.3 (0.2)	0.02 (0.9)	-0.4 (0.03)	-0.3 (0.06)	-0.01 (0.9)	-0.03 (0.9)
RV	-0.3 (0.1)	-0.1 (0.6)	-0.3 (0.06)	-0.3 (0.08)	-0.1 (0.5)	-0.1 (0.5)
FL	0.5 (0.01)	-0.2 (0.2)	0.7 (< 0.01)	0.7 (<0.01)	-0.2 (0.3)	-0.3 (0.2)
FSA	0.4 (0.02)	-0.3 (0.1)	0.7 (< 0.01)	0.6 (<0.01)	-0.2 (0.3)	-0.3 (0.1)
FV	0.4 (0.03)	-0.3 (0.1)	0.7 (< 0.01)	0.6 (<0.01)	-0.3 (0.2)	-0.3 (0.06)
PKL	-0.4 (0.05)	0.01(0.06)	-0.5 (0.02)	-0.5 (0.01)	0.03 (0.9)	0.01 (0.7)
TS	-0.03 (0.9)	0.1 (0.7)	0.1 (0.5)	-0.1 (0.7)	0.2 (0.5)	0.1 (0.8)

D = Average diameter, L = Total length, SA = Surface area, RV = Root volume, FL = % length of fine root, FSA = % Surface area of fine root, FV = % volume of fine root, PKL = Peak load, TS = Tensile strength

Table 4.6. Pearson's correlation coefficient (p-values) between the measured root traits.

	D	L	SA	RV	FL	FSA	FV	PKL	TS
D	1.00	-	-	-	-	-	-	-	-
L	0.7 (<0.01)	1.00	-	-	-	-	-	-	-
SA	0.9 (<0.01)	0.9 (<0.01)	1.00	-	-	-	-	-	-
RV	0.9 (<0.01)	0.7 (<0.01)	0.9 (<0.01)	1.00	-	-	-	-	-
FL	- 0.8 (<0.01)	-0.7 (<0.01)	-0.8 (<0.01)	-0.7 (<0.01)	1.00	-	-	-	-
FSA	-0.8 (<0.01)	-0.7 (<0.01)	-0.8 (<0.01)	-0.7 (<0.01)	0.9 (<0.01)	1.00	-	-	-
FV	-0.7 (< 0.01)	-0.7 (<0.01)	-0.6 (<0.01)	-0.5 (<0.01)	0.9 (<0.01)	0.9 (<0.01)	1.00	-	-
PKL	0.7 (<0.01)	0.6 (<0.01)	0.7 (<0.01)	0.7 (<0.01)	-0.7 (<0.01)	-0.7 (<0.01)	-0.6 (<0.01)	1.00	-
TS	-0.2 (0.4)	0.02 (0.9)	-0.1 (0.6)	-0.2 (0.4)	-0.1 (0.5)	-0.1 (0.6)	-0.1 (0.5)	0.4 (0.06)	1.00

D = Average diameter, L = Total length, SA = Surface area, RV = Root volume, FL = % length of fine root, FSA = % Surface area of fine root, FV = % volume of fine root, PKL= Peak load, TS = Tensile strength

CHAPTER 5

APPLICATION OF A NON-LINEAR DETACHMENT MODEL FOR COHESIVE SOIL IN BANK STABILITY AND TOE EROSION MODEL[2]

Abstract

Cohesive sediment detachment is typically modeled for channels, levees, spillways, earthen dams, and internal erosion using a linear excess shear stress approach. However, mechanistic nonlinear detachment models, such as the Wilson model, have recently been proposed in the literature. Questions exist as to the appropriateness of nonlinear relationships between applied shear stress and the erosion rate. Therefore, the objective of this research was to test the appropriateness of linear and nonlinear detachment models for cohesive sediment detachment using streambank erodibility as quantified by jet erosion tests (JETs) for the linear excess shear stress equation and the nonlinear Wilson model across a small range of shear stress (1 to 4 Pa). The Wilson model was also incorporated into the Bank Stability and Toe Erosion Model (BSTEM) as an option for simulating fluvial erosion and used to simulate bank retreat in the streambank erodibility study The Wilson model was shown to be an appropriate particle detachment rate model.

---

[2]Published as:

Khanal, A., Kalvon, K., Fox, G., Daly, E.(2015) "Comparison of Linear and Nonlinear Models for Cohesive Sediment Detachment: Rill Erosion, Hole Erosion Test, and Streambank Erosion Studies". *Journal of Hydraulic Engineering. doi: 10.1061/(ASCE)HY.1943-7900.000147*

The use of a nonlinear detachment model alleviated questions about the .most appropriate solution technique for deriving erodibility parameters from JETs. In situ and laboratory tests sometimes use a limited range of applied shear stress, and therefore, users of these measurement techniques should be aware of the potential nonlinear behavior of cohesive sediment detachment especially at higher shear stress.

Introduction

Many water management issues, including river channel degradation, bank stability, bridge scour, culvert scour, earthen spillway erosion, and levee and earthen dam overtopping, stem from excessive sedimentation and erosion. Therefore, the ability to accurately predict cohesive soil erosion is a significant necessity for engineers worldwide. Prediction is a challenge due to numerous factors influencing soil erodibility such as soil texture, structure, unit weight, water content, swelling potential, clay mineralogy, and pore water chemistry (Utley and Wynn, 2008).

Typically, the erosion rate of a cohesive soil is predicted using using a model that relates soil erodibility to a measure of hydraulic forces on the soil. The most common model is known as the excess shear stress equation (Partheniades 1965). The model states that the erosion rate is proportional to the difference between the applied boundary shear stress and the critical shear stress

$$\varepsilon_r = k_d(\tau - \tau_c)^a \qquad (5.1)$$

where ε_r is the detachment rate (m s^{-1}), k_d is the erodibility coefficient (m^3 N^{-1} s^{-1}), τ is the applied shear stress (Pa), and a is an exponent. The value of the exponent (a) is usually assumed to be one (Hanson et al., 2002). . The k_d and τ_c are collectively called the erodibility parameters of the excess shear stress equation. The τ_c is defined as the

hydraulic stress at which erosion will initiate. The τ_c was originally defined for non-cohesive soils. There is no precise definition of τ_c for a cohesive soil as there is rarely a defining τ at which erosion of a cohesive soil starts (Utley and Wynn, 2008).

Linear Detachment Rate Assumption

This linearization of the τ versus ε_r relationship is typically justified as a necessary condition to simplify the complex description of the detachment process (Zhu et al., 2001; Knapen et al., 2007). However, whether or not the assumption of linearity holds over the entire range of possible τ in experiments still remains unanswered. In their comprehensive study of all available data relating soil erodibility and concentrated flow, Knapen et al. (2007) found that few authors attempt to search for the equation that best fits their experimental results. Some authors found that the linear relationship proved to fit well for a narrow range of τ (e.g., Ghebreiyessus et al., 1994; Prosser et al., 1995; Ghidey and Alberts, 1997; van Klaveren and McCool, 1998); while other authors found a power relation better described ε_r (e.g., Hollick, 1976; Knisel, 1980; van Liew and Saxton, 1983; Franti et al., 1999; Zhu et al., 2001). Most research has concluded that although the linear model has the advantage of being simple in application, it suffers from significant lack of fit when applied to experimental data encompassing a wide range of τ. Some authors (e.g., Lyle and Smerdon, 1965; Parker et al., 1995; Zhu et al., 1995, 2001) proposed using two different linear models by splitting the range into separate sections to overcome the deficiency of the linear model (Knapen et al., 2007). In summary, there is no consensus among researchers on the nature of the relation between ε_r and τ. Theoretical assumptions for linearity or nonlinearity have not been tested

completely. Nevertheless, the type of relationship chosen has important consequences for the values of erodibility parameters and estimation of ε_r (Knapen et al., 2007).

Wilson (1993a, b) introduced an alternative to the excess shear stress model, and Al-Madhhachi et al. (2014a, b) modified the model to account for additional forces that influence detachment. The model, hereafter called the Wilson model, is based on the balance of all the forces and moments driving and resisting detachment of a two-dimensional particle or aggregate

$$\varepsilon_r = \frac{b_0\sqrt{\tau}}{\rho_b}\left[1-\exp\left\{-\exp\left(3-\frac{b_1}{\tau}\right)\right\}\right] \tag{5.2}$$

where ρ_b is the bulk density and Wilson's model has two parameters b_0 (g m^{-1} s^{-1} $N^{-0.5}$) and b_1 (Pa). These parameters, unlike parameters of the excess shear stress equation, are mechanistically defined. The parameters of the Wilson model (b_0 and b_1) require knowledge of several soil particle and aggregate paramteres that are difficult to estimate.

According to the excess shear stress equation, once the thresh old of τ_c is exceeded, ε_r increases linearly with applied τ. The Wilson model predicts no such critical threshold but does predict a similar increase in εr at lower applied τ . At higher τ, ε_r increases with the square root of applied τ. This nonlinear shape of the Wilson model has proven to fit observed data from rill erosion studies better than the linear excess shear stress equation (Wilson 1993b).

Estimating erodibility parameters

Different techniques such as large flumes, small flumes, HETs, and JETs have been employed to obtain experimental data required for quantifying erodibility

parameters. Flumes are the most traditional and frequently used technique for studying erosion characteristics of natural channels (Hanson, 1990b).

The JET has proven to be among the most useful instruments because the test can be carried out *in situ*. JETs consist of a submerged jet of water impinging upon a soil surface creating a scour hole. The depth of scour hole is measured at different time intervals. Details of the apparatus and methods employed for JETs are described by Hanson (1990b). The experimental data obtained from the JETs can be analyzed using three different solution routines to derive the erodibility parameters of the linear excess shear stress model. The most popular method of analysis, referred to as Blaisdell's solution (Blaisdell et al., 1981), was developed by Hanson and Cook (1997, 2004). The solution method was based on principles of fluid diffusion presented by Stein and Nett (1997) and a hyperbolic-logarithmic function modeling the progression of the scour hole depth as developed by Blaisdell et al. (1981). This solution method first determines the τ_c based on the equilibrium depth of the scour hole. The equilibrium depth is defined as the maximum depth beyond which the water jet cannot further erode the soil and is determined by using the hyperbolic curve fit to estimate the scour depth as time approaches infinity. The k_d is then iteratively solved for to minimize the error between the measured time and predicted time based on an integrated solution of the excess shear stress equation.

Two alternatives to the Blaisdell solution have been suggested recently: the iterative solution (Simon et al., 2010) and the scour depth solution (Daly et al., 2013). In contrast to the Blaisdell solution, the scour depth and iterative solutions solve for both τ_c and k_d simultaneously through iterations. The scour depth solution simultaneously solves

for k_d and τ_c values to minimize the squared errors between the observed JET scour depths and the predicted scour depths computed by the excess shear stress equation (Daly et al., 2013). The iterative solution is initialized using the values of erodibility parameters determined by the Blaisdell solution (Simon et al., 2010). The scour hole is assumed to reach the equilibrium depth at the end of each test. An upper bound on τ_c is calculated using this equilibrium depth and is set as a constraint preventing the final estimated τ_c from exceeding this value. The final value of τ_c and k_d are then solved for simultaneously by minimizing the squared errors between the measured time to reach observed scour depths and the times calculated to reach the observed depths using the excess shear stress equation. Note that the parameters (b_0, b_1) of Wilson's model are also estimated from the JET data by minimizing the sum of squared error between the predicted scour depth data and observed data from the JET. The details of the procedure are described in Al-Madhhachi et al. (2013).

Previous research has indicated that the Blaisdell solution estimates lower τ_c than the scour depth and iterative solutions (Simon et al., 2010; Daly et al., 2013). Because each method assumes that the τ-k_d relation is linear, the estimation of k_d by the Blaisdell solution is also lower than that estimated by scour depth and iterative solutions. At higher applied τ, ε_r predicted by the scour depth solution and the iterative solution are thus much higher due to their higher estimated k_d values. When used in stability models such as BSTEM, k_d is frequently used as a calibration parameter, and it has been observed that k_d estimated from JETs using the scour depth and iterative solutions requires significant scaling down to match the predicted and observed bank retreat (Daly et al., 2015). This necessity raises questions about the assumption of linearity between ε_r and τ.

Objectives

The range of shear applied during a JET depends on the constant head under which the test is carried out. The range of shear stress applied in a channel simulation depends upon the river stage. The range of applied shear stress during JETs is usually smaller than the range of applied shear stress in a simulation, especially if the simulation is carried out for a long time period with extreme events. A narrower range of applied shear stresses are used to estimate k_d but then applied across a wider range of shear stress in stability models. This study proposes that the linearity of excess shear stress causes inflation of the erosion rate when using scour depth and iterative solutions at higher applied shear stress caused by high river stages.

The objectives of this study are to demonstrate that the non-linear detachment rate models like Wilson's model provide improved predictions of fluvial erosion when used in stability models. This study carried out BSTEM simulations with three different erodibility parameters derived from different solution routines and with Wilson's model in place of the excess shear stress equation. Predictions from all simulations were compared with the observed bank retreat.

Methods and Materials

The Bank Stability and Toe Erosion Model (BSTEM) is one of the most popular process-based models for simulating streambank erosion and failure (Simon et al., 2000). This model was developed by the National Sedimentation Laboratory in Oxford, Mississippi. The model is implemented as a spreadsheet application for one-dimensional stability modeling of a composite streambank under a continuous flow event defined by a stage hydrograph. The importance of incorporating bank heterogeneity into a model has

been shown in previous research (Sutarto et al., 2014). BSTEM addresses this issue by enabling user input of up to five soil layers. At each time step of the hydrograph, BSTEM evaluates bank stability as a combination of two processes: fluvial erosion and geotechnical erosion. The model first simulates the fluvial erosion of the bank face and determines the extent of bank undercutting.

The model also evaluates overall stability of the bank by calculating a factor of safety (FOS) as a ratio of resisting forces to driving forces. BSTEM computes the FOS using three different limit equilibrium-method models of the bank: horizontal layers, vertical slices, and cantilever shear failure. The FOS is calculated across all horizontal soil layers as follows:

$$FOS = \frac{\sum_{i=1}^{I} c_i' L_i + (\mu_a - \mu_w) L_i \tan\phi_i^b + [W_i \cos\beta - \mu_{ai} L_i + P_i \cos(\alpha' - \beta)] \tan\phi_i'}{\sum_{i=1}^{I} [Wi \sin\beta - Pi \sin(\alpha - \beta)]} \quad (5.3)$$

where c_i' is effective cohesion of i^{th} layer (kPa), μ_a is the air pressure, μ_w is the pore-water pressure (kPa), ϕ^b is an angle that describes the relationship between shear strength and matric suction (degrees) (Fredlund and Rahardjo, 1993), L_i is the length of the failure plane incorporated within the i^{th} layer (m), W_i is weight of the i^{th} layer (kN), P_i is the hydrostatic confining force due to external water level (kN m^{-1}) acting on the i^{th} layer, β is failure-plane angle (degrees from horizontal), α' is local bank angle (degrees from horizontal), ϕ'_i is the soil internal angle of friction of the i^{th} layer (degrees from horizontal), and I is the number of layers. Failure is assumed to occur when the driving forces exceed the resisting forces (i.e., when FOS is less than one), and various

combinations of the failure plane angle and shear emergence elevation (on the bank face) are considered within the model in order to determine the failure plane with the lowest FOS. A more detailed description of the model is provided by Simon et al. (2000) and Simon et al. (2011).

BSTEM simulations were carried out for a streambank on Barren Fork Creek located in eastern Oklahoma and previously modeled with the linear excess shear stress equation by Midgley et al. (2012) and Daly et al. (2015). Barren Fork Creek is a fourth order stream that originates in northwestern Arkansas and flows through Boston Mountains and Ozark Highland ecoregions before meeting the Illinois River at Lake Tenkiller near Tahlequah, Oklahoma (Miller et al., 2014). The modeled bank was located 2.2 km downstream from Eldon Bridge USGS gage station (35.90°N, 94.85°W) (Midgley et al., 2012). The composite bank consisted of Razort and Elsah silt loam topsoil overlying an unconsolidated gravel deposit (Miller et al., 2014). The depth of topsoil layer varied across the 146 m reach. Following Midgley et al. (2012), the height of bank at the site was 3.15 m. The depths of top soil layer and gravel layer were taken as 0.74 m and 2.41 m, respectively. The slope of the stream reach was 0.002 m m^{-1}.

Bank location surveys were carried out between April 18th and October 15th, 2009 using a TOPCON HiperLite Plus global positioning system configured with a base station and rover unit (Midgley et al., 2012). Borehole shear tests were carried out to estimate cohesion (c' = 0.7 kPa) and friction angle (ϕ' = 22.7^{o}), and the values used in the model matched those used by Midgley et al. (2012). Soil samples were collected to estimate the bulk density and median particle size (d_{50}). Ground water elevations were collected from shallow groundwater monitoring wells (Fuchs et al., 2009; Heeren et al., 2010) and

default soil hydraulic parameters were used for the silt loam topsoil layer. The discharge hydrograph for the stream was collected from Eldon Bridge U.S. Geological survey gage station. The discharge hydrograph was converted to a stage hydrograph using a stage-discharge rating curve and the gage reading was assumed to be the same at the study site (Midgley et al., 2012). 29 JETs weres carried out on the cohesive layer using a mini-JET device (Al-Madhhachi et al., 2013, 2014a, 2014b) to estimate the erodibility parameters on the same location (Daly et.al., 2015). Unique to this research, erodibility parameters (k_d, τ_c) for the cohesive soil layer were estimated from the JET data with three different solution routines using the spreadsheet tool described in Daly et al. (2013). Average of the erodibility parameters derived from these JETs was used for the BSTEM simulations.

The goodness of fit of each detachment model to the observed data was quantified using the Normalized objective function (NOF). NOF is defined as the ratio of root mean squared deviation of each solution routine and overall mean of the observed data:

$$NOF = \frac{\sqrt{\frac{\sum_{i=1}^{N}(x_i - y_i)^2}{N}}}{X_a} \tag{5.4}$$

where x_i and y_i are the observed data, respectively, N is the number of observations and X_a is the mean of observed data. Smaller the values of the NOF, better is the goodness of fit of predictions of a particular model to the observed data. (Fox et al., 2006; Al-Madhhachi et al., 2013, 2014a,b).

Inclusion of Wilson's model in BSTEM

. In order to run BSTEM simulations with the nonlinear detachment model, the excess shear stress equation in BSTEM was replaced with the Wilson model in the 'Shear

stress' module. The performance of BSTEM with the Wilson model was initially evaluated by running several simulations with a range of Wilson model input parameters (b_0 and b_1) for a fictitious streambank and flow event to test whether the model was stable and output was reasonable. BSTEM was stable across the range of input parameters and predicted reasonable bank retreat.

The τ_c for the noncohesive soil was estimated using following equation developed by Millar and Quick (1993):

$$\tau_c = 0.048 \tan(\phi')\rho g(s-1)d_{50}\sqrt{1-\frac{\sin^2\theta}{\sin^2\phi'}} \tag{5.5}$$

where ϕ' is the effective internal angle, ρ is the density of water, g is gravitational acceleration, s is the specific gravity, d_{50} is the mean particle diameter of soil and θ is the bank angle (assumed to be 25° for the gravel toe or the streambank). Following Hanson and Simon (2001), the k_d was then estimated based on the estimated τ_c using the following relationship described by Criswell et al. (2015):

$$k_d = 2.23\tau_c^{-0.5} \tag{5.6}$$

The k_d and τ_c derived from equations (5.5) and (5.6) were adjusted based on the stream curvature following Daly et al. (2015). In order to estimate the Wilson model parameter, b_1, of the gravel layer, the following relationship between τ_c and b_1 was used, as reported by Wilson (1993a, 1993b) for noncohesive particles:

$$\tau_c = \frac{b_1 C_v \sqrt{6}}{\pi} \tag{5.7}$$

where C_v is the coefficient of variation due to turbulence.

To estimate b_0 for the gravel layer, separate BSTEM simulations were carried out with just the gravel layer and b_0 was changed in these simulations until the predicted retreat of the gravel layer matched the retreat predicted with excess shear stress equation. This calibration process was deemed reasonable because the focus of the simulations was on the erodibility of the cohesive topsoil layer of the streambank. Therefore, the b_0 from this calibration process and b_1 obtained from equation (5.7) were used in the BSTEM simulation with the Wilson Model.

The stage hydrograph with a time step of one hour spanned across seven years (July 2003 to August 2010) and covered flow events producing applied τ ranging from 0.3 to 32.7 Pa. The corresponding range in the applied τ for the JETs on the cohesive soil layer were 1 to 4 Pa. The groundwater elevation was assumed to be 1.73 m at the start of the simulation based on observed water levels in observation wells. The groundwater elevation was then updated by BSTEM as the simulation progressed.

A total of four simulations were performed. Three uncalibrated simulations for the cohesive topsoil layer were carried out with different erodibility parameters (Blaisdell, scour depth solution, and iterative solution) for the linear excess shear stress equation. One uncalibrated simulation for the cohesive topsoil layer was carried out with the Wilson Model. The final bank profile at the end of each simulation was extracted from BSTEM. Distance between the top of the original bank profile and the final bank profile were calculated as the bank retreat and compared to observed bank retreat.

Results and Discussion

The JET-estimated values of k_d, τ_c, and the Wilson model parameters are shown in Tables 5.1 and 5.2 . The scour depth progression predicted by the scour depth and iterative solutions more closely fit the observed scour depth data measured during the JET based on NOF values. Figures 5.1 and 5.2 show the extrapolated values of ε_r obtained by applying the excess shear stress equation and Wilson model to a wide range of applied τ, using parameters shown in Tables 5.1 and 5.2. Note that Figure 5.2b highlights the range of applied τ typically measured during the JETs, which was much smaller than the range of applied τ simulated by BSTEM in the streambank stability study. The Blaisdell solution predicted erosion to begin at much lower τ_c. In comparison, the scour depth and iterative solutions predicted a higher τ_c of 1.8 and 1.6 Pa respectively. The k_d predicted by the Blaisdell solution was lower than those predicted by the scour depth and iterative solutions (Table 5.1).

Previous research has suggested that the τ_c estimated by the scour depth solution and iterative solution were more representative of the actual applied τ at which the particle detachment was initiated in flow events (Daly et al., 2013The τ_c estimated from the Blaisdell solution was 0.6 Pa which was closer to the reported minimum average τ applied across the Barren Fork Creek (0.3 Pa) . This led to over prediction of ε_r at low τ and under prediction of ε_r at high τ. The scour depth and iterative solutions estimated τ_c to be 1.8 Pa and 1.6 Pa, respectively. This estimation was closer to the mean of the average applied shear across the bank (1.8 Pa). However, they also estimated higher k_d which led to over prediction of ε_r at higher τ. The Wilson model does not have the threshold value of the τ_c. At smaller values of the applied τ, ε_r increased almost linearly

and followed close to the iterative solution (Figures 5.1 and 5.2). At larger values of applied τ, the predicted ε_r increased with the square root of the applied shear and almost scaled to ε_r predicted by the Blaisdell solution at high τ (Figure 5.1 and 5.2).

Final bank profiles predicted by BSTEM simulation runs with uncalibrated topsoil erodibility parameters are presented in Figure 5.3. The original bank profile and base of cohesive soil layer are also shown for reference. Observed bank retreat during the simulation period was 34.6 m. As expected, all BSTEM simulations predicted similar retreats of the gravel layer at the base because of the calibration process for the gravel layer. The retreat of the cohesive layer depended on the solution routines used to derive the erodibility parameters. The Blaisdell, iterative, and scour depth solutions predicted bank retreats of 18.04 m, 50.75 m, and 83.23 m, respectively. The Wilson model predicted a retreat of 21.35 m, closest to the observed retreat. The smaller bank retreat predicted by the Wilson model and the Blaisdell solution of the linear excess shear stress equation was due to the prediction of retreat by the Blaisdell solution at small τ (< 1.0 Pa. The erodibility parameters derived from the linear detachment models, especially with the iterative and scour depth solvers, over predicted the bank retreat. The magnitude of the over prediction was proportional to the derived k_d values. Also, note that even greater differences may be observed in longer simulations.

Conclusions

In many cases, erodibility tests are performed across a small range of applied shear stress in which a linear detachment model appears appropriate. Measurement techniques that utilize greater applied shear stress illustrate the nonlinear behavior of

cohesive sediment detachment especially at higher applied shear stress. Erodibility parameters from these tests are typically used in erosion models that may simulate detachment under conditions of much greater applied stress. The Wilson model was shown to be an appropriate erosion rate model as it alleviated questions regarding the most appropriate analysis technique for *in situ* jet erosion tests, as demonstrated by the modeling of a composite streambank in this study. Interestingly in the reach-scale streambank stability modeling, the linear excess shear stress approach with erodibility parameters derived with the Blaisdell solution predicted similar bank retreat as simulations with the Wilson model. Such results suggest the advantageous nature of the nonlinear Wilson detachment model, but also identify the need for additional research to evaluate the various detachment models for laboratory HETs and in situ JETs across a wider range of soil types and additional reach-scale streambank erosion studies.

Acknowledgements

The authors acknowledge the financial support of the Buchanan Family Trust through the Buchanan Endowed Chair and the Oklahoma Agricultural Experiment Station at Oklahoma State University. This project was also supported by Agriculture and Food Research Initiative Competitive Grant no. 2013-51130-21484 from the USDA National Institute of Food and Agriculture and through a FY 2012 US EPA 319(h) Special Project #C9-00F56701.

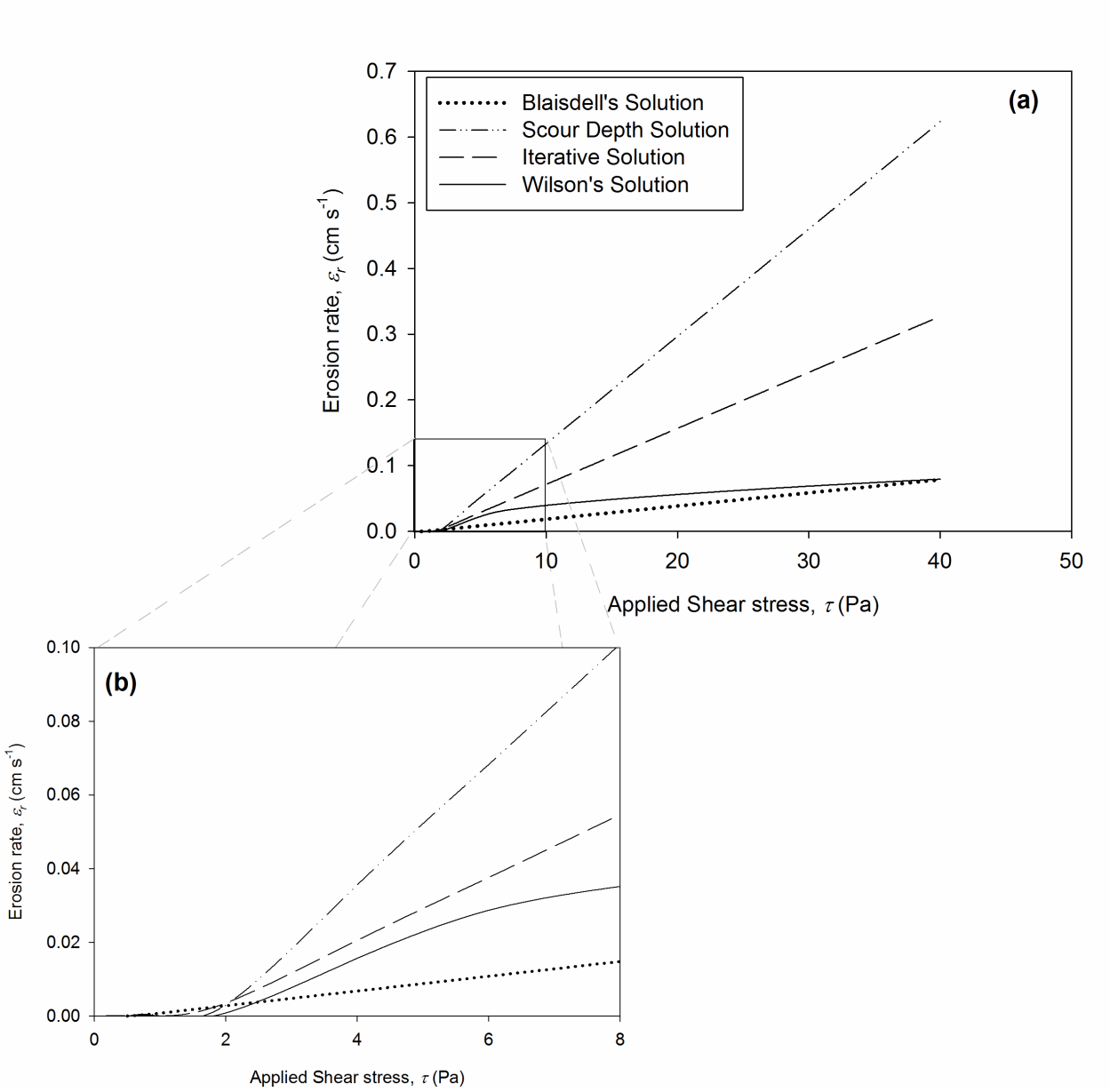

Figure 5.1. Theoretical erosion rates predicted with the average erodibility parameters from 29 JETs (a) erosion rates predicted at wider range of applied shear stress and (b) erosion rates predicted at lower values of applied shear stress. (Data from Daly et al. 2015b).

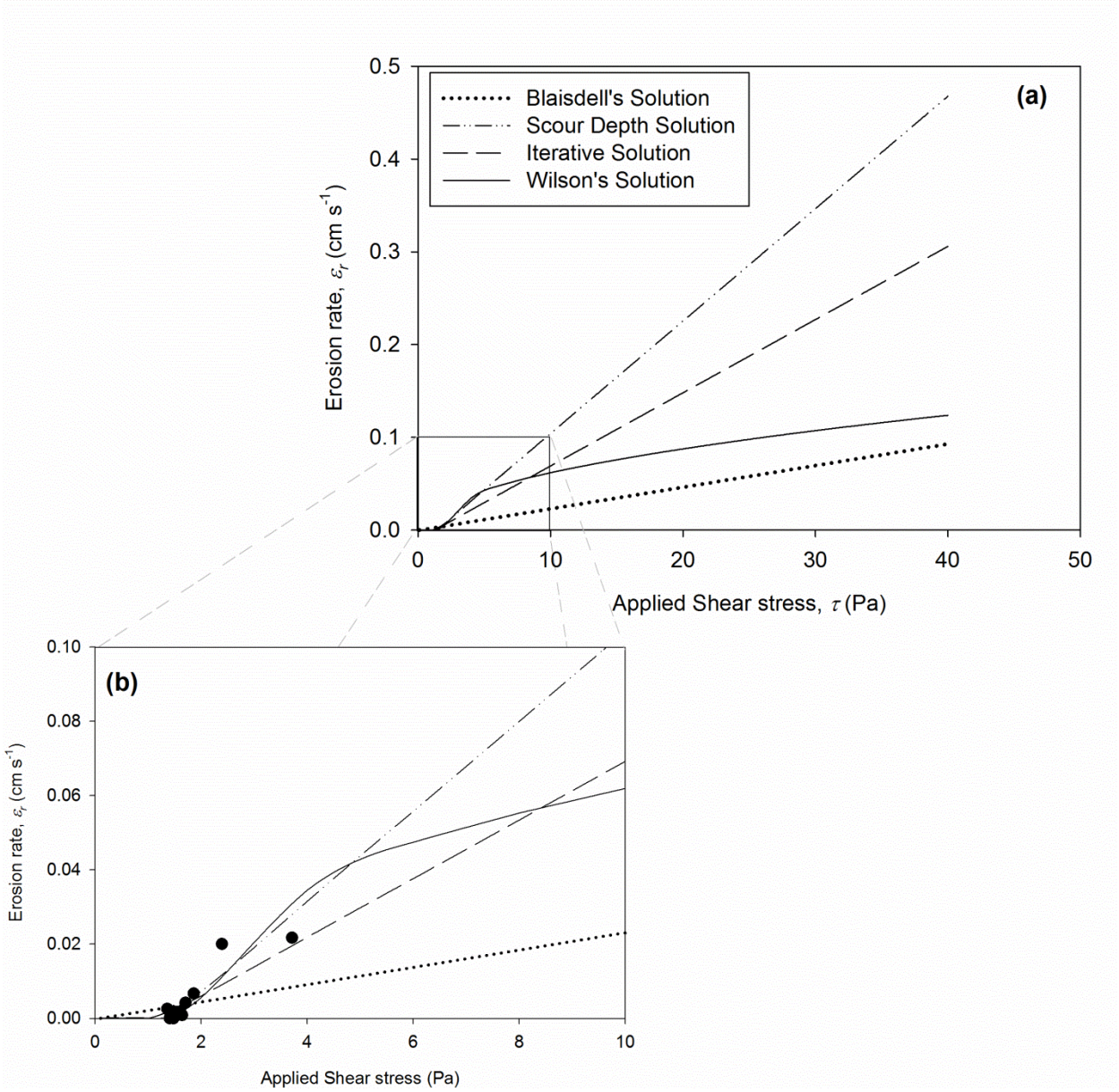

Figure 5.2. Theoretical erosion rates predicted with the erodibility parameters reported in Table 5.2. (a) Erosion rates predicted at wider range of applied shear stress and (b) erosion rates predicted at lower values of applied shear stress. An example of measured JET data is shown in (b).

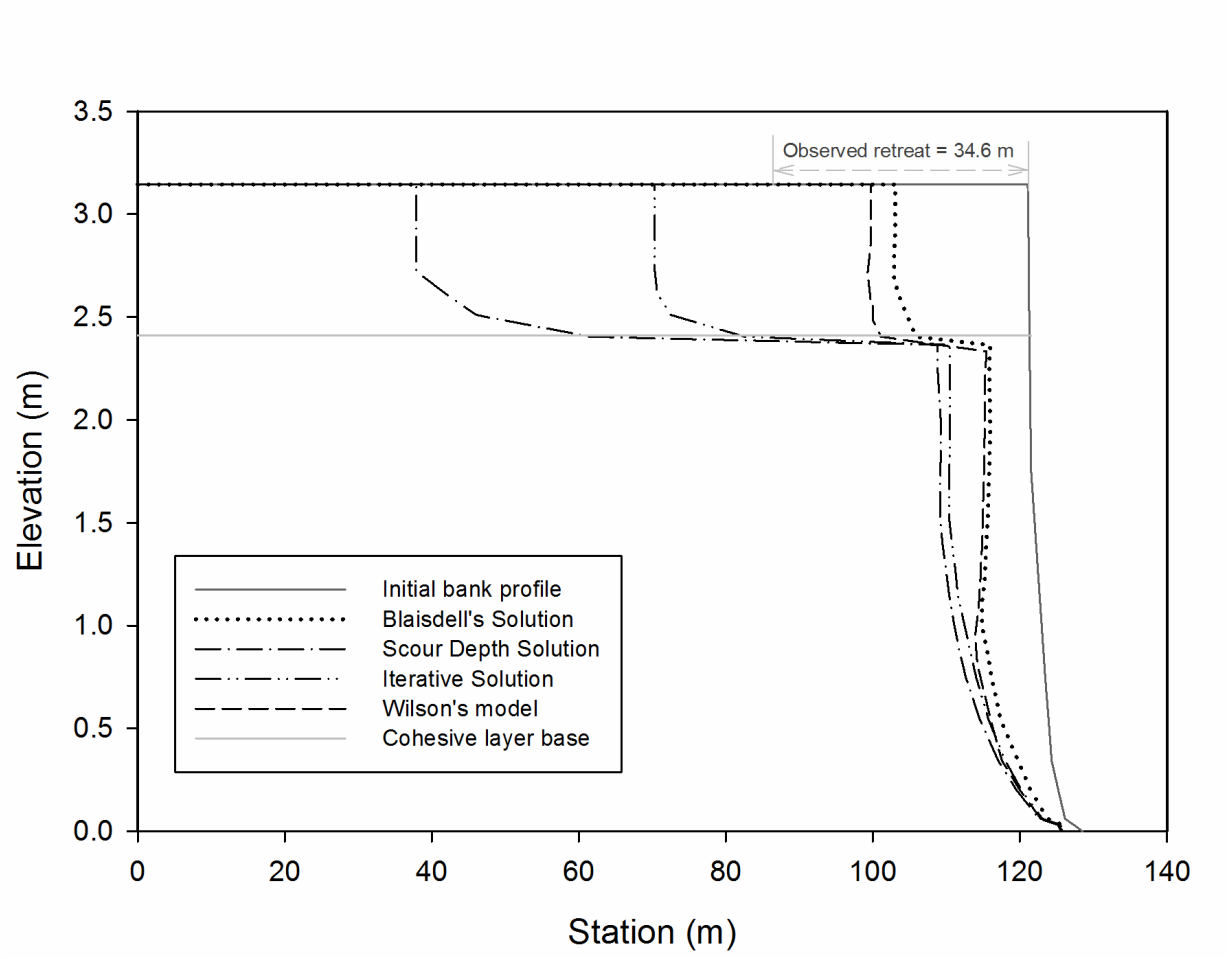

Figure 5.3. Bank profiles predicted by BSTEM for different solution routines of the linear excess shear stress model and Wilson's model.

Table 5.1. Average values of erodibility parameters for the Barren Fork Creek cohesive streambank layer derived from JETs (n = 29).

	k_d ($cm^3\ N^{-1}\ s^{-1}$)	τ_c (Pa)
Blaisdell Solution	20.04	0.62
Scour Depth	163.3	1.82
Iterative Solution	85.22	1.59
	b_0 ($g\ m^{-1}\ s^{-1}\ N^{-0.5}$)	b_1 (Pa)
Wilson Model	176.2	12.1

Table 5.2. Erodibility parameters for the Barren Fork Creek cohesive streambank layer derived from one example JETs and NOF values for the fit to the erosion rate data observed during the JET.

	k_d **($cm^3\ N^{-1}\ s^{-1}$)**	τ_c **(Pa)**	**NOF**
Blaisdell Solution	23	0.1	3.4
Scour Depth	121	1.4	0.1
Iterative Solution	79	1.2	0.2
	b_0 ($g\ m^{-1}\ s^{-1}\ N^{-0.5}$)	b_1 (Pa)	
Wilson Model	255	9.0	0.1

CHAPTER 6

CONCLUSION AND RECOMMENDATIONS

Modeling and predicting detachment of cohesive particles and consequently erosion of cohesive soil remains an unconquered problem. The complexity of the problem has led early attempts of modeling the cohesive soil erosion to take an empirical approach. However, many studies in recent years have showed that the empirical models do a poor job of estimating the erosion rates for natural conditions and call for a process based approach. The excess shear stress model and the Wilson model are two of the prominent process based models used extensively. The parameters of these models can be statistically estimated from various experimental methods. Most of these experimental methods, such as the flumes and HET, are limited in their application as they cannot be used in situ. The in situ measurement of the erodibility of cohesive soil is important as it is influenced by a number of factors which cannot be adequately resembled in laboratory conditions. The Jet Erosion Test (JET) is a relatively novel method that can be used to estimate the parameters of these models. The interest in application of JETs has been growing since they were introduced in 1990, primarily to measure the erodibility of earthen dams. The JET has also evolved in form and function over the last two decades. A miniaturized version of the JET called the mini-JET was introduced in 2010. Mini-JETs have the added advantage of portability and in-situ use. However, there is no

uniformity in operation of the device due to lack of a standard operating procedure. This can lead to wide variability in estimation of the parameters of the erodibility equation. Besides the operation of the device, data analysis procedures are also not adequately established.

There are three different solution techniques in current practice that can be used to estimate the parameters of the linear model and there is no consensus on which is the best solution technique. The variability of the parameters estimated from the JET data is also one of the major concerns. The variability in field conditions is attributed to heterogeneity of different intrinsic properties of the soil and the extrinsic environmental factors. However, the influence of these factors on the JET data has not been studied in isolated and controlled conditions. There is also a broader discussion on the appropriateness the linear model for predicting the erodibility of the cohesive soil and possibility of replacing it with a non-linear model. This study focused on the operation of the mini-JET device and the solution techniques to derive the parameters of the erodibility models from the mini-JET, added new information to the discussion, and answered the aforementioned questions. The major conclusions drawn from this dissertation are as follows:

1. The erodibility parameters of more erodible sandy loam soil were less variable than less erodible clay loam soil.
2. In general, the erodibility parameters of the linear model were estimated with the least variability when using the scour depth (SD) solution technique.

3. The b_0 parameter of the nonlinear model was more variable than the corresponding k_d in the linear excess shear stress model, with similar variability between b_1 and τ_c.
4. Laboratory mini-JETs on disturbed and repacked soil samples may be used to establish benchmark values of in situ erodibility parameters.
5. Variability of the erodibility parameters estimated from the laboratory tests was two to three orders of magnitude less than those estimated from the field tests.
6. Conducting three to five mini-JETs to quantify the erodibility of a soil in the laboratory will typically provide a good estimate of the mean with 25% precision at a 95% confidence.
7. Selection of the initial and termination time intervals were most influential at larger applied pressure heads.
8. An initial time interval of at least 30 s is recommended for mini-JETs for easily erodible sandy soils.
9. A termination time interval of 300 s is recommended for less erodible soils.
10. Smaller head setting should be preferred to higher head setting if the field conditions permit.
11. The influence of moisture content on the erodibility of soil varies with the solution technique used to derive the parameters.
12. The τ_c and b_1 increased significantly at the highest moisture contents of both soil types.

13. Increasing moisture content of packed soil influences the erodibility of soil and the influence can be detected in the estimated parameters of the linear and non-linear models.
14. The τ_c and b_1 were higher on average for vegetated samples than bare soil samples.
15. Significant correlations were observed among the parameters of the excess shear stress model and the Wilson's model; especially high correlation was observed between τ_c and b_1 parameters for vegetated samples.
16. Root traits like average diameter, length and surface area were negatively correlated with the k_d and b_0 parameters.
17. The percentage of finer roots was positively correlated with these parameters which were attributed to limited development of roots.
18. Power relationships between the k_d and root traits, especially with root diameter, were observed which can prove to be useful in simulating the erosion mitigation abilities of roots in process based models.
19. The Wilson model was shown to be the most appropriate erosion rate model from used in a reach scale streambank modeling study.

Recommendations for Future Studies

The operation of mini-JET should be standardized so that this very useful device can be used universally and results from the JETs can be interpreted with uniformity. This study has provided a basis to standardize the JET with respect to the precision of the apparatus, applied head, initial time interval and the termination time interval. The

recommendations from this study should be verified on other soil types and expanded to a larger sample set, both in field and in laboratory.

A lot of confusion seems to stem from the options of the solution methods available for the estimation of the parameters of the linear model. The traditional BL method has been shown to severely under-predict the τ_c parameter due to it's reliance on the equilibrium scour depth. The SD and IT techniques, alternatives to the BL technique, estimate a more representative value of the τ_c. However, the k_d parameter estimated from these techniques was shown to over predict the erosion rate at higher values of the applied shear stress. The SD technique was most consistent as the variability of the parameters estimated from this technique was the least. Hence, further discussion should concentrate on a consensus of the best solution technique to estimate the parameters of the linear model.

The modeling of cohesive soil erosion is complicated by the interaction effect of many factors. This study tried to isolate the effect of two of those factors: vegetation roots and moisture content. Application of the mini-JET in a controlled laboratory study was useful in reducing the complexity of the problem. More research is required in quantifying the effect of the roots on fluvial erosion. The τ_c and b_1 increasing effect with increasing moisture content was counter intuitive and unexpected. Further research is required on whether this is due to a limitation of the mini-JET or can be physically explained.

The non-linear model was shown as a sound alternative to the linear model from an application point of view of. The validity and appropriateness of the linear model

should be debated further and more research is required to establish the non-linear model in common practice.

CHAPTER 7

REFERENCES

Adhikari, A. R., M. R. Gautam, Z. Yu, S. Imada, and K. Acharya. 2013. Estimation of root cohesion for desert shrub species in the Lower Colorado riparian ecosystem and its potential for streambank stabilization. *Ecological Engineering*, 51, 33-44.

Al-Madhhachi, A. T., G. J. Hanson, G. A. Fox, A. K. Tyagi, and R. Bulut. 2013b. Deriving parameters of a fundamental detachment model for cohesive soils from flume and jet erosion tests. *Transactions of the ASABE*, 56(2), 489-504.

Al-Madhhachi, A., G. Hanson, G. Fox, A. Tyagi, and R. Bulut. 2013a. Measuring soil erodibility using a laboratory "mini" JET. *Transaction of the ASABE*, 56(3), 901-910.

Amezketa, E. 1999. Soil aggregate stability: a review. *Journal of Sustainable Agriculture*, 14(2-3), 83-151.

Anderson, M. G., and K. S. Richards. 1987. *Slope stability: Geotechnical Engineering and Geomorphology*. John Wiley & Sons.

ASCE Task Committee on Hydraulics, Bank Mechanics, and Modeling of River Width Adjustment. 1998. River width adjustment. I: Processes and mechanisms. *Journal of Hydraulic Engineering*, 124(9), 881-902.

ASTM. 2006. *Annual Book of ASTM Standards, Section 4: Construction*. Philadelphia, PA, ASTM.

Belsky, A., A. Matzke, and S. Uselman. 1999. Survey of livestock influences on stream and riparian ecosystems in the western United States. *Journal of Soil and Water Conservation*, 54(1), 419-431.

Bernhardt, E. S., M. Palmer, J. Allan, G. Alexander, K. Barnas, S. Brooks, J. Carr, S. Clayton, C. Dahm, and J. Follstad-Shah. 2005. Synthesizing U. S. river restoration efforts. *Science (Washington)*, 308(5722), 636-637.

Blaisdell, F. W., G. G. Hebaus, and C. L. Anderson. 1981. Ultimate dimensions of local scour. *Journal of the Hydraulics Division*: 107(3). 327-337.

Burylo, M., F. Rey, N. Mathys, and T. Dutoit. 2012. Plant root traits affecting the resistance of soils to concentrated flow erosion. *Earth Surface Processes and Landforms*, 37(14),1463-1470.

Carson, M. A., and M. J. Kirkby. 1972. *Hillslope form and process*. Cambridge University Press Cambridge.

Cossette, D., K. A. Mazurek, and C. D. Rennie. 2012. Critical shear stress from varied methods of analysis of a submerged circular turbulent impinging jet test for determining erosion resistance of cohesive soils. *6th International. Conference on Scour and Erosion (ICSE6)*, 11-18. Paris, France: Société Hydrotechnique de France (SHF).

Cetin, H., M. Fener, M. Söylemez, and O. Günaydin. 2007. Soil structure changes during compaction of a cohesive soil. *Engineering Geology* , 92(1), 38-48.

Curran, J. C., and W. C. Hession. 2013. Vegetative impacts on hydraulics and sediment processes across the fluvial system. *Journal of Hydrology*, 505, 364-376.

Daly, E. R., G. A. Fox, A.-S. T. Al-Madhhachi, and D. E. Storm. 2015. Variability of fluvial erodibility parameters for streambanks on a watershed scale. *Geomorphology,* 231, 281-291.

Daly, E., G. Fox, A. Al-Madhhachi, and R. Miller. 2013. A scour depth approach for deriving erodibility parameters from jet erosion tests. *Transactions of the ASABE* , 56(6), 1343-1351.

Darby, S. E. 2010. Reappraising the geomorphology-ecology link. *Earth Surface Processes and Landforms,* 35(3), 368-371.

De Baets, S., and J. Poesen. 2010. Empirical models for predicting the erosion-reducing effects of plant roots during concentrated flow erosion. *Geomorphology,* 118(3), 425-432.

De Baets, S., J. Poesen, G. Gyssels, and A. Knapen. 2006. Effects of grass roots on the erodibility of topsoils during concentrated flow. *Geomorphology*, 76(1), 54-67.

Fan, C.C. and C.F. Su. 2008. Role of roots in the shear strength of root-reinforced soils with high moisture content. *Ecological Engineering,* doi 10.1016/j.ecoleng.2008.02.013, 33(2), 157-166.

Florsheim, J. L., J. F. Mount, and A. Chin. 2008. Bank erosion as a desirable attribute of rivers. *BioScience,* 58(6), 519-529.

Fox, G.A., Wilson, G.V. 2010. The role of subsurface flow in hillslope and stream bank erosion: a review. *Soil Science Society of America Journal,* 74(1), 717-733.

Franti, T., J. Laflen, and D. Watson. 1999. Predicting soil detachment from high-discharge concentrated flow. *Transactions of the ASAE,* 42(2), 329-335.

Fredlund, D. G., and H. Rahardjo. 1993. *Soil mechanics for unsaturated soils*. John Wiley & Sons.

Fuchs, J. W., G. A. Fox, D. E. Storm, C. J. Penn, and G. O. Brown. 2009. Subsurface transport of phosphorus in riparian floodplains: Influence of preferential flow paths. *Journal of Environmental Quality,* 38(2), 473-484.

Ghebreiyessus, Y., C. Gantzer, E. Alberts, and R. Lentz. 1994. Soil erosion by concentrated flow: shear stress and bulk density. *Transactions of the ASAE*, 37(6), 1791-1797.

Ghidey, F., and E. Alberts. 1997. Plant root effects on soil erodibility, splash detachment, soil strength, and aggregate stability. *Transactions of the ASAE,* 40(1), 129-135.

Goodwin, C. N., C. P. Hawkins, and J. L. Kershner. 1997. Riparian restoration in the western United States: overview and perspective. *Restoration Ecology,* 5(4S), 4-14.

Govers, G., and R. Loch. 1993. Effects of initial water content and soil mechanical strength on the runoff erosion resistance of clay soils. *Soil Research,* 31(5), 549-566.

Gray, D. H. 1974. Reinforcement and stabilization of soil by vegetation. *Journal of the Geotechnical Engineering Division,* 100(6), 695-699.

Gray, D. H., and A. T. Leiser. 1982. *Biotechnical slope protection and erosion control*. Van Nostrand Reinhold Company Inc.

Gurnell, A. 2013. Plants as river system engineers. *Earth Surface Processes and Landforms,* 39(1), 4-25.

Gyssels, G., J. Poesen, E. Bochet, and Y. Li. 2005. Impact of plant roots on the resistance of soils to erosion by water: a review. *Progress in Physical Geography,* 29(2), 189-217.

Hanson, G. J., K. M. Robinson, and D. M. Temple. 1990. Pressure and stress distributions due to a submerged impinging jet. *ASCE National Conference on Hydraulic Engineering,* New York, 525-530.

Hanson, G. J., K. Robinson, and K. Cook. 2002. Scour below an overfall: Part II. Prediction. *Transactions of the ASAE,* 45(4), 957-964.

Hanson, G., and K. Cook. 1997. Development of excess shear stress parameters for circular jet testing. *ASAE Paper*, St Joseph, MI, 972227.

Hanson, G., and K. Cook. 2004. Apparatus, test procedures, and analytical methods to measure soil erodibility in situ. *Applied engineering in agriculture*, 20(4), 455-462.

Hanson, G., and K. Robinson. 1993. The influence of soil moisture and compaction on spillway erosion. *Transactions of the ASAE*, 36(5), 1349-1352.

Hanson, G., and S. Hunt. 2007. Lessons learned using laboratory JET method to measure soil erodibility of compacted soils. *Applied engineering in agriculture*, 23(3), 305-312.

Heeren, D. M., R. B. Miller, G. A. Fox, D. E. Storm, T. Halihan, and C. J. Penn. 2010. Preferential flow effects on subsurface contaminant transport in alluvial floodplains. *Transaction of the ASAE,* 53(1), 127-136.

Hollick, M. 1976. Towards a routine test for the assessment of the critical tractive forces of cohesive soils [Erosion of cohesive soils by flowing water]. *Transactions of the ASAE,* 19(6), 1076-1081.

Khanal. A., K. Klavon, G.A. Fox, and E.R. Daly. 2015. Nonlinear Detachment Model for Cohesive Sediment Detachment: Application to Laboratory, Rill and Streambank Erodibility Studies. *Journal of Hydraulic Engineering* , doi:10.1061/(ASCE)HY.1943-7900.0001147.

Khanal, A., Fox, G., Al-Madhhachi, A. T. 2016b. "Variability of Erodibility parameters from Laboratory mini jet erosion tests". *Journal of Hydrologic Engineering. doi:10.1061/(ASCE)HE.1943-5548.0001404.*

Knapen, A., J. Poesen, G. Govers, G. Gyssels, and J. Nachtergaele. 2007. Resistance of soils to concentrated flow erosion: A review. *Earth-Science Reviews,* 80(1), 75-109.

Knisel, W. G. (1980). *CREAMS, A field-scale model for chemicals, runoff, and erosion from agricultural management systems. Conservation Rep. No. 26*. USDA Agricultural Research Service, Washington, D.C.

Lawler, D. M. 2008. Advances in the continuous monitoring of erosion and deposition dynamics: Developments and applications of the new PEEP-3T system. *Geomorphology,* 93(1), 17-39.

Le Bissonnais, Y., B. Renaux, and H. Delouche. 1995. Interactions between soil properties and moisture content in crust formation, runoff and interrill erosion from tilled loess soils. *Catena,* 25(1), 33-46.

Lipiec, J. 1990. *Soil physical conditions and plant growth*. CRC Press Inc.

Lovern, S., G. Fox, and R. Miller. 2013. Quantifying the erodibility and geotechnical strength of cohesive alluvial soils following streambank reconstruction. *American Society of Civil Engineers Environmental Water Resources Institute Annual Meeting,* May 19–23, 2000-2008.

Luk, S.-h. 1985. Effect of antecedent soil moisture content on rainwash erosion. *Catena,* 12(1), 129-139.

Lyle, W., and E. Smerdon. 1965. Relation of compaction and other soil properties to erosion resistance of soils. *Transactions of the ASAE,* 8(3), 419-422.

Midgley, T. L., G. A. Fox, and D. M. Heeren. 2012. Evaluation of the bank stability and toe erosion model (BSTEM) for predicting lateral retreat on composite streambanks. *Geomorphology,* 145, 107-114.

Millar, R. G. 2000. Influence of bank vegetation on alluvial channel patterns. *Water Resources Research*, 36(4), 1109-1118.

Millar, R. G., and M. C. Quick. 1993. Effect of bank stability on geometry of gravel rivers. *Journal of Hydraulic Engineering*, 119(12), 1343-1363.

Miller, R. B., G. A. Fox, C. J. Penn, S. Wilson, A. Parnell, R. A. Purvis, and K. Criswell. 2014. Estimating sediment and phosphorus loads from streambanks with and without riparian protection. *Agriculture, Ecosystems & Environment*, 189, 70-81.

Osborn, B. 1954. Effectiveness of cover in reducing soil splash by raindrop impact. *Journal of Soil and water Conservation*, 9, 70-76.

Palmer, M., E. Bernhardt, J. Allan, P. Lake, G. Alexander, S. Brooks, J. Carr, S. Clayton, C. Dahm, and J. Follstad Shah. 2005. Standards for ecologically successful river restoration. *Journal of Applied Ecology*, 42(2), 208-217.

Parker, D. B., T. G. Michel, and J. L. Smith. 1995. Compaction and water velocity effects on soil erosion in shallow flow. *Journal of Irrigation and Drainage Engineering*, 121(2), 170-178.

Partheniades, E. 1965. Erosion and deposition of cohesive soils. *Journal of the Hydraulics Division, ASCE*, 91(1), 105-139.

Poesen, J., D. Torri, and K. Bunte. 1994. Effects of rock fragments on soil erosion by water at different spatial scales: a review. *Catena*, 23(1), 141-166.

Pollen, N. 2007. Temporal and spatial variability in root reinforcement of streambanks: accounting for soil shear strength and moisture. *Catena*, 69(3), 197-205.

Pollen, N., A. Simon, and A. Collison. 2004. Advances in assessing the mechanical and hydrologic effects of riparian vegetation on streambank stability. *Riparian Vegetation and Fluvial Geomorphology*, doi: 10.1029/008WSA10, 125-139.

Pollen, N., and A. Simon. 2005. Estimating the mechanical effects of riparian vegetation on stream bank stability using a fiber bundle model. *Water Resources Research*, doi:10.1029/2004WR003801, 41(7).

Pollen-Bankhead, N., and A. Simon. 2009. Enhanced application of root-reinforcement algorithms for bank-stability modeling. *Earth Surface Processes and Landforms*, 34(4), 471-480.

Pollen-Bankhead, N., and A. Simon. 2010. Hydrologic and hydraulic effects of riparian root networks on streambank stability: Is mechanical root-reinforcement the whole story? *Geomorphology*, 116(3–4), 353-362.

Polvi, L. E., E. Wohl, and D. M. Merritt. 2014. Modeling the functional influence of vegetation type on streambank cohesion. *Earth Surface Processes and Landforms*, 39(9), 1245-1258.

Prosser, I. P., W. E. Dietrich, and J. Stevenson. 1995. Flow resistance and sediment transport by concentrated overland flow in a grassland valley. *Geomorphology*, 13(1), 71-86.

Regazzoni, P. L., G. J. Hanson, T. Wahl, D. Marot, and J. R. Courivaud. 2008. The influence of some engineering parameters on the erosion of soils. *4th International Conference on Scour and Erosion (ICSE-4)*. Tokyo, Japan: Japanese Geotechnical Society

Renard, K. G., Foster, G. R., Weesies, G. A., McCool, D. K., & Yoder, D. C. 1997. Predicting soil erosion by water: a guide to conservation planning with the revised universal soil loss

equation (RUSLE). *Agriculture Handbook no. 703* Washington, D.C.: U.S. Dept. of Agriculture, Agricultural Research Service.

Reinhardt, L., D. Jerolmack, B. J. Cardinale, V. Vanacker, and J. Wright. 2010. Dynamic interactions of life and its landscape: feedbacks at the interface of geomorphology and ecology. *Earth Surface Processes and Landforms*, 35(1), 78-101.

Regents Instruments Inc.. 2014. *WinRHIZO introduction manual and reference manual*. *www.regentinstruments.com/assets/images_winrhizo/WinRHIZO2014.pdf*

Simon, A., A. Curini, S. E. Darby, and E. J. Langendoen. 2000. Bank and near-bank processes in an incised channel. *Geomorphology*, 35(3), 193-217.

Simon, A., and A. J. Collison. 2002. Quantifying the mechanical and hydrologic effects of riparian vegetation on streambank stability. *Earth Surface Processes and Landforms* 27(5), 527-546.

Simon, A., and S. Darby. 1999. The nature and significance of incised river channels. *Incised River Channels: Processes, Forms, Engineering and Management. John Wiley & Sons, Chichester*:3-18.

Simon, A., R. Thomas, and L. Klimetz. 2010. Comparison and experiences with field techniques to measure critical shear stress and erodibility of cohesive deposits. *2nd Joint Federal Interagency Conference, Las Vegas, NV*.

Stein, O., and D. Nett. 1997. Impinging jet calibration of excess shear sediment detachment parameters. *Transactions of the ASAE,*40(6), 1573-1580.

Thorne, C. 1982. Processes and mechanisms of river bank erosion. *Gravel-bed rivers*, Wiley, Chichester, England (1982), 227-259.

Trimble, S. W. 1997. Contribution of stream channel erosion to sediment yield from an urbanizing watershed. *Science,* 278(5342), 1442-1444.

Utley, B., and Wynn, T. M. 2008. Cohesive soil erosion: Theory and practice. *Proc., World Environmental and Water Resources Congress,* doi: 10.1061/40976(316)289.

Van Klaveren, R., and D. McCool. 1998. Erodibility and critical shear of a previously frozen soil. *Transactions of the ASAE,* 41(5), 1315-1321.

Van Liew, M., and Saxton, K. (1983). Slope steepness and incorporated residue effects on rill erosion. *Tranaction of the. ASABE,* 26, 1738-1743.

Waldron, L. 1977. The shear resistance of root-permeated homogeneous and stratified soil. *Soil Science Society of America Journal,* 41(5), 843-849.

Waldron, L., and S. Dakessian. 1981. Soil reinforcement by roots: calculation of increased soil shear resistance from root properties. *Soil Science* , 132(6), 427-435.

Wan, C.F., and R. Fell. 2004. Laboratory test on the rate of piping erosion od soils in embankment dams. *Geotechnical Testing Journal,* 27(3), 295-303.

Wilson, B. 1993a. Development of a fundamentally based detachment model. *Transactions of the ASAE,* 36(4), 1105-1114.

Wilson, B. 1993b. Evaluation of a fundamentally based detachment model. *Transactions of the ASAE,* 36(4), 1115-1122.

Wu, T. H., W. P. McKinnell III, and D. N. Swanston. 1979. Strength of tree roots and landslides on Prince of Wales Island, Alaska. *Canadian Geotechnical Journal,* 16(1), 19-33.

Wynn, T., and S. Mostaghimi. 2006. Effects of riparian vegetation on stream bank subaerial processes in southwestern Virginia, USA. *Earth Surface Processes and Landforms,* 31(4), 399-413.

Zhu, J., C. Gantzer, S. Anderson, R. Peyton, and E. Alberts. 1995. Simulated small-channel bed scour and head cut erosion rates compared. *Soil Science Society of America Journal,* 59(1), 211-218.

Zhu, J., C. Gantzer, S. Anderson, R. Peyton, and E. Alberts. 2001. Comparison of concentrated-flow detachment equations for low shear stress. *Soil and Tillage Research,* 61(3), 203-212.

VITA

Anish Khanal

Candidate for the Degree of

Doctor of Philosophy

Thesis: A COMPARATIVE STUDY OF ERODIBILITY MODELS AND INVESTIGATION OF INFLUENTIAL FACTORS IN ESTIMATION OF THEIR PARAMETERS FROM LABORATORY MINI-JETS

Major Field: Biosystems Engineering

Biographical:

Education:

Completed the requirements for the Doctor of Philosophy in Biosystems Engineering at Oklahoma State University, Stillwater, Oklahoma in May, 2016.

Completed the requirements for the Master of Science in Civil Engineering at Southern Illinois University Carbondale in 2012.

Completed the requirements for the Bachelor of Science in Civil Engineering at Tribuvan University, Nepal in 2008.

Experience:
2012 -2016 Graduate Research Assistant, Oklahoma State University
2010 -2012 Graduate Research Assistant, Southern Illinois University Carbondale